Novel functional imaging approaches for investigating brain plasticity in multiple sclerosis and Parkinson's disease: from research to clinical applications

Giulia Bommarito

Department of Neuroscience, Rehabilitation, Ophthalmology, Genetics, and Maternal and Children's Sciences (DINOGMI)

University of Genova

Supervisor

Matilde Inglese

In partial fulfillment of the requirements for the degree of

Doctor of Philosophy

May 19th, 2020

To my sister, my family, Demetrius, and to whoever made me smile.

'Tis e'en so: the hand of little employment hath the daintier sense.

W. Shakespeare, Hamlet, Act V, Scene I.

-Dilla dunque, la cosa. -Già lo sai. Quei loro incontri.

C. Pavese, Dialoghi con Leucò

Il faut imaginer Sisyphe heureux.

A. Camus, Le mythe de Sisyphe.

Abstract

Neuronal plasticity, as the capacity of the brain to respond to external demands or to injury, has emerged as a crucial mechanism to preserve, at least in part, an adequate behavioral functioning after an injury and as the process underlying improvements in disability during rehabilitation. Brain plasticity can be detected with both structural and functional magnetic resonance imaging and more and more processing techniques have been developed to better capture the occurring changes and to better define the potential plasticity. Gait and balance are affected in patients with multiple sclerosis since the early stages of the disease with sensory deficits playing a major role in determining both balance and gait impairment. Moreover, gait disorders are one of the major causes of disability in patients with Parkinson's disease, in particular if suffering from freezing of gait. With this work we aimed at i) investigating the functional reorganization occurring in multiple sclerosis at both early and late stages of the disease, ii) characterizing the functional pattern underlying sensory impairment in patients with early multiple sclerosis and iii) verifying the neural correlates of action observation of gait in patients with Parkinson's disease. These different studies fit into a larger framework where neuroimaging techniques, in particular functional imaging, would support the clinicians in identifying tailored rehabilitation treatments and the patients who would better benefit from them. We found that pa-

tients with early multiple sclerosis showed a higher brain functional flexibility, expressed in terms of blood oxygen level dependent signal variability, which correlated to clinical disability, representing a possible compensatory mechanism. In patients with early multiple sclerosis we also observed subtle position sense deficits, not detectable with a standard neurological examination, and which affected still standing balance. Moreover, these deficits were related to a structural damage at the level of the corpus callosum and to functional activity patterns mainly involving the frontoparietal regions. On the contrary, patients with multiple sclerosis at the progressive stages presented with more subtle changes in the resting state functional connectivity which, nonetheless, were related to clinical disability. Lastly, the presence of freezing of gait in patients with Parkinson disease influenced the neural activation underpinning the action observation of walking. Altogether, these results offer an better insight into the pathophysiological mechanisms underlying disability in patients with multiple sclerosis and constitute a groundwork for the enhancement of rehabilitation protocols to improve gait and balance in both multiple sclerosis and Parkinson's disease, supporting the embracing of new strategies such as sensory integration and action observation training.

Acknowledgements

Several thanks are needed, because of the contributions and support I received during these years.

Thanks to Prof. Matilde Inglese, for the continuous incitements and the incredible perseverance, for giving me the chance to frequent her Lab at the Icahn School of Medicine in NYC, where I learnt the basis of neuroimaging processing, and for believing in me through these years.

Thanks to Prof. Giovanni Luigi Mancardi, for welcoming me in the Neurologic Clinic of Genova, where I learnt to be a neurologist, and for strongly backing the main project of this thesis.

Thanks to Prof. Maura Casadio and to Riccardo Iandolo for the fundamental contribution to the design and fulfillment of part of this work.

Thanks to Prof. Mauro Dam and Prof. Renzo Manara for the introduction to the neuroimaging world and the invaluable teaching.

Thanks to my friends and colleagues in Genova, in particular to Maria and Giacomo, but also to Caterina, Giovanni, Chiara, Elvira, Nicolò, Simona, Niccolò, Riccardo, Angela, for all the tips and laughs together.

Thanks to the people from the Lab at Mount Sinai: Maria, Catarina,

Serena, Carla, for the precious training and the amazing moments together in NYC.

A special thanks to Prof. Van De Ville and the MipLab people: Anjali, Younes, Lorena, Vanessa, Alessandra, Daniela, Giulia, Laura, Miljan, Raphael, Nico, Nawal, Serafeim, Thomas, Elvira. The two years I spent in this Lab, with these incredible people, have been extraordinarily stimulating and a special professional and personal learning experience.

Thanks to my friends in Padova and to Nathan and Gemma for the strong and devoted support.

Thanks to Daniel, for the time together.

Thanks to my singing teachers, Carmen and Adriana, because their singing lessons have always been crucial moments during these years, making me feel better each and every time, even in the worst occasions.

Above all, a huge thanks to my family: my sister, my mum and dad, Angelo, my aunts and uncle, my achievements have never been possible without them and their love.

At last, an infinite thanks to Demetrius, with whom I'm learning to love, understand and respect life as an adult human being would.

Publications

Journal Articles

Published

- Boffa G, Tacchino A, Sbragia E, Schiavi S, Droby A, Piaggio N, Bommarito G, Girardi G, Mancardi GL, Brichetto G, Inglese M. Preserved brain functional plasticity after upper limb task-oriented rehabilitation in progressive multiple sclerosis. *European Journal of Neurololy* 2020 Jan;27(1):77-84

- Cellerino M, Cordano C, Boffa G, Bommarito G, Petracca M, Sbragia E, Novi G, Lapucci C, Capello E, Uccelli A, Inglese M. Relationship between retinal inner nuclear layer, age, and disease activity in progressive MS. *Neurology Neuroimmunology Neuroinflammation* 2019 Aug 12;6(5).

- Pardini M, Gualco L, Bommarito G, Roccatagliata L, Schiavi S, Solaro C, Mancardi G, Uccelli A, Capello E, Inglese M. CSF oligoclonal bands and normal appearing white matter periventricular damage in patients with clinically isolated syndrome suggestive of MS. *Multiple Sclerosis Related Disorders* 2019 Jun;31:93-96.

- Iandolo R, Carè M, Shah VA, Schiavi S, Bommarito G, Boffa G, Giannoni P, Inglese M, Mrotek LA, Scheidt RA, Casadio M. A two alternative forced choice method for assessing vibrotactile discrimination thresholds in the lower limb. *Somatosensensory and Motor Research.* 2019 Jun;36(2):162-170.

- Lapucci C, Saitta L, Bommarito G, Sormani MP, Pardini M, Bonzano L, Mancardi GL, Gasperini C, Giorgio A, Inglese M, De Stefano N, Roccatagliata L. How much do periventricular lesions assist in distinguishing migraine

with aura from CIS? *Neurology.* 2019 Apr 9;92(15):e1739-e1744

- Petracca M, Margoni M, Bommarito G, Inglese M. Monitoring Progressive Multiple Sclerosis with Novel Imaging Techniques. *Neurology and Therapy.* 2018 Dec;7(2):265-285.

- Piaggio N, Schiavi S, Martino M, Bommarito G, Inglese M, Magioncalda P. Exploring mania-associated white matter injury by comparison with multiple sclerosis: a diffusion tensor imaging study. *Psychiatry Research Neuroimaging.* 2018 Nov 30;281:78-84.

- Milanese L, Martini C, Scaroni C, Dassie F, Ceccato F, Della Puppa A, Denaro L, Bommarito G, Citton V, Ermani M, Maffei P, Manara R. Radiotherapy in acromegaly: Long-term brain parenchymal and vascular magnetic resonance changes. *Journal of Neuroradiology* 2018 Sep;45(5):323-328.

- Bommarito G, Cellerino M, Prada V, Venturi C, Capellari S, Cortelli P, Mancardi GL, Parchi P, Schenone A. A novel prion protein gene-truncating mutation causing autonomic neuropathy and diarrhea. *European Journal of Neurololy* 2018 Aug;25(8):e91-e92

- Iandolo R, Bellini A, Saiote C, Marre I, Bommarito G, Oesingmann N, Fleysher L, Mancardi GL, Casadio M, Inglese M. Neural correlates of lower limbs proprioception: An fMRI study of foot position matching. *Human Brain Mapping.* 2018 May;39(5):1929-1944

- Bommarito G, Bellini A, Pardini M, Solaro C, Roccatagliata L, Laroni A, Capello E, Mancardi GL, Uccelli A, Inglese M. Composite MRI measures and short-term disability in patients with clinically isolated syndrome suggestive of MS. *Multiple Sclerosis Journal* 2018 Apr;24(5):623-631

- Tacchino A, Saiote C, Brichetto G, Bommarito G, Roccatagliata L, Cordano C, Battaglia MA, Mancardi GL, Inglese M. Motor Imagery as a Function of Disease Severity in Multiple Sclerosis: An fMRI Study. *Frontiers in Human Neuroscience*. 2018 Jan 11;11:628.

- Mormina E, Petracca M, Bommarito G, Piaggio N, Cocozza S, Inglese M. Cerebellum and neurodegenerative diseases: Beyond conventional magnetic resonance imaging. *World Journal of Radiology* 2017 Oct 28;9(10):371-388.

- Pardini M, Petracca M, Harel A, Fleysher L, Oesingmann N, Bommarito G, Fabian M, Chard D, Lublin F, Inglese M. The relationship between cortical lesions and periventricular NAWM abnormalities suggests a shared mechanism of injury in primary-progressive MS. *Neuroimage Clinical* 2017 Jul 4;16:111-115.

- Saiote C, Tacchino A, Brichetto G, Roccatagliata L, Bommarito G, Cordano C, Battaglia M, Mancardi GL, Inglese M. Resting-state functional connectivity and motor imagery brain activation. *Human Brain Mapping* 2016 Nov;37(11):3847-3857

- Iandolo R*, Bommarito G*, Falcitano L, Schiavi S, Piaggio N, Mancardi GL, Casadio M, Inglese M. Position Sense Deficits at the Lower Limbs in Early Multiple Sclerosis: Clinical and Neural Correlates. Neurorehabilitation and Neural Repair. 2020 Mar;34(3):260-270 * to be considered joint first authors.

Submitted

- Bommarito G, Putzolu M, Avanzino L, Abbruzzese A, Marchese R, Inglese M, Pelosin E. Functional correlates of action observation of gait in patients with Parkinson's disease. Submitted to Journal of Parkinson Disease.

Lectures

- "Aggiornamento su diagnosi e terapie farmacologiche della SM" nell'ambito del corso di "Recenti acquisizioni nella sclerosi multipla", corso AISM, Genova 16-17 marzo 2018.

Conferences

- Bommarito G, Cellerino M, Capello E, Prada V, Ventura C, Curotto A, Cortelli P, Mancardi GL, Parchi P, Schenone A. Peripheral dysautonomia caused by PRNP gene mutations: a case report. Sesta riunione annuale ASNP, Mondello, 14 aprile 2016.

- Bommarito G, Iandolo R, Falcitano L, Schiavi S, Piaggio N, Mancardi G.L , Casadio M, Inglese M. Position sense deficits at the lower limbs in early multiple sclerosis: clinical and neural correlates. ECTRIMS, Stockholm, 11-13 September 2019

- Bommarito G, Martino M, Magioncalda P, Petracca M, Mancardi G.L, Inglese M. Investigating resting-state BOLD variability in early Multiple Sclerosis. ECTRIMS, Paris, 25-28 October 2017

Funding

Part of the work presented in this thesis has been supported by a research fellowship FISM, Fondazione Italiana Sclerosi Multipla, Cod. : 2017/B/2, and financed or co-financed with the '5 per mille' public funding.

Contents

List of Figures

LIST OF FIGURES

List of Tables

LIST OF TABLES

Chapter 1

Introduction

1.1 Rationale and objectives

"When an axon of Cell A is near enough to excite a Cell B and repeatedly or persistently takes part in firing it, some growth process or metabolic change takes place in one or both cells such that A's efficiency, as one of the cells firing B, is increased" [1], with these words, Donald O. Hebb described neural plasticity, at a synaptic level, in 1949. Defined as the brain capacity to respond to experienced demands with structural changes that alter the behavioral repertoire, the capacity of the brain to adapt relies on mechanisms involving both the grey and the white matter and can be detected at a macroscopic level, using neuroimaging techniques such as diffusion tensor imaging and functional magnetic resonance imaging. Besides the research made on healthy subjects, the study of neural plasticity by means of neuroimaging techniques in neurological disorders has received more and more attention in the last two decades, resulting in significant and interesting developments.

The first studies on changes occurring after brain injury focused on stroke, e.g. after an ischemic damage. Afterwards, research extended to a large number of

neurological disorders including Parkinson's disease and multiple sclerosis (MS). A response to injury is already detectable in the first days after an acute damage, e.g. stroke, but adaptation occurs over the following weeks and months. While in the case of an acute damage the course of the response modulation is more discernible, for chronic diseases or for a disorder such as multiple sclerosis, which embraces acute events and ongoing degenerative processes at the same time, it is harder to disentangle the different steps of neural adaptation.

Neural plasticity has also emerged as the mechanism underlying the effects of rehabilitation in neurological disorders, in particular for gait and balance impairment. In patients with multiple sclerosis, evidence from previous studies suggests that somatosensory deficits play a major role in determining gait and balance disorders and rehabilitation protocols for balance including sensory integration training resulted in a better outcome. Besides, patients with Parkinson's disease might benefit from novel rehabilitation strategies to improve gait, including action observation training. Despite the progresses in discovering and developing new drugs for neurological disorders, rehabilitation remains a crucial therapeutic tool and more and more efforts have been put in the direction of designing personalized rehabilitation protocols. However, to reach this aim, a comprehensive understanding of the baseline plastic changes underlying the clinical disability is necessary.

Against this background, the work described in this thesis aimed at investigating the functional changes occurring in multiple sclerosis at both the early and late stages of the disease and the position sense deficits in terms of both behavioral and neural correlates. A last study on patients with Parkinson disease aimed at analyzing the functional neural patterns underlying action observation of walking in presence or absence of freezing of gait.

1.2 Overview of the thesis

- In the chapter 2 an overview of the state of the art of the imaging methods used to investigate brain plasticity is provided, together with a summary of the neurophysiology of gait, focusing on the role of position sense. It also includes a description of multiple sclerosis and Parkinson's disease.

- In the chapter 3 the first study is presented, investigating the variability of the BOLD signal, as a measure of the functional flexibility of the brain, in patients at the early stages of multiple sclerosis.

- In the chapter 4 the main project, aiming at investigating the position sense in patients at the early stages of multiple sclerosis, is described.

- The chapter 5 illustrates the work exploring functional connectivity in patients with progressive multiple sclerosis.

- In the chapter 6 is reported the study characterizing the neural correlates of action observation of gait in patients with Parkinson's disease in presence and absence of freezing of gait.

The chapters 3, 4, 5 and 6 contain sections including the background, aims, methods and discussion specific for each study.

- Lastly, the chapter 7 contains the concluding remarks and future directions of the work done so far.

Chapter 2

Background

Summary

In this chapter a description of the main imaging techniques used in this work as well as a background for multiple sclerosis and Parkinson's disease are provided, emphasizing the studies on gait and balance and on brain plasticity unveiled by functional neuroimaging.

2.1 Brain plasticity

In neuroscience, the term plasticity is referred to the ability of the brain to change in response to an internal or external stimuli. This concept have been widely used and developed through centuries. Between the end of the 19th century and the beginning of the 20th fundamental discoveries were made in the field of neurophysiology. During these decades, Cajal defined the neuron as the basic building block of the nervous system and Sherrington called synapsis the connection between two neuronal cells. The term plasticity has been introduced within this context. Although probably already used by Freud referred to nervous system and

learning, in 1890, it was William James who associated plasticity with behavioral habits. In the meantime Lugaro, based on the hypothesis of his teacher Eugenio Tanzi, was the first one linking plasticity to synaptic transmission. The synaptic theory of learning underwent a strong debate until 1949, when Hebb published the Organization of Behavior [1]. This essay would lead to a wide acceptance of synaptic changes as one of the basic mechanisms underlying behavioral changes. A comprehensive and detailed review of the history of the term plasticity is beyond the purposes of this thesis and for further details see [2; 3]. However, a brief summary was needed to introduce the modern concept of brain plasticity and the impact it had on the interpretation of changes occurring within the central nervous system (CNS). Nowadays, plasticity is a term reserved to reactive phenomena, reflecting a secondary change in response to a primary change and authors differentiate it from the existing capacity to optimize brain's performance to the occurring demands, which is instead indicated as flexibility. [4].

Mechanisms underlying brain plasticity are multiple and occur at different levels. At a molecular and cellular levels, changes affect both the white and grey matter and include neurogenesis, synaptogenesis, changes in neuronal morphology, in the number of axons, in axon diameter, in the density of fibers, in axonal branching and trajectories, in myelination, in glia cells and angiogenesis [5]. These changes resonate in modifications at a columnar, cortical map and systems level, [6] and are detectable by magnetic resonance (MR) imaging. However, the neuroimaging of plasticity in human brain has drawn the attention only in the last two decades. The first studies explored differences between individuals that reflected skills or knowledge [7; 8; 9] or, with longitudinal studies, the learning of a new skill[10]. Both structural and functional imaging can capture changes due to plasticity and advances have been made in gaining more and more details of the tissue micro structure and function, i.e. cortical layer functional

Magnetic Resonance Imaging (fMRI) [11]. Plasticity is influenced by genetic and environmental factors, which would determine a different ability in responding to a specific stimulus, for each individual. Therefore, both the characteristic of the demand and the baseline ability to respond to it can determine the amount of plastic changes.

In neurological diseases, plasticity limits the impact that damage has on behavior, thus limiting the clinical disability. In acute neurological diseases, such as stroke, plasticity investigated by means of fMRI revealed increased functional activity in areas distant from the lesion early after the stroke and a later relative normalization [12]. This course mirrors what observed in healthy subjects during learning, with a decrease in cortical activity specialized in that skill over time, which occurs in parallel with an increase in effective connectivity [13]. The detection of changes due to plasticity in chronic and spatially diffuse neurological diseases such as multiple sclerosis is more challenging. However, the understanding of plasticity phenomena occurring in neurological patients in response to injury is of utmost importance for the development of novel and more effective rehabilitation strategies [14; 15].

2.2 Functional Magnetic Resonance Imaging

Since 1992, when it was firstly described as an increase in water proton MR signal in the visual cortex after visual stimulation, on a gradient-echo sequence [16], brain functional MR imaging has been broadly applied and its results have been extensively interpreted to better understand the brain function in both health and disease status. Functional MR imaging, specifically blood-oxygen-level-dependent (BOLD) fMRI imaging, reflects the interplay between cerebral blood flow (CBF), cerebral blood volume (CBV) and metabolic rate of oxygen

consumption (MRO_2C).

According to the classical model, a linear relationship subsists between CBF, MRO_2C, metabolic rate of glucose consumption and brain activity. Although this is plausible during resting state, when focal neural activation occurs a more recent theory (feedforward control) states that only MRO_2C remains linearly correlated to neural activity and in particular to synaptic activity [17]. BOLD signal is considered to arise from a linear coupling between neural activity and MRO_2C and from a more complex coupling with CBF. During focal neural activity, CBF increases in excess of MRO_2C, thus the rate of oxygen reaching the cortex exceeds its consumption rate, resulting in an increased ratio of oxygenated to deoxygenated hemoglobin. Since the former is diamagnetic and the latter paramagnetic, the higher ratio augments the MR signal, producing the BOLD response.

Recently, it emerged how astrocytes participate in the neurovascular and neurometabolic coupling. In fact, astrocytes are closely connected to both synapses and vessels, creating a neurogliovascular unit which has an impact on the neurometabolic coupling. Interestingly, studies on rat brain showed that, even at resting state, glucose consumption is similar between astrocytes and neurons, despite the much higher energy demand of the latter, compared to the former. A possible explanation is that glucose, in astrocytes, is primarily metabolized through the less efficient pathway, glycolysis, while neurons would use the oxidative pathway and tricarboxylic acid cycle, generating more adenosine triphosphate, given the same amount of glucose. Moreover, it has been hypothesized that the lactate produced by glycolysis would be shifted from astrocytes to neurons, and, converted to pyruvate, would enter the tricarboxylic acid cycle as well. This mechanism, called astrocyte-neuron lactate shuttle, is, in turn, modulated by synaptic activity and in particular, by glutamate release.

In the feedforward control hypothesis, focal activity and in particular glutamate also induces an increase in CBF through both a neuronal and an astrocytic pathway which induce vasodilation, using different cascades and mediators. The neurovascular coupling is modulated by the balance between the two pathways and other regional and central processes. This complex modulation underlies the variable and non-linear coupling between synaptic activity and CBF. However it does not explain the disproportionate rise in CBF relative to MRO_2C, the conditio sine qua non to have BOLD signal. A possible explanation for the increase in CBF to be much higher than what apparently needed would be to constitute a reserve in case of activity-related hypoxia.

The complex relationship between neural activity and metabolic or vascular processes suggests that the BOLD signal is causally better correlated with the integrated synaptic input activity rather than with the spike output activity and in a complex way, depending on the afferent input, on the target neuronal subpopulation and on the vascular response. However, correlation between BOLD signal and spike output activity has been also reported.

BOLD signal is measured using a T2*-weighted sequence. When a radiofrequency pulse is applied, a transverse magnetization is obtained which rotates in the transverse plane at the Larmor frequency and induces an MR signal in the radiofrequency coil. The decay of the transverse magnetization (or relaxation) starts as protons begin going out of phase. The characteristic time representing the decay of the signal by 1/e is called T2 relaxation time and 1/T2 is the transverse relaxation rate. Transverse relaxation is mainly related to intrinsic field caused by adjacent protons and thus reflects the interactions at atomic and molecular levels. Additional dephasing fields arise from local field inhomogeneities and its characteristic time is the T2* relaxation. In gradient echo sequences the latter is a combination of T2 relaxation and relaxation caused by local magnetic

field inhomogeneities, as expressed by:

$$\frac{1}{T2^*} = \frac{1}{T2} + \gamma \Delta B_{inhom}$$

or

$$\frac{1}{T2^*} = \frac{1}{T2} + \frac{1}{T2'}$$

where $\frac{1}{T2'} = \gamma \Delta B_{inhom}$, ΔB_{inhom} is the magnetic field inhomogeneity across a voxel and lambda is the gyromagnetic ratio.

Deoxyhemoglobin is paramagnetic thus perturbing the surrounding magnetic field, while oxyhemoglobin, containing unpaired electrons, is diamagnetic with no perturbation effects. Briefly, the magnitude of the resulting local field perturbations is proportional to intravascular oxygen saturation and to the strength of the external field:

$$\Delta B_z \propto [dHb] x B_0$$

After a radiofrequency excitation, the signal decay occurs faster with higher levels of deoxyhemoglobin. As aforementioned, the level of deoxyhemoglobin is affected by CBF, MRO2C and CBV. During brain activation, the increase in CBF is much higher than the increase of MRO_2C and the effect of CBV is relatively small. Therefore, the result is a net decrease in the level of deoxyemoglobin, in turn resulting in a slower rate of T2* relaxation and a higher T2*-weighted signal.

The relative signal change between the baseline and the activation condition can be expressed by:

$$\frac{\Delta S}{S_0} = \frac{S_a - S_0}{S_0} = \frac{S_a}{S_0} - 1 = \frac{e^{-R^*_{2(a)} \cdot TE}}{e^{-R^*_{2(0)} \cdot TE}} - 1 = e^{-\Delta R^*_2 \cdot TE} - 1 \approx -\Delta R^*_2 \cdot TE$$

where S_0 and S_a are the signals in the baseline and activated conditions,

respectively, $R^*_{2,(0)}$ and $R^*_{2,(a)}$ are the baseline and activated relaxation rates, respectively, $\Delta R^*_2 = R^*_{2,(a)} - R^*_{2,(0)}$ and the (linear) approximation applies because ΔR^*_2 is small.

Therefore, the fractional change in T^*_2-weighted signal is proportional to the absolute change in T^*_2 relaxation rate. In fact, in the total transverse relaxation rate R^*_2, the intrinsic T2 relaxation is fixed and the change in R^*_2 depends only on the perivascular field perturbations. Relaxation due to spatial magnetic field perturbation is, in turn, proportional to the magnitude of such perturbation ΔB_z and to the vascular volume fraction

$$R'_2 \propto \Delta B_z \cdot V$$

.

Since

$$\Delta B_z \propto [dHb]B_0$$

the relaxation rate is directly proportional to the deoxyhemoglobin concentration, the vascular volume fraction and the magnetic field strength is given by:

$$R'_2 \propto [dHb]B_0V$$

.

However, by including the diffusion effect (for which each spin samples a wide range of fields around vessels modifying its phase history) and the effect of intravascular spins, the model is described now by:

$$R'_2 \propto ([dHb]B_0)^\beta V$$

Assuming that the arterial oxygenation saturation is 100 % and thus that the

fractional deoxygenation is equal to the oxygen extraction fraction (E):

$$R_2' \propto ([Hb] \cdot E \cdot B_0)^\beta \cdot V$$

.

Therefore,

$$\Delta R_2^* = \Delta R_2' = R_{2,(a)}' - R_{2,(0)}' \propto (B_0[Hb]E_0)^\beta V_0[(\frac{E_a}{E_0})^\beta(\frac{V_a}{V_0}) - 1]$$

.

Since E is related to CBF by $E = \frac{MRO_2C}{(CBF \cdot [O_2]_a rt)}$,

$$\frac{E_a}{E_0} = \frac{\frac{MRO_2C_{2,(a)}}{MRO_2C_{2,(0)}}}{\frac{CBF_a}{CBF_0}} = \frac{m}{f}$$

where m and f are the MRO_2C and CBF normalized to their baseline values. Similarly, as the normalized blood volume $v = \frac{V_a}{V_0}$, substituting it into the fractional BOLD signal changes the expression into:

$$\frac{\Delta S}{S_0} = M\Big[1 - v\Big(\frac{m}{f}\Big)^\beta\Big]$$

where

$$M = k \cdot TE \cdot V_0 \cdot (B_0[Hb]E_0)^\beta$$

.

The constant M: 1) sets a ceiling on BOLD effect e.g. the limiting case in which CBF increases so much compared to MRO_2C and CBV that the baseline deoxyhemoglobin is all washed out, 2) is dependent on vessel geometry, total baseline deoxyhemoglobin content and MR parameters (TE and B0). At 1.5 T, M values have been found to be 0.08, thus giving a theoretic maximal BOLD

effect of 8%. Lastly, the Davis model includes an empiric power law relationship between CBF and CBV, resulting in:

$$\frac{\Delta S}{S_0} = M[1 - f^{\alpha-\beta} m^{\beta}]$$

.

In conclusion, with an empirical value of M=8%, n=2-3 and an increase in CBF of 50%, the model predicts a BOLD signal change of 0.8-1.5%.

The BOLD response after a neural impulse is dispersed over seconds and this accounts for the poor temporal resolution of the fMRI. The function describing it, the hemodynamic response function (HRF), presents an initial dip in the curve which reflects an initial increase in deoxyemoglobin and has been inconsistently observed. Then, CBF rises and so does the BOLD signal, reaching the peak in about 5-6 seconds and then decreasing towards baseline at about 10 seconds and lastly falling below baseline with an undershoot whose origin is uncertain. A general linear model (GLM) is applied to the statistical analysis of fMRI data, decomposing the signal y (vector of voxel signal measurements at the sampled time points) into the model estimate $y = \beta X$ and the residual error e, resulting in:

$$y = \beta X + e$$

where y ($y_1 ... y_n$) are the observed time series for each voxel, X is the design matrix, containing the exploratory variables and η are the residuals. [17]

2.2.1 Task functional MR imaging

Task-based fMRI is used to evaluate the variation in the BOLD signal during a task condition compared to a control condition. There are two different designs used: block design and the event-related design. In the block design activation

and control conditions alternate, each lasting a time interval of about 15-30 seconds, called block. During the activation block the subjects perform an action (generally a motor or cognitive task) continuously. Advantages are the simplicity and the power for detection of the activation response. In fact, the hemodynamic response over each activation block is summed, resulting in a relatively high BOLD signal-to-noise ratio.

2.2.2 Resting state functional MR imaging

Functional MR imaging at rest, in absence of external stimuli, is referred to as resting state fMRI. At baseline, neural activity accounts already for the 20% of body energy consumption and activation induces only a small increase in this consumption, e.g. for stimulation of the visual cortex it is estimated between the 5% [18] and 15% [19], depending on the task. Moreover, thalamo-cortical synapses represent only a small fraction of all synapses, the majority consisting of ones between non-primary areas neurons which support the activity at rest.

A correlation between time courses of low frequency fluctuations in different brain regions was found by Biswal et al. in 1995 [20]. Since then, resting state fMRI (rs-fMRI) has been widely used and applied to study brain activity at rest, with a continuous development of different methods of analysis.

The advantages of rs-fMRI, in particular when applied to patients with neurological or psychiatric conditions, is its independence on the ability of the patient to understand the instructions and perform a specific task. The most used rs-fMRI design consists in asking the subjects to keep their eyes closed, not to think about anything in particular and not to fall asleep.

Resting state fMRI activity can be measured, in specific areas, with the amplitude of low frequency fluctuations (ALFF) or with the regional homogeneity (ReHo). Instead, the resting state functional connectivity (rs-FC) between dif-

ferent areas of the brain can be measured using the functional connectivity density analysis, the seed-based functional connectivity, the independent component analysis method or the graph analysis[21]. In the latter, brain connectivity is intended as networks of brain regions connected by functional associations [22]. Consistent functional resting state networks are observed in studies on healthy subjects [23].

Differences in rs-FC between task and rest can be subtle but still detectable. Cole et al. showed that up to 38% of connections differ significantly between rest and task. However, compared to rest, the task condition differs in several ways: within-network connectivity decreases during task periods; changes in across-network connectivity is observed during task in both an increased and reduced direction; reorganization of the hubs during task; the contribution of frequencies within the 0.01-0.1 Hz changes, with a more balanced contribution of all frequencies during task; ReHo, reflecting local rs-FC, is reduced during task; moment-to-moment fluctuations in rs-FC are more stable during task than rest; the variability of the dynamics of inter-network connectivity increases with age at rest while during task is higher in younger subjects; a higher global integration state is observed during task. [24].

2.2.3 Functional MR imaging preprocessing

The fMRI preprocessing includes multiple steps which can be performed using different software available or automated preprocessing pipelines that have been implemented, although the use of different pipelines and the order of the preprocessing steps have been showed to affect the results. Here are reported the main steps: [25].

- Initial stabilization: when the sequence acquisition starts, the scanner takes some seconds to completely stabilize its gradients and the tissues require

few seconds to reach the necessary excitation. For this reason, usually the first volumes acquired are discarded from the analysis.

- Slice timing correction: since the fMRI is a 2D sequence there is a delay between the acquisition of the first and last slice, which depends on the TR. The slice timing correction adjusts the time course at each voxel level, interpolating the information in each slice to match the one of the reference slice (usually the first or the mean one).

- Motion correction: head motion is a major issue in fMRI data and it has been addressed with several methods. A classic one is to realign each volume to a reference one using a rigid body transformation. It has been suggested to discard volumes which present a motion range greater than a single voxel dimension. Other methods to reduce motion artifacts are: expansion to 24 or 36 motion parameters regression, independent component analysis denoising and scrubbing, the latter based on framewise displacement.

- Spatial transformation: consists in the alignment of the functional data to another sequence, usually to the anatomical one or to a standard space. Linear and nonlinear transformations or surface registration techniques are available.

- Spatial smoothing: in this step data points are averaged with the neighbors, increasing the signal to noise ratio but reducing the actual spatial resolution. The spatial smoothing is achieved by convolving the fMRI signal to a Gaussian function of a specific width. Typical smoothing values range from 5 to 8 mm.

- Temporal Filtering: consists in removing the effect of confounding signals with known or expected frequencies, fMRI data are usually filtered using a

high pass filter (0.008-0.01 Hz) for task fMRI and band pass filter (usually 0.01-0.08 Hz) for rs-fMRI.

2.2.4 BOLD signal variability

Brain activity has been showed to vary from moment to moment. This variability has been detected at different level, from a single neuron level to networks oscillations. The interpretation and biological meaning of variability in brain function is still unknown. It has been typically regarded as noise but recently its role in better unveiling brain functioning has emerged [26]. An hypothesis is that brain variability could derive from coherent spontaneous oscillations throughout the cortex [27] and therefore BOLD signal variability may reflect functional connectivity between brain regions and in particular the dynamic range of FC, with a greater dynamic range allowing a better adaptability and efficiency of neural systems.

Temporal signal variability reflects the magnitude of moment-to-moment variability in a fMRI time series. It can be measured as variance, standard deviation and mean square successive differences.

A higher variability of brain signals has been associated with a better behavioral performance, it's low during resting state, increases during internally focused tasks and is highest during externally focused tasks [28]. BOLD signal variability has been shown to change across lifespan but results are divergent with some studies finding a u-shaped lifespan developmental curve, increasing from infancy to young adulthood and then decreasing to elderly [29] while others differentiating the course based on the brain regions, with most of the networks showing a decrease of variability across the lifespan [30]. Brain signal variability has been applied to neurological and psychiatric disorders with discordant results on schizophrenia and Alzheimer disease but more consistent results in other dis-

eases such as traumatic brain injury and autism, pointing towards a decreased variability in patients compared to healthy subjects.

2.2.5 Dynamic functional connectivity

Functional connectivity has been showed to vary over time, with fluctuations occurring within time scales of seconds to months [31; 32; 33]. However, the ones that received more attention are changes happening over seconds and therefore detectable within a standard rs-fMRI acquisition. Numerous approaches have been recently proposed to better capture FC dynamic. The classic sliding window method is based on the choice of a temporal window to segment the timecourses and on the comparison of the FC obtained within single windows. The sliding window approach has some of limitations, such as the appropriate choice of the window length and the different measures to assess the FC within the window. Moving from a sliding window analysis towards an observation of single frames and retaining only the significant time points, e.g. over a certain threshold, a point process analysis (PPA) [34] was developed, according to the hypothesis that meaningful information could be retrieved from short periods of time. Similarly, co-activation-patterns (CAP) [35] select the time points only within the seed while maintaining the non-thresholded timecourses at the selected timepoints for temporal clustering. A further step involved the computation of whole-brain co-activation patterns based on transients in fMRI signal, rather than using peaks, leading to innovation-driven co-activation-patterns (iCAPs) [36]. The latter, compared to CAPs, indicate brain regions which simultaneously activate or deactivate, but without information about the direction [37].

2.3 Diffusion Tensor MR Imaging

Diffusion MR imaging of the brain has been applied since the early 1990s, with striking consequences on the early diagnosis of stroke and, in 1994, the use of diffusion tensor for MR imaging was proposed by Basser [38]. Diffusion tensor imaging is sensitive to cellular structure, measuring the diffusion of water molecules. Brownian motion is the constant random molecular motion due to heat. At a fixed temperature the diffusion rate can be described by:

$$< r^2 >= 6Dt$$

where $< r^2 >$ refers to the mean squared displacement of the molecules, t is the diffusion time, and D is the diffusion coefficient, a constant of proportionality for the particular substance being measured. Among the several methods for modelling diffusion in biological systems, the simplest one would be to assume free diffusion. However, the diffusivity measured in clinical setting depends on experimental parameters (in particular the diffusion time that for clinical diffusion-weighted imaging is 10-50 ms) and on the sample, therefore the term apparent diffusion coefficient (ADC) has been introduced [39]. The diffusion measured in tissues is not the same in all directions (anisotropic) and reflects the microscopic tissue heterogeneity [38].

A diffusion-weighted pulse sequence is built adding a pair of diffusion-sensitizing gradients, known as motion-probing gradients, to a T2-weighted spin-echo sequence. The gradients are applied along the same directional axis before and after the 180° refocusing pulse, a procedure known as the Stejskal-Tanner diffusion encoding [40]. The MR signal (S) depends on the diffusion coefficient (D),

repetition time (TR) and echo time (TE) according to the following equation [41]:

$$S = PD(1 - e^{-TR/T_1})e^{-TE/T_2}e^{-bD}$$

where PD is the proton density, T_1 and T_2 the signal relaxation times after excitation which are related to the tissue properties and b is the diffusion-weighting parameter. The b factor depends on the strength, duration and temporal spacing of the diffusion-sensitizing gradients, according to:

$$b = \gamma^2 G^2 \delta^2 (\Delta - \delta/3)$$

where λ is a constant (gyromagnetic ratio), G the amplitude of diffusion gradient, delta is the duration of each diffusion gradient, Delta is the interval between the onset of the of the diffusion gradient before the refocusing pulse and that after the refocusing pulse. Typical b values used in clinical applications range from 600 to 1500 seconds/square millimeter. The increase in b values determines an increase in the degree of diffusion-weighting, as well as an increase of G and delta. ADC values can be thus derived:

$$ADC_i = \frac{-\ln\left(\frac{S_i}{S_0}\right)}{b}$$

where S0 is the signal intensity in the absence of diffusion-sensitizing gradient, derived from an image acquired at b=0 s/mm3. ADC maps can be thus derived using a set of diffusion-weighted images acquired at high b factor and a second set acquired at a lower b factor. Applying the two diffusion-sensitizing gradients, S_1 can be calculated by:

$$S_1 = PD(1 - e^{-\frac{TR}{T_1}}e^{-\frac{TE}{T_2}}e^{-b_1 D}) = S_0 e^{-b_1 D}$$

$$S_1 = PD(1 - e^{-\frac{TR}{T_1}} e^{-\frac{TE}{T_2}} e^{-b_2 D}) = S_0 e^{-b_2 D}$$

The ratio

$$\frac{S_2}{S_1} = e^{-(b_2 - b_1)D}$$

leads to

$$D = \frac{-\ln\left(\frac{S_2}{S_1}\right)}{b_2 - b_1}$$

The first pulse causes the water molecules to resonate and when it ends the molecules will be out of phase. The second pulse causes a phase refocusing and if, in the meantime, the molecules have moved, the phase refocusing would fail causing a signal loss. The refocusing process is linked to the strength of the gradient pulse and to the interval between the two pulses. Pure water at body temperature shows an isotropic diffusion and in human brain an isotropic diffusion can be found at the CSF level. Instead white matter is characterized by tightly packed coherently oriented fiber bundles thus hindering water displacement perpendicular to the direction of the fibers, resulting in higher ADC_i values parallel to the fibers than perpendicular to them. It's noteworthy that diffusion measurements detect water motion only along the applied gradient axis. Combining the gradients along the three axes ADC can be measured along any orientation. However, measurements along the X, Y and Z axes are not enough because fiber orientation is almost always oblique to the axes, so theoretically measurements along thousand of axes should be made. To simplify this the concept of diffusion tensor was introduced, fitting the measurements along different axes to a 3D ellipsoid [41]. The properties of this ellipsoid, e.g. the length of the longest, middle and shortest axes (eigenvalues lambda 1 2 3) and their orientation (eigenvectors) can be defined by 6 parameters. The measurements of ADC along 6 axes are enough

to obtain the ellipsoid. In this way the degree of diffusion anisotropy can be obtained by:

$$(\lambda_1 - \lambda_2)^2 + (\lambda_1 - \lambda_3)^2 + (\lambda_2 - \lambda_3)^2$$

and if diffusion is isotropic e.g. $[(\lambda_1 = \lambda_2 = \lambda_3)]$ this measure becomes 0 while large numbers indicate high diffusione anisotropy. One of the most used metrics of diffusion anisotropy is the fractional anisotropy (FA), defined as

$$FA = \sqrt{\frac{1}{2}} \frac{\sqrt{\left((\lambda_1 - \lambda_2)^2 + (\lambda_2 - \lambda_3)^2 + (\lambda_3 - \lambda_1)^2\right)}}{\sqrt{\lambda_1^2 + \lambda_2^2 + \lambda_3^2}}$$

A decrease in FA value is associated with white matter disruption.

2.4 Gait and balance

Locomotion is one of the most important sensori-motor behaviors in humans. The act of standing and walking requires coordination of the limbs and muscles, a multi-sensory integration, and robust control mechanisms.

The start of the alternating muscle activity and the locomotor rhythm are produced by spinal neural networks called central pattern generators (CPGs) [42], even in absence of afferent or descending projections. However, a complex sensori-motor dynamic interaction is needed during walking and the CPGs are controlled by both central commands and proprioceptive feedback [43; 44]. This dynamic sensori-motor interaction is recognized as fundamental in shaping the CPG function, particularly in guiding post-lesional plasticity mechanisms [45]. Components of this interaction system include: 1) cutaneous inputs which have a role in facilitating or inhibiting locomotion but, in particular, are involved in the correct positioning of the limb during normal locomotion or after perturbations;

2) muscle afferents to modulate the timing of the step cycle, the duration of the subsequent phases of the cycle and the amplitude of muscle activation during each phase; 3) joint afferents (discharge at knee level has been showed by Loeb et al. during movement and stance [46]); 4) the mesencephalic and diencephalic locomotor region, which are sites of sensori-motor integration, and other parts of the brainstem including vestibular nuclei, medial longitudinal fascicle, reticular pathways; 5) cerebral cortex and cerebellum [47].

The musculoskeletal and biochemical mechanisms involved in gait are well studied and used in rehabilitation protocols; however the underlying neural control organization, necessary for a stable gait, in particular at the supraspinal level, is less clear in humans. The difficulty in studying supraspinal control mechanisms during gait relies in the assessment of the neuronal processes during movement.

Cortical activity during gait has been recorded with functional near infrared spectroscopy (fNIRS) [48], electroencephalography (EEG)[49] and single photon emission tomography [50], showing an increased activation in the primary sensorimotor regions (M1/S1) and in the supplementary motor area (SMA), the involvement of a fronto-posterior cortical network and of sub-cortical structures. Further, it was demonstrated that bilateral cortical activity in M1/S1, anterior cingulate cortex (ACC) as well as in the parietal cortex is dependent on the gait cycle phase [51]. Studies with functional Magnetic Resonance Imaging (fMRI) have been performed in healthy subjects during the execution of single-joint movement of the lower limbs to mimic walking; they found an involvement of M1/S1, of the secondary somatosensory cortex (S2), and SMA, cerebellum and the basal ganglia (i.e., the putamen) [52; 53; 54; 55; 56]. A recent study with a MR compatible stepping robot found an activation of several cortical and sub-cortical areas of the sensorimotor network, with higher relative activation of those areas during active movement than during passive movement [57].

During still standing, the position of the center of gravity (COG) or center of mass (equal in this context) must be maintained vertically over the base of support. During quiet standing the body center of mass is approximately located at the level of the sacral vertebrae and positioned in front of the ankles. The upright posture is unstable due to gravity, breathing, heart rate and intrinsic noise in the motor and sensory system. The state of someone's balance is described in terms of angular displacement of the center of gravity from the gravitational vertical. The neural processes for determining the center of gravity position and for moving it are highly integrated but a coarse separation can be made into sensory and motor processes. When the first is affected, the position of the COG relative to the base of support is not accurately sensed. Instead, when the motor component is affected, the automatic movements required to bring the COG to a balanced position are not timely or effectively coordinated. In the "sensory processes" locution we intend, here, the combination of visual, vestibular and somatosensory (tactile, deep pressure, position sense and kinesthetic movement sense) input components. Thus, the integration of somatosensory inputs (providing information on the orientation of the body parts relative to one another and to support surface), the vestibular inputs (providing gravitational, linear and angular accelerations of the head in space) and the visual inputs (providing the position and orientation of the body in relation to surrounding space and objects) is needed to guarantee the balance ability. Moreover, in case of conflict of sensory inputs, brain must select the one providing the more accurate information and ignore the misleading ones [58]. Regarding the motor process, multiple components as the myotatic strech reflex and both the spinal cord and cortical control of the legs and trunk muscles, muscle spindles and tendons are involved. Different biomechanical models have been proposed to describe the complex integrated process that allows postural control, among them the inverted pendulum model [59]. In neurological disease,

balance disorders can derive from motor weakness, altered muscular tone, sensory loss, perceptual deficits and altered spatial cognition with reference to the postural body scheme. Focusing on the somatosensory cues contributing to balance, inputs derive from muscles, joints and skin receptors. In particular, muscle length and velocity are encoded by primary and secondary afferents innervating muscle spindles, the active muscle force production is recorded and provided by the Golgi tendon organs; lastly the dynamic skin deformation and skin vibration are encoded by fibers innervating the Meissner and Pacinian corpuscles, respectively, while the skin indentation and static skin stretch information are provided by afferents originating from Merkel and Ruffini cells, respectively. [60] Lower limbs somatosensory information is the most sensitive, among sensory inputs, in detecting whole body sway. [61]

2.4.1 Proprioception at the lower limbs

In 1906, the English neurophysiologist Sir Charles Sherrington coined the term "proprioception" to give a term for the sensory information derived from receptors embedded in joints, muscles and tendons that enable a person to know where parts of the body are located at any time. He defined it as "the perception of joint and body movement as well as position of the body, or body segments, in space" [62].

Proprioception is classically comprised of both static (i.e. joint position sense) and dynamic (i.e. kinesthetic movement sense) components. Following the early observations of Sherrington (1906), the proprioceptive feedback has been found to derive from muscle spindles, mediating the conscious perception of movement and limb position; moreover cutaneous and joint mechanoreceptors are also important for determining the position of distal body segments and/or signaling extremes in range of motion.[63] For the execution of functional movements in daily activities, exercise, and sports, central processing receives proprioceptive

information from a variety of mechanoreceptors, which need to be integrated. To examine proprioceptive mechanisms, three main testing techniques are reported in the literature: threshold to detection of passive motion (TTDPM), joint position reproduction (JPR), also known as joint position matching, and active movement extent discrimination assessment (AMEDA). [64] Differences in these tests exist since they have been developed from different concepts, are conducted under different testing conditions, and assess different aspects of proprioceptive modalities.

These three techniques to assess proprioception refer to three classical methods used in psychophysical experiments: the method of adjustment, the method of limits and the method of constant stimuli. In the method of adjustment, also known as the method of average error, the participant is required to control the level of the stimulus, starting with a level that is clearly less or greater than a reference stimulus, and then to adjust the level until they feel that the level of the stimulus is the same as the level of the reference stimulus. The difference between the adjustable stimulus and the reference one is recorded as the participant's error, and the average error is calculated as the measure of sensitivity. The current JPR proprioception test protocol is one form of the method of adjustment, where participants are usually asked to match or reproduce the previously experienced reference joint positions, using their ipsilateral or the contralateral limb.[64]

The JPR testing method is conducted under either passive or active conditions for criterion and reproduction movements. There are three types of JPR tasks described in the assessment of proprioception: ipsilateral JPR; and two contralateral JPR approaches. For the ipsilateral testing, a predetermined target joint position is passively or actively presented to the participant for a few seconds; then, the joint is returned to the initial start position, either passively by the experimenter or actively by the participant. Participants are then required

to reproduce the target joint position previously experienced by either indicating the target position by pressing a stop-button when the joint is passively moved into the same range, or by actively moving the joint to the target position. Therefore, in the ipsilateral test, participants need to remember the target position and reproduce the position using the same limb. In the contralateral tests, one procedure is identical to the method for ipsilateral testing in terms of experiencing the target joint position, but differs in that the participant is asked to reproduce the joint position by using the contralateral limb; in this case, participants need to remember the target joint position and use the opposite limb to reproduce the position. The second contralateral test differs in that once one joint is moved to the target position, it remains in that position and the contralateral limb is required to reproduce the target joint position; this test does not require a memory of the target position, but participants can use the information in the position task to help them to replicate the position on the contralateral side.

The ipsilateral and contralateral tests differ since participants use also other networks for central processing. In fact, in the ipsilateral matching tasks, where the same arm serves to establish both the reference and matching locations, it is inherently necessary to use memory in order to accurately match the target position; in this situation, when the test is used in clinical practice, the error in performing the task could reflect cognitive or memory deficits, rather than any decrease in proprioception itself. In the contralateral matching tasks on the other hand the reference joint angle is available throughout the task from the opposing limb and the use of memory is not required. However, contralateral position matching tasks are subject to other limitations: due to the involvement of both arms in the task, it is difficult to ascertain whether the measured error arises from the reference arm, the matching arm, or both; additionally, based on the anatomical pathways involved in the transmission of peripheral proprio-

ceptive input to the brain, it is almost certain that matching using the opposite limb requires greater interhemispheric communication compared with ipsilateral matching. Bilateral matching tasks have shown higher matching error magnitude with respect to unilateral task both for the upper [65; 66] and lower limbs [67].

Goble et al. found that the non-dominant arm has an advantage in proprioceptive position matching tasks. In a study where both left-handed and right-handed healthy subjects performed an elbow position matching task, they showed that matching was more accurate by the non-preferred arm and that the magnitude of arm asymmetry favoring the non-preferred arm also was relatively increased with greater cognitive demands. Specifically, although preferred arm errors were progressively larger when comparing the contralateral condition with the ipsilateral and contralateral remembered conditions, non-preferred arm matching errors were similar in magnitude across all tasks. In a follow-up study involving also visual matching, it was shown that non-preferred arm position matching advantages were evident only in the proprioceptive version of the matching experiment [65; 68; 69].

There is currently evidence in the literature that enhanced non-preferred left arm matching is linked to a right hemisphere specialization for the processing of proprioceptive inputs.[70; 71] Besides the studies by Naito, also Ben-Shabat et al. showed the activation of the right supramarginal gyrus during matching tasks with both non-dominant and dominant wrist and suggested a right hemisphere dominance for upper limb proprioception [72]. The proprioceptive asymmetry in the upper limb is associated with differences in performance and control strategies between the two arms [73; 74].

The different limb specialization in everyday life activities could either induce or reinforce different brain activation patterns in the two hemispheres during both motor and proprioceptive tasks [75; 76]. Some studies suggested that foot later-

alization may be a better indicator than handedness to study brain lateralization since the feet were less biased by use-dependent motor behavior than the upper limbs [77; 78].

A clear relationship exists also between the target amplitude and the magnitude of matching error, with further targets inducing greater matching errors; in fact, participants make smaller errors when matching a reference position that is established through their own active movement, rather than the same target position determined passively by the experimenter [79]. This effect is thought to be the consequence of 2 movement-related features: 1) the sensitivity of muscle spindles (key proprioceptors) is enhanced during active movements via the gamma motor system 2) an "efferent copy" of the motor command used to get to the target position may be called upon to inform subsequent matching movements. Another point of concern for clinical researchers is the "tau effect." The tau effect manifests as a strong interdependence between time and space, such that movements of longer duration are perceived as traveling farther than those of shorter duration. For position matching experiments, this finding implies that, if during the establishment of the target joint angle an experimenter takes a long versus a short amount of time, the participants will perceive the target as being further from the starting joint angle than it actually is [66].

Despite the impact of lower limb position sense on everyday life activities such as posture control and gait the neural correlates of proprioception have received little attention. To date, two studies have investigated the neural basis of lower limbs proprioception by focusing on proprioceptive-related activity elicited by vibro-tactile stimulation; authors found cluster of neural activity, in response to muscle-spindle stimulation, in the bilateral inferior parietal cortex, inferior frontal gyrus, supplementary motor area, anterior insula, basal ganglia and thalamus; right hemisphere-specific activations were seen in ventral premotor

area, orbital frontal cortex, dorsolateral prefrontal cortex (BA 9/46), and dorsal anterior cingulate [80; 81]. Although muscle spindle vibration could induce a proprioceptive illusion [82], no studies focused on the cortical activation induced by specific position sense tasks.

2.4.2 The role of the ankle

The analysis of ankle dorsiflexion has been suggested as a potentially practical way to assess the integrated cortical, subcortical, and spinal sensori-motor network involved with gains in skillful walking [83].

In fact, an appropriate control of the ankle joint is necessary for maintaining the standing posture,[84] for the foot clearance during the swing phase and the push-off at the terminal stance of gait.

Moreover the ankle dorsi-flexion has been used to assess the supraspinal sensori-motor network and to evaluate the effects of rehabilitation training also in neurological diseases, as stroke.[52] Previous fMRI studies showed that during active (i.e., movement generated by the participant) or passive (i.e., movement generated by an experimenter or an actuated external device) single-joint movements of the ankle an activation of M1/S1, secondary somatosensory cortex (S2), and SMA is observed. Subcortical activations were seen in the cerebellum and the basal ganglia (i.e., the putamen). Generally, it has been found that passive movements, when compared to active ones, elicit weaker peak activations in the subcortico-cortical sensori-motor network and increased activation in the ACC, in the precuneus and in the right premotor cortex [52; 55; 56; 83]. In the study of Dobkin et al. the motor learning related to active ankle dorsi-flexion in both a healthy subjects and a small group of stroke patients during a course of locomotor rehabilitation was assessed. The stroke patients had fewer activated voxels in the contralateral sensori-motor cortex for active ankle dorsi-flexion compared with

the healthy group, potentially indicating fewer available cortical motor neurons for the task. After 2–6 weeks of rehabilitative therapy the number of activated voxels during active task was shown to increase within the contralateral sensorimotor and cingulate motor cortex, with this increase being correlated with motor performance [52]. In patients with MS recent studies found that a reduced push-off due to insufficient ankle plantar-flexion force production strongly contributes to gait disturbances [85; 86].

The behavioral aspects of proprioception at the level of the ankle has been studied [87], showing that the accuracy and precision of ankle joint position sense decrease with aging [88] and fatigue [89].

2.5 Multiple sclerosis

Multiple sclerosis (MS) is defined as a chronic immune-mediated, demyelinating disease of the central nervous system.

2.5.1 Classification

The most common form is relapsing-remitting multiple sclerosis and affects about 85% of patients; the onset, in this case, is characterized by an acute episode of neurological deficit (clinically isolated syndrome (CIS)) lasting at least 24 hours and in most cases interesting the optic nerve, brainstem, spinal cord or cerebellum, followed by a remission period of clinical recovery. The clinical course of relapsing remitting (RR) MS is typically marked by recurring relapses and remissions; relapses are characterized by focal inflammation and demyelination in the CNS. Approximately 15-30% of these patients develop secondary progressive (SP) MS, over a long-term follow-up. About 10-15% of patients with MS are diagnosed with primary progressive (PP) disease, which is characterized by a progressive

disability from the outset and the absence of relapses. A new phenotype description has been introduced, for the three forms (RR, PP and SP), which further subdivide them according to disease activity and progression.[90]

2.5.2 Epidemiology

Multiple sclerosis is the most common demyelinating disease seen in high-income countries, and the main cause of non-traumatic chronic disability in young adults, with the average age at diagnosis being 30 years [91].

Prevalence and incidence. The global prevalence of MS has been estimated, in 2016, as 30.1 cases per 100000 population. Age-standardised prevalence has increased from 1990 to 2016, in particular in east Asia and Canada. The highest estimates have been registered in high-income North America (164.6), western Europe (127.0) and Australasia (91.1) while the lowest in eastern and central sub-Saharan Africa (3.3 and 2.8, respectively) and Oceania (2.0). In a recent systematic analysis, a significant association was found between prevalence and both latitude and the socio-demographic index [92]. The constant increase in MS prevalence [92] [93] is probably due to concomitant factors: the higher rate in survival, the higher incidence and the improvements in the diagnosis, with an easier access to medical facilities and the revisions of McDonald Criteria. [93] The global median incidence of MS is 2.5 per 100000 [94], with higher rates in Europe (3.8), Eastern Mediterranean (2), Americas (1.5), Western Pacific and Africa. Early epidemiological studies and reviews reported a north to south and a high- to low-income gradient in MS prevalence. However, despite the differences among continents, the traditional view of a latitudinal gradient has been questioned, in particular in Europe and North America, where, when considering the incidence instead of prevalence, no correlation is found with latitude.[95]

Gender ratio. At the beginning of the last century MS was considered a

disease affecting predominantly males. However, in the last decades the gender ratio (female:male) showed an increase in both Europe and Canada, where it changed from 1.9 between 1936 and 1940 to 3.2 for patients born between 1976 and 1980 [96]. Gender ratio negatively correlates with latitude but increases with incidence and time [95]. Reasons to explain the increase in gender ratio over time could be the improvements in access to healthcare and the fact that there are more benign cases of MS in women, which are now being identified more quickly with the use of MR imaging and new diagnostic criteria.

Mortality. According to one published series [97], 70–88% of patients are still alive 25 years after clinical onset, and the median time from onset to death ranges from 24 years to over 45 years. The age-standardised mortality decreased from 1990 to 2016 by 11.5%, at a global level [92]. Factors associated with a better vital prognosis include a relapsing–remitting phenotype, MS clinical onset before 25 or 30 years of age, initial symptoms such as optic neuritis and sensory problems, a low level of disability during the first years of the disease, and a long time lag between the first and second neurological episode [98].

2.5.3 Risk factors

Multiple sclerosis does not have a single cause, with both genetic susceptibility and environmental exposure playing a role in the disease development.

Environmental risk factors. Multiple environmental factors have been associated with MS. In their umbrella review, Belbasis et al. examined the meta-analyses of observational studies, concluded that three risk factors showed a strong, consistent evidence of an association with MS with no suggestion of bias: immunoglobulin G (IgG) seropositivity to Epstein Barr virus (EBV) nuclear antigen; infectious mononucleosis; smoking. The association between the following risk factors and MS was found to be null or to have very small effect:

several vaccinations (tetanus, diphtheria, influenza, BCG, mumps, measles and rubella, poliomyelitis, hepatitis B virus, and typhoid fever), biochemical factors, presence of dental amalgam, past surgeries and traumatic events (tonsillectomy, adenoidectomy, and traumatic injury), and presence of allergies, eczema, and chronic cerebrospinal venous insufficiency. The authors also concluded that the evidence for low $25-(OH)-D$ levels to be a risk factor for MS is weak and deserves further studies [99].

Environmental factors could contribute to the disease development through different mechanisms such as molecular mimicry, generation of new autoantigens, release of segregated CNS autoantigens in the periphery or determining a pro-inflammatory environment. Two main mechanisms have been hypothesized to explain the role EBV could have in determining MS: according to the first one a reactivation of the virus within the CNS would activate B cells, while the second one implies a general dysregulation of the immune response.[100]

Genetics. Genetic factors play a main role in causing MS, as evidenced by the higher concordance for MS in monozygotic twin pairs (25.9%), compared to dizygotic ones (2.3%) [101]. The association between MS and variations in the genes encoding human leukocyte antigens (HLAs) within the major histocompatibility complex was first observed several decades ago. The HLA-DRB1 gene, and in particular the HLA-DRB1*15:01 allele common in European population, showed to have the strongest association with MS with an average odds ratio of about 3 for this allele [102]. MS patients carrying the DRB1*15:01 haplotype are more likely to be female and an earlier disease onset but it's not associated to disease severity or progression. Moreover, this haplotype is associated with presence of oligoclonal bands and IgG levels in the cerebrospinal fluid of MS patients. Instead, alleles which have a protective effect include class I HLA-A*02:01 and class II DRB1*14:01 [102]. More than 150 single nucleotide polymorphisms have

been associated with MS, in genes including the ones encoding for the α-chains of interleukin-7 and interleukin-2 receptors [100]. Probably, both central tolerance mechanisms and changes in the threshold of peripheral immune cell activation contribute to this genetically determined pathogenetic pathways. Recently, differences in the expression of genes involved in inflammatory and immunological pathways have been found between patients with mild relapsing-remitting MS and patients with primary progressive MS, further underlining the gap between these two clinical phenotypes of MS [103].

2.5.4 Pathogenesis

MS is considered, in the traditional way, an autoimmune inflammatory disorder affecting the CNS. The hallmark of the disease are focal inflammatory lesions, mostly perivenular [104], caused by the disruption of the blood-brain barrier, resulting in an infiltrate of lymphocytes, microglia activation, demyelination, axonal damage and, ultimately, alteration of the neuronal signaling.

In broad terms, MS develops in genetically susceptible subjects who occur to be exposed to environmental risk factors, triggering an autoimmune response against the CNS. The primum movens is still uncertain and disentangling the role inflammatory cells have in triggering or sustaining the pathological process is difficult. Two different models implicate that the immune response initiates in the periphery or in the CNS itself. In the former one, autoreactive T cells are activated in peripheral sites and then move to the CNS with activated B cells and monocytes. On the contrary, in the "CNS-intrinsic" model, events (i.e. viral infection or neurodegeneration) occurring within the CNS trigger the immune response, releasing CNS antigens in the periphery which secondly attracts autoreactive lymphocytes. Within this "central" model frame, some authors claim that MS is primarily a degenerative disorder and that inflammation is secondary

to neurodegeneration [105]. Observations supporting this hypothesis are, among others, the lack of effect of the available disease modifying drugs (DMD) on the primary progressive clinical phenotypes of the disease and the independence of the inflammatory relapse activity and the degeneration, as they were driven by two different processes [106]. According to this hypothesis, PP MS would be the primary disease and RR and SP phenotypes would represent variants with an abnormal inflammatory response. Instead, traditionally, neurodegeneration is considered as secondary to the both acute and chronic inflammation phase of the disease and PP MS a clinical variant with a feebler inflammatory component. In both cases, whether the process starts in the periphery or within the CNS, antigens released from the CNS reach the periphery and activate a further immune response and the invasion of CNS by lymphocytes. Microglia activation contributes to the initiation of tissue damage and to the protraction of the disease.

Inflammation is present at all stages of MS, but it is more pronounced in acute phases than in chronic phases. Perivenular inflammatory lesions are the ones characterizing the disease, showing an infiltrate of macrophages and CD8+ T cells, and a lower number of CD4+ T cells, B cells and plasma cells. Oligodendrocyte and demyelination occur as result of inflammation. In the progressive phase of the disease, the immune response is more confined to the CNS and tissue damage consist in diffuse demyelination, axonal injury, microglia activation and cortical involvement with the formation of tertiary lymphoid structures. This results in a more pronounced atrophy of the grey and white matter. Axonal and neuronal loss are the main responsible of the permanent clinical disability, axonal damage occurring both in the acute and later stages while neuronal loss is mainly due to the deficit of myelin trophic support and mitochondrial dysfunction.[100]

2.5.5 Pathology

The focal lesions are characterized by primary demyelination and astrocytic scaring, but also by axonal and neuronal injury and they affect not only in the white matter but also the grey matter, deep nuclei, brainstem and spinal cord. Remyelination to variable extent is present in focal lesions. Focal lesions can be distinguished in classical active lesions, chronic active or slowly expanding lesions with a low degree of demyelination and no major BBB damage and representing about 30% of lesions in patients in the progressive phase, inactive lesions and remyelinated shadow plaques.

Cortical lesions have been recently recognized as a major substrate of MS pathology but, in vivo, only the 10-15% of cortical lesions can be identified by MR imaging. Most lesions involve the cortex and the subcortical white matter (cortico-subcortical lesions) but also intracortical and subpial lesions have been identified. Subpial lesions are associated with meningeal inflammation and tertiary lymph follicles can be observed, especially in patients with SP MS and PP MS with rapid disease progression. Active cortical demyelination starts on surface with an outside-in gradient and is associated with a severe axonal and neuronal degeneration. Focal grey matter lesion and a diffuse neuronal loss interest also the deep gray matter nuclei since the early stages of the disease and their number and size only moderately increases over time.

Diffuse injury is found in the "normal appearing" white and grey matter, in particular in the progressive stage of the disease. In the white matter the injury consists of small perivascular inflammatory infiltrates, diffuse axonal injury, astrocytic scaring and microglia activation. However, the extent of the cortical demyelination is even more severe in the progressive stage, characterized by neuronal loss, thus driving additional axonal neurodegeneration in the white matter. [104]

2.5.6 Clinical features

Clinical onset and symptoms from relapses broadly vary, based on the spatial dissemination of lesions within the CNS and the degenerative process over time.

Common clinically isolated syndrome presentations include acute unilateral optic neuritis, a partial myelitis, or a brainstem syndrome.[107] On the contrary, the onset of primary progressive MS by contrast is characterized by slowly progressive symptoms, most often an asymmetric paraparesis that evolves over months or years or, less commonly, a progressive hemiparesis or cerebellar ataxia or very rarely, visual failure or dementia.

However, the symptomatology and the clinical course of the disease are very heterogeneous and a univocal pathogenetic and pathophysiological corresponding pattern to each of the clinical phenotypes is still lacking. Prognosis, in terms of disability accumulation, depends on age at diagnosis, gender, higher disability at baseline and brain atrophy.

2.5.7 Diagnosis

A definite diagnosis of MS is not provided by a single test, including tissue biopsy. Therefore, the diagnosis is based over the integration of clinical, imaging and laboratory features and on the demonstration of dissemination of the disease in space (DIS) and time (DIT). The reference criteria for MS diagnosis are the McDonald criteria which are periodically revised. The current diagnostic criteria for MS are the revised McDonald criteria of 2017 [108]. The diagnosis of MS requires objective evidence of CNS lesions disseminated in time and space, that there is no better explanation for the clinical presentation and that alternative diagnoses are considered and excluded. Using the McDonald 2017 criteria, a diagnosis of MS can still be made on clinical grounds alone. However, MR imaging role has become more and more important in the disease diagnosis since criteria for both

DIS and DIT include the presence of new lesions in specific brain and spinal cord areas and the simultaneous presence of a gadolinium enhancing and non-enhancing lesions, respectively. Additionally, MR imaging has a complementary main contribute in the exclusion of alternative diagnoses that can mimic MS [108; 109; 110].

In most patients with typical clinical and MR imaging findings, examination of cerebrospinal fluid (CSF) is not usually necessary but can provide supportive evidence of MS and its importance has been highlighted in the last 2017 McDonald criteria, where the presence of CSF oligoclonal bands can represent DIT, thus allowing the diagnosis if also DIS criteria is satisfied. CSF findings include a normal or mildly raised white cell count (< 25 cells per cm^3; predominantly lymphocytes) and protein (usually < 1 g/L), a raised IgG index, and IgG oligoclonal bands not present in serum.

Neurophysiological testing of evoked potentials in visual, sensory, or auditory pathways can also provide supportive evidence of MS through identification of a clinically silent lesion in the CNS, indicating dissemination in space and the urgency for studies validating the visual evoked potentials as a tool to fulfil DIS has been stressed in the last revision.

2.5.8 Treatment

In the last five years, several drugs have been approved for patients with RR MS. Their main target is the inflammatory component of the disease, with limited effects on the neurodegenerative component and thus on the progressive forms of MS. The disease-modifying drugs for MS (DMD) currently approved for use in the EU for the treatment of RR MS include interferon-beta ($IFN-\beta$), glatiramer acetate (GA), teriflunomide, dimethyl fumarate (DMF), fingolimod, natalizumab, alemtuzumab, cladribine and ocrelizumab.

The latter drug has been approved also for PP MS patients, showing an effect of slowing progression. Two main strategies are used in choosing and prescribing the more appropriate drug: an escalation and an induction strategy, the first consisting in starting with a first-line treatment and then changing in case of no response, the second providing an higher effective drug as first choice to obtain a fast disease remission, mostly used in patients with a disease characterized by high activity since the beginning. Autologous haemopoietic stem cell transplantation has been used in patients not responding to DMD. Guidelines to help in the choice of the most appropriate drugs have been recently published [111].

Rehabilitation has been used since the first phases of the disease. In order to make rehabilitation protocols more efficient and tailored to the single patient, further studies investigating the mechanisms of cortical plasticity and the way the rehabilitative treatments modulate the neural plasticity are needed [15].

2.5.9 Structural and functional MR imaging studies in multiple sclerosis

As previously mentioned, the hallmark of MS are focal inflammatory lesions which, on MR imaging, appear as hyperintense lesions on T2-weighted and hypointense on T1-weighted sequences, interesting mainly the periventricular, juxtacortical and infratentorial regions. The lesion load on T2-weighted sequences has been found to correlate with the global clinical disability (expressed in terms of the expanded Disability Status Scale (EDSS)). Lesions affecting the spinal cord are detectable in 80-90% of patients with established MS and in up to 50% of patients with CIS [112]. Despite the relationship between lesion load and global clinical disability, still MR imaging features do not extensively explain disability in MS, resulting in the clinico-radiological paradox of MS.

Guidelines have been released to optimize the MR imaging clinical protocol

for MS in order to increase the diagnosis accuracy and to monitor the disease, in terms of relapses and progression [113].

Besides a standardized protocol for brain and spinal cord MR imaging [114], other more innovative MR imaging techniques have been applied to better characterize the pathophysiological mechanisms underlying the onset and progression of the disease. The lymphoid follicles and leptomeningeal inflammation can be visualized in 25-50% of cases of MS, using a delayed high resolution post-contrast T2 fluid-attenuated-inversion-recovery sequence (FLAIR) sequence and in 90% of patients, at ultra-high field MR imaging, using a postgadolinium magnetization prepared FLAIR.

The demyelination, occurring non only at the level of the focal lesion, but diffusively in the white matter and affecting also the grey matter and the deep grey matter nuclei, can be detected using the magnetization transfer ratio (MTR) maps, although they reflect also the inflammation, edema and axonal loss. Together with MTR, the myelin water fraction and the computation of MR imaging ration maps of T1 and T2 weighted images, have been showed to reflect myelin content and thus could be valuable markers of demyelination.

The concentration of N-acetyl-aspartate, obtained using spectroscopy MR, and the total sodium concentration, by means of sodium MR imaging (or 23Na-MR imaging) have been used to detect neurodegeneration, in terms of neuroaxonal loss and cellular metabolic dysfunction/irreversible damage, respectively. An indirect indicator of neurodegeneration is the tissue atrophy, which has emerged as a mechanism taking place since the early stages of the disease and interesting also the deep grey mater nuclei that, in particular, correlates with disability [115]. Brain and spinal cord atrophy can be measured using 3D T1-weighted images. However, the estimation of brain tissue loss is affected by concurrent pathophysiological states such as hydration, inflammation and the concurrent therapies, by

technical factors such as MR imaging contrast quality, signal-to-noise ratio, field inhomogeneity and by the reliability of the post-processing algorithms used [116].

Resting state fMRI has been widely applied to MS patients. A comprehensive review of fMRI studies in MS is beyond the aim of this thesis. However, I'll try to summarize the major findings in this field, examining the multiple studies based on the stage of the disease they have been applied to.

Studies on functional connectivity in patients at the early stages of the disease, in particular patients with CIS, showed an increased synchronization (using a variance-normalized time-series) in CIS patients compared to healthy subjects (HS) in the executive function network, the attention network, and the sensori-motor network and also in CIS patients compared to RR MS in attention, default mode and frontoparietal networks [117]. In a more recent studies on CIS, using graph properties, no differences were observed in the functional network metrics between CIS patients and HS, while, at 1 year follow-up, the betweennes centrality was significantly increased in CIS patients but no region survived after multiple comparison correction for nodal-level comparison. Since authors found differences in structural network properties at the baseline and a structural-functional decoupling they suggested that structural abnormalities precede functional reorganization [118]. In another study on both CIS and MS patients, Liu et al., after detecting the modules of functional connectome, found no differences between HS and CIS but a decreased inter-module efficiency between sensori-motor and frontoparietal network and between visual and frontoparietal netweork in RR MS patients compared to both HS and CIS [119]. Instead, examining the structural connectivity of the same networks, changes in structural inter-module efficiency was detected already in CIS patients. Similarly, Shu et al found alterations in structural connectome but not in functional connectome in CIS patients, functional changes becoming evident only in the definite stage of the disease [120; 121].

Further evidence of the interdependence between structural damage and functional connectivity derives also from a study by Patel et al. where, using a computational model, they demonstrated that structural disconnection contributes to the observed increase in functional connectivity. Authors also commented how the results from previous studies, indicating an early increase in FC, followed by a pseudonormalization and an eventual reduction in later stages, could be explained by the accumulation of subcortical pathology [122]. In another modeling study authors simulated both grey and white matter damage and for each simulation quantified functional connectivity. They found that cortical and thalamic damage induced an increase in FC, while the white matter damage resulted in an early increase and subsequent decrease in FC and that both white and grey matter damage resulted in a reduced network integration [123].

A recent study on a large sample of patients including RR and SP MS, revealed that disability had a direct linear relation with frontal FC but a non linear one with cerebello-temporal and cerebello-frontal FC. Moreover, applying mathematical modeling to find the best describing EDSS vs functional or structural measures they found that, in cortical regions, FC increased together with structural model for EDSS scores < 3 and decreased for higher values of the disability scale, suggesting an exhaustion of compensatory mechanisms at more advanced disability stages [124]. Lastly, Pinter and co-authors, on a large sample including CIS, RR MS and SP MS patients, found out that the connectivity in the central area of the sensori-motor network was related to focal damage but not to global atrophy [125]. Studies on RR MS, besides the results above mentioned, are the majority, the RR MS phenotype being the most represented among MS forms. However, studies on rs-fMRI, in particular the early ones, gave discordant results, some finding and increase FC compared to HS, while others finding a reduced FC. Although RR MS is the most frequent form, it is also very heterogeneous,

with patients varying in severity of clinical disability and severity of traditional imaging features such as lesion load and atrophy. Therefore, this could at least partially account for the incongruous results when exploring rs-fMRI. Hawellek et al., including CIS and RR MS patients, found an increased functional connectivity in patients compared to control despite a disruption in white matter integrity [126]. An increase in FC in RR MS patients was also observed by Faivre et al. in most of the functional networks found by means of independent component analysis, negatively correlated with clinical disability [127]. Furthermore, the analysis of functional activity, by means of exploring the differences in the ALFF between RR MS and HS patients showed an increase of ALFF in bilateral thalami, right insula and right superior temporal gyrus, the latter two correlating with EDSS [128].On the contrary, Rocca et al., in RR MS patients, found both an increase and a decrease in FC, depending on the network regions examined, with salience, executive control, working memory, sensori-motor, and DMN showing a reduced FC correlating with disability and lesion load on T2-weighted images and an increase of FC in other regions of executive control and auditory networks [129]. Focusing on specific networks such as the sensori-motor and the default mode network (DMN) an increase in FC was found in patients, including RR and SP MS, compared to HS and in RR MS compared to SP MS in the sensori-motor network while the opposite, SP MS greater than RR MS, was observed for DMN regions [130]. Lastly, DMN has been showed to have a reduced intrinsic FC in patients compared to HS, with the reduction in the PCC being worse in cognitively impaired patients [131].

Even results of fMRI studies using graph properties showed different results in MS patients. Available studies included both RR and SP MS patients. Schoonheim et al did not find any differences in clustering coefficient values between patients and controls, the only difference being in the network efficiency

when the analysis was restricted to male patients and controls [132]. In a subsequent study the eigenvector centrality mapping values were increased in patients in the thalami and PCC and decreased in the sensori-motor and ventral stream areas [133]. Instead, Rocca et al. found reduced global graph properties values, in particular degree, global efficiency and hierarchy and a higher path length and assortativity in MS patients compared to HS and an altered distribution of hubs between the two groups and between different MS phenotypes (RR and SP MS) [134]. In a 1-year longitudinal study, an increase in local graph properties, such as modularity, clustering coefficient, local efficiency and transitivity, was observed in patients with RR MS but not in HS and beyond detectable atrophy [135]. The same authors, in another study, suggested that the increase in modularity in patients, indicating an increase in local connectivity and a reduced strength of long range connections and suggested that concomitant beneficial and detrimental changes in FC occurs in close proximity in MS [136].

The relationship between functional connectivity and cognitive status has been considerably explored in patients with MS. A study exploring functional networks related to cognitive function revealed a decrease in functional connectivity in RR MS patients compared to HS [137]. Similarly, on a larger sample of MS patients, a reduced functional connectivity was found in the default mode network, fronto-parietal and salience network in cognitive impaired patients compared to both cognitively reserved patients and HS [138]. Using, as a measure of preservation of functional connectivity, the z-scored connectivity matrices (based on a sample of age and sex matched HS) Fuchs et al., found that a preserved functional connectivity reduced the impact of white matter damage on cognitive performance [139]. Longitudinal changes in FC within cognitive related networks were also showed to predict cognitive performance after cognitive rehabilitation. Studies on rs-FC in patients at the progressive stages of the disease are more lim-

ited. In a early study Rocca et al., focusing on the relation between functional activity in the DMN and cognitive status, found a reduced activity in both PP and SP MS patients compared to HS, but the reduction concerned different cortical areas (pre-central gyrus and medial prefrontal cortex for PP and SP MS, respectively); moreover, the activity in the anterior cingulate cortex was increased in SP MS compared to PP MS but reduced in cognitively impaired patients compared to cognitively preserved. Functional activity in the medial prefrontal cortex correlated also with cognitive test scores [140] A study using BOLD signal variability and functional connectivity measures in cognitively impaired and cognitively preserved patients with PP MS found an increased variability in patients, compared to HS and in cognitively impaired vs cognitively preserved patients; in the same study variability correlated with cortical lesion load at the level of the cingulate and superior frontal gyrus [141]. Altogether, these studies point out the following hypothesis: white matter damage drives changes in functional connectivity in the early stages of the disease and these functional changes are compensatory and occur until a threshold of damage, thereafter getting insufficient or maladaptive.

Task fMRI in patients with MS has been used to explore mainly the functional neural correlates underlying cognitive or motor impairment. In a cross-sectional study on patients at different stages of the disease, Rocca and co-authors found a progressively altered functional recruitment, with patients at the late stage of the disease presenting larger and bilateral activation [142]. In another study including CIS, RR MS and SP MS, using a Go/No-go discrimination task, Loitfelder and colleagues found that the task-related activation pattern changed more in the late stages of the disease, e.g. in SP MS. In particular, they did not observe any significant differences between CIS and HS, but both RR MS and SP MS patients showed an increase activation in several cortical areas, compared to CIS. These results were interpreted as an adaptive functional reorganization to, at least par-

tially, compensate and guarantee a normal clinical performance [143]. Task fMRI has also been applied to evaluate the occurrence of brain plasticity after motor or cognitive rehabilitation in patients wit MS. A first study by Rasova and colleagues using a thumb and index flexion task before and after a motor rehabilitation program found no differences between patients and HS and no relationship between changes in motor performance and functional activation [144]. On the contrary, Tomassini et al. found a reduction in task-related activation at the level of occipital and parietal cortices in patients after long term training of a visuomotor task while in HS the reduction was observed only a the level of the occipital cortex [145]. Plasticity after cognitive rehabilitation has been investigated even more widely. Altogether, results point towards an increase in functional connectivity, explored with task fMRI, after cognitive rehabilitation, in regions including the cingulate cortex, frontal and parietal areas and cerebellum [146].

Dynamic FC approach has been recently used to investigate functional reorganization occurring in patients with MS, in particular in relation to their cognitive status. In a study including 29 patients with MS and 18 age- and gender-matched HS performing both rs-fMRI and cognitive task fMRI authors did not find any differences between the two groups but, in MS group, the variance in the cognitive performance was predicted by the cortical volume and by the difference between dynamic FC of the DMN during rest and during task, the latter accounting for an increase of the 26% of the explained variance [147]. In a cross-sectional study, cognitively impaired RR MS patients, compared to cognitively preserved patients showed slower inter-network connectivity and authors suggested this could contribute to cognitive dysfunction [148]. In a longitudinal study, CIS patients showed an increase in dynamic functional network connectivity, which became significant after 2-years of follow-up, interesting mainly the DMN [149]. Lastly, in a study involving rehabilitation using action observation training (AOT) pa-

tients presented with reduced dynamic rs-FC at baseline, compared to HS, but an increase in dynamic FC after training involved the sensori-motor and cognitive networks in patients and not in HS [150].

2.5.10 Gait and balance in multiple sclerosis

Dysfunction of gait is present in MS since the early stages, also in patients with minimal disability. The ability to walk is a feature which mainly contribute to assigning a disability score,according to the most used scale (EDSS), in particular in the more advanced stages [151]. Patients with MS walk more slowly, with a shorter step and stride length, reduced cadence, increased double support time and increased swing phase time, compared to healthy subjects [152]. Lastly, patients with MS walk more slowly and present more timing variability also when walking while performing a cognitive task, compared to healthy controls [153].

The disturbances of gait in MS can result can rely on the damage in one of the CNS areas involved in sensory, motor, coordination functions and it is probably a main contributor to the risk of falls. However, evidence suggests that gait impairment are most likely the result of sensory and particularly proprioceptive impairments and/or central processing deficits rather than deficits in strength, vision, or other neurologic functions affected by MS.[154; 155; 156].

Ankle motion is affected since the earliest stages of the disease although often underestimated due to the limited sensitivity and reproducibility of the conventional clinical measures. Moreover Benedetti et al. found an enhanced degree of EMG coactivation resulting from premature recruitment and/or late relaxation of ankle antagonist muscles, and supposed that stiffening of the ankle joints may serve as a nonspecific superimposed protective mechanisms acting whenever the perceived reliability of balance control is lowered [157].

Balance deficits occur in 50-80% of patients with MS, being present through-

out the course of the disease but detected since the early stages even in patients with minimal or no disability detected with clinical scales [158]. As a preserved balance is the result of the integration of several brain functions such as coordination, vestibular function, proprioception, sight, cognition and muscular strength, there is no a single brain structure responsible of balance dysfunction in patients with MS. In fact, as the whole neuraxis can be affected by focal lesions or diffuse damage in MS, all the different areas concurring to preserve balance can be damaged as well as the integration between them. Although balance has been extensively studied in patients with MS it is still not known which component, among the cerebellar, vestibular, proprioceptive and visual, plays a main role or how their interaction is affected [151].

Balance dysfunction can result in a decreased ability to mantain position, a limited and slowed movement towards limits of stability and a delayed response to postural displacement and perturbations. The first has been studied by means of dynamic posturography or more simply during standing still with several studies showing that patients with MS sway more compared to healthy controls and maintain standing for less time with a reduced base of support [159; 160]. Patients with MS also move less far and less quickly when trying to reach or step from a standing position, they have a worse trunk control [161] and delayed postural responses when the support surface moves. While the latter deficit has been correlated with delays in spinal somatosensory conduction, cerebellar dysfunction seems to have a minor contribution to the delays in postural responses in patients with MS [151].

Taken together, these observations suggest that the sensori-motor impairment at the level of the ankle may be a primary factor that determines mobility and balance impairments in people with MS. Previous fMRI studies during the execution of active and passive ankle movements [56; 162] have shown greater fMRI

activation in MS patients than controls in the superior temporal gyrus, rolandic operculum, and putamen. However, no studies focused on the neural correlates of proprioception in patients with MS.

Once again, rehabilitation and exercise are of utmost importance in improving both gait and balance and reducing the risk of falls, in particular in the progressive stage of the disease. Identifying the role proprioception has in the gait and balance impairment would help in the selection of the most appropriate rehabilitation strategy. In line with these observation, rehabilitation strategy aimed at improving the central integration of the sensory inputs resulted in greater improvement in balance and risk of falls, compared to a standard rehabilitation protocol [163].

2.6 Parkinson's disease

Parkinson's disease (PD) is a neurodegenerative disease of the nervous system characterized by the loss of dopaminergic neurons I the pars compacta of the substantia nigra. The classical clinical features are represented by bradykinesia, tremor, rigidity and postural and gait impairment [164]. Among gait disorders, the freezing of gait has a high disabling impact, affecting the quality of life and increasing the risk of falls [165].

2.6.1 Epidemiology

Parkinson's disease is the second most frequent neurodegenerative disease diagnosed. Annual incidence in the high-income countries is about 14 per 100000, increasing to 160 per 100000 if the population aged 65 years or over is considered [166]. The lifetime risk is slightly higher for men (2% than for women (1.3%) in individuals aged 40 years. From 1999 to 2009 a decrease in the incidence of PD

disease diagnosis was reported, interpreted as an improved diagnosis of different parkinsonian syndromes [167]. After 50 years the incidence increase rapidly until a peak at around 80 years. In elderly the incidence decrease is probably due to an increasing prevalence of dementia which is an exclusion diagnostic criteria for PD. The male:female ratio is reported to vary from 1.3 to 2.[168]

2.6.2 Risk Factors

Both genetic and environmental factor contribute to PD pathogenesis. Monogenic forms of the disease result in both autosomal dominant (genes involved: SNCA, LRRK2, VPS35, EIF4G1, DNAJC13,CHCHD2) and autosomal recessive types (genes involved: Parkin, PINK1, DJ-1) [164]. Moreover, subjects with a family history of PD or tremor present an increased risk and, so far, a mutation in the β-glucocerebrosidase is the greatest genetic risk factor for developing the disease and recently 24 genetic loci have been associated with disease risk [169]. Environmental risk factors include the consumption of dairy products, the exposure to pesticides (in particular the 1,1'-dimethyl-4,4'-bipyridinium dichloride),metamphetamine, previous traumatic brain injuries. on the contrary, smoking, the consumption of coffee and physical activity have been indicated as protective factors. [168]

2.6.3 Pathology and pathogenesis

The main neuropathological features of PD are the loss of dopaminergic neurons in the pars compacta of the substantia nigra and the presence of Lewy bodies (abnormal aggregates of α-synuclein) in the surviving nigral neurons. Lewy bodies have been showed to spread from enteric and autonomous nervous system to brainstem and to higher part of the neuraxis [170]. Nonetheless the clinical features seem to be more correlated to neuronal loss than to the extent of Lewy

bodies pathology. The presence of the Lewy bodies in the neocortex has been associated with midiline motor symptoms (postural instability and difficulty of gait) and with more severe bradykinesia [171]. Lastly, also the severity of freezing of gait (FOG) was related to the density of Lewy bodies containing neurons in the cortex [172].

Other pathological features include neuroinflammation, the neuronal loss in many other brain regions (locus ceruleus, nucleus basalis of Meynert, pedunculopontine nucleus, raphe nucleus, dorsal motor nucleus od the vagus, amygdala ans hypothalamus) and the presence of other protein aggregates such as β-amyloid plaques and tau neurofibrillary tangles. With the discovery of monogenic forms of PD, the clinical features of PD have been found to occur also in absebce of Lewy pathology [164; 173].

Several pathogenetic mechanisms have been proposed, from the toxicity of protein aggregates, mitochondrial dysfunction, synaptic dysfunction, neuroinflammation and prion-like transmission of α-synuclein.

2.6.4 Clinical features

Parkinson's disease is characterized by motor symptoms including bradykinesia, muscular rigidity, rest tremor, postural and gait impairment. Empirical clinical observations suggest two major forms, a tremor-dominant and a non-tremor-dominant. The former is usually associated with a slower rate of progression and less functional disability [164]. Other non-motor features include olfactory dysfunction, cognitive impairment, psychiatric symptoms, sleep disorders, autonomic dysfunction, late dementia. In particular, some of them are characteristic of the prodromal phase of the disease characterized by impaired olfaction, constipation, depression, excessive daytime sleepiness and rapid eye movement sleep behavior disorder. Falls, impaired gait and postural instability are frequent in patients with

PD. Freezing of gait is present in up to 80% of patients with PD after about 17 years of the disease [174] and this condition has been associated with extranigral pathology, including cortical cholinergic denervation and beta-amyloid deposition

2.6.5 Diagnosis

The diagnosis is based on the clinical motor features after the exclusion of red flags who would suggest a different cause of parkinsonism [175]. although the gold standard is the neruopathological assessement there re no generally accepted standard pathological diagnostic criteria [176]. Genetic testing is recommended in monogenic forms but most of them do not show a complete penetrance making a definite diagnosis in asymptomatic subjects not possible[164]. Positron emission topography and single photon emission tomography can help in the differential diagnosis with other causes of parkinsonism.

2.6.6 Treatment

The symptoms of the disease are treated with drugs that increase intracerebral dopamine concentrations or stimulating dopamine receptors and include levodopa, dopamine agonists, monoamine oxidase type B inhibitors, catecholOmethyltransferase inhibitors and amantadine. A surgical treatment, with deep brain stimulation, is considered when the motor fluctuations and dyskinesia become disabling [164].

However disease modifying drugs are not available yet and the physical activity and rehabilitation, aimed in particular at reducing the risk of fall and improving balance and gait, play a major therapeutic role [173; 177].

2.6.7 Action observation in Parkinson's disease

Motor imagery and Action observation (AO) has been proposed as a rehabilitation strategy to improve freezing of gait in patients with PD. These two approaches rely on different, although partially overlapping, neural substrates [178]. While Motor Imagery ability has been showed to be substantially preserved in patients with Parkinson's disease, this is not the case for AO. AO training is based on the finding that during the observation of an action a similar pattern of brain activity is observed as during the actual execution of the same action. The neurophysiological basis of AO relies in the mirror neuron system which is defined as the brain areas containing mirror neurons, e.g. neurons that discharge during both the execution of a goal-directed action and the observation of other subjects performing the same action [179; 180].

A previous study on PD patients with FOG showed that after physical AO training patients significantly reduced the number of episodes of FOG and an overall improvement in motor performance and quality of life when compared to a control group without AO training [181]. Nonetheless, the integrity of the MNS in patients with PD is still a matter of discussion, and the neural correlates of AO in these patients have not been investigated yet. Moreover, the neural correlates of gait and of AO could be of aid in the choice of a specific or even personalized rehabilitation protocols [182]).

2.6.8 Functional MR imaging studies in Parkinson's disease

MR imaging had a secondary role in the diagnosis and prognosis of Parkinson's disease but with the advent of sequences that better capture the functional and structural brain organization more and more studies are emerging. Altered func-

tioning in the cortico-striatal network and a reduced functional connectivity between the striatum and other brain regions such as thalamus, midbrain pons and cerebellum have been found [183; 184]. Reduced cortico-subcortical sensori-motor connectivity and dysfunction of the cognitive networks have also been observed [185; 186] as well as a disruption in the functional networks with altered global graph metrics correlating with cognitive symptoms and local ones with motor features [187]. A recent study using dynamic functional connectivity revealed an abnormal global integration and a reduction in the functional segregation among networks, which was correlated with the clinical severity [188].

Patients with FOG presented a reduced functional connectivity between the basal ganglia network and the cognitive control network during a virtual reality gait task and this reduction was associated to the frequency of freezing behaviors [189].

Gait and gait alterations have been studied in patients with Parkinson's disease by means of single photon emission tomography with results showing a reduction of brain activity in the medial frontal motor area [190] and of positron emission tomography. The latter study in particular revealed that, during a gait mental imagery task, premotor-parietal and brainstem area where activated in patients in the off(-medication) phase, while a brain activity pattern more similar to the healthy controls' one was observed in the on(-medication) phase [191].

A task fMRI study using motor imagery of gait in patients with and without freezing of gait showed that patients with FOG had an increased activity at the level of mesencephalic regions but decreased at the level of fronto-parietal regions, compared to FOG- patients. [192]. Altogether these studies point out towards a compensatory functional activation of brainstem regions and an altered brain response at the level of the fronto-parietal areas in patients either in off-medication phase or with FOG, defining a role for these regions in gait abnormalities.

Chapter 3

BOLD signal variability in early multiple sclerosis

Summary

Here are presented the rationale and methods of the study of BOLD signal variability in patients with Multiple Sclerosis at the early stage of the disease, the results and their interpretation.

3.1 Introduction

Resting state fMRI (rs-fMRI) analysis has been classically based on the study of temporal coherence of the blood oxygenation level dependent (BOLD) signal between different areas of the brain, resulting in measures of resting state functional connectivity (rs-FC) [20]. It is now widely accepted that a disruption of resting state functional networks and a subsequent functional reorganization occur in patients with multiple sclerosis (MS) as a consequence, albeit in part, of structural damage [193]. However, the clinical impact and the precise role of the

rs-fMRI connectivity changes remain a matter of debate [194].

Variability of the BOLD signal is emerging as an index of the complexity and efficiency of neuronal networks [27]. This measure can be quantified in different ways such as multiscale entropy or as the amplitude of low frequency fluctuations (ALFF). In this work it will be defined as the standard deviation (SD) of the temporal fluctuation of the BOLD signal [26]. Initially discarded as "noise", temporal variability has recently received greater attention and has been showed to characterize both physiological and pathological conditions, such as systemic inflammation, bipolar disorder and progressive multiple sclerosis [141; 195]. In particular, low-frequency oscillations have been shown to be consistent within cortical regions [196]; moreover, fluctuations within sub-bands of the low-frequency spectrum of 0.01-0.1 Hz, i.e. Slow-4 (0.027-0.073 Hz) and Slow-5 (0.01-0.027 Hz), have also been shown to be more restricted to the gray matter (GM) compared to the white matter (WM)[197; 198]. Lastly, the amplitude of low-frequency fluctuations correlated with cognitive symptoms in previous rs-fMRI studies on patients with neurological diseases [199].

Neuronal variability has been investigated in patients with progressive MS, showing increased values within areas of the attention and executive control network especially in cognitive impaired patients [141]. Nonetheless, it is still unknown whether variability is altered in patients at the very early stages of the disease. The MS onset is, in most cases, characterized by a neurological event, referred as clinically isolated syndrome (CIS). In up to 82% of cases, patients with a CIS develop a clinically defined relapsing-remitting MS (RR-MS) [200]. While no previous studies have explored the change in neuronal variability in these two populations of patients, studies on rs-FC alterations in patients with CIS or RR-MS have reported different results, controversial in terms of both the comparison between patients and healthy subjects (HS) and between CIS and

RR-MS [117; 128].

Therefore, the aims of our study were: a) to investigate the presence and extent of neuronal variability changes as function of disease severity in patients with CIS and RR-MS; b) to assess the relationship between variability changes and rs-FC; c) to explore the clinical relevance of variability changes.

3.2 Materials and methods

Participants. Thirty-seven outpatients (17 with CIS and 20 RR-MS) were consecutively recruited. Twenty-seven HS with no history of neurological or psychiatric disorders were included as control group. CIS patients were defined as subjects presenting with a first neurological event, suggestive of a demyelinating disease. The diagnosis was made upon clinical examination, and supported by radiological and cerebrospinal fluid (CSF) findings, according to McDonald's criteria 2010 [201]. Patients were excluded if they presented pregnancy, an active major organ disease or any other neurological or psychiatric disorder. RR-MS patients had to be free from clinical relapses in the three months preceding the scan.

On the same day, all subjects underwent MRI and symbol-digit-modality test (SDMT) while CIS and RR-MS patients additionally underwent a neurological assessment, including Expanded Disability Status Scale (EDSS).

The study conforms to the standard of the declaration of Helsinki and was approved by the institutional ethical committee. All subjects provided written informed consent prior to participation into the study.

MRI acquisition. All subjects underwent MRI at 1.5T (SignaHDxt scanner, GE MEDICAL Systems), using a 8-channel brain array coil. The protocol

included the following sequences: 1) axial PD-T2-weighted ($TR/TE1/TE2$ = 2340/102/38.25 ms; FA = 90°; $voxelsize$ = 0.94x0.94x4 mm^3); 2) sagittal 3D-T1-weighted fast-spoiled-gradient-echo ($TR/TE/TI$ = 11.56/5.048/500 ms; FA = 8°, $voxelsize$ = 1x1x1 mm^3); 3) gradient-echo Echo Planar Imaging (EPI) sensitive to BOLD signal with 150 volumes for resting-state fMRI (TR/TE = 3000/60 ms; FA = 90°, $voxelsize$ = 3.3x3.3x3.3 mm^3). During rs-fMRI, participants were explicitly instructed to keep their eyes closed and to relax.

Structural MRI analysis. WM T2 and T1 lesion volumes (LV) were measured on the PD-T2-weighted and the 3D-T1-weighted images respectively, using a semi-automated technique (Jim version 7; Xinapse Systems, `http://www.xinapse.com`). A lesion mask obtained on the 3D-T1-weighted images was obtained for each patient and used to fill-in the T1-hypointense lesions [202].

Statistical analysis of demographic, clinical and structural MRI data. Chi-square test was used to assess significant differences in terms of gender among the three groups. The normality of distributions and homogeneity of variances for age, disease duration, SDMT, T2LV and T1LV were checked with Shapiro-Wilk test and Levene's Test, respectively. Since the two conditions were not satisfied, Mann-Whitney U test and Kruskal-Wallis 1-way analysis of variance (ANOVA) were used to compare the above-mentioned variables between RR-MS and CIS or among RR-MS, CIS and HS, respectively.

Resting state fMRI preprocessing. All pre-processing steps were implemented in Analysis of Functional NeuroImages (AFNI version 17.0.13) (`http://afni.nimh.nih.gov/afni`) if not otherwise specified. The first 3 volumes of each time-series were discarded. Subsequently, the remaining volumes underwent despiking and slice-timing correction. Head motion estimation along six dimen-

sions (three rotational axes and three translational axes) was then performed. All subjects showed head motion $< 2mm$ (translation) and $< 2°$ (rotation) (mean values and range of the six motion parameters per each group are reported in Table 3.1). T1 images were registered to the standard space (Talairach, using the TT N27 space, i.e. the "talairached" version of the Colin N27 atlas). rs-fMRI data were thus normalized to standard space and spatially smoothed (6mm). The filled T1-weighted images were segmented using FAST (FSL version 5.0.9) and WM and CSF masks, thresholded at 0.99 and binarized (using Fslutils, part of FSL), were registered to the standard space; subsequently, the nuisance signal from the WM and CSF was obtained. Linear interpolation was used for all the transformations to the standard space, performed in AFNI. The estimated 6 head motion parameters and the mean time series from CSF and WM were used as covariates in the correlation computation. Data were subsequently filtered between 0.01 and 0.1 Hz, obtaining the standard frequency band (SFB). Moreover, we analyzed two separate bands within the standard range: Slow-4 (0.027-0.073 Hz) and Slow-5 (0.01-0.027 Hz).

Variability analysis. Variability of the BOLD signal was measured by calculating the SD of the time-series amplitude, in each frequency band (SFB, Slow-4 and Slow-5). However, as the fractional amplitude of the fluctuations of BOLD signal at low frequencies (fALFF) has been found to be more robust, with a higher sensitivity and specificity for the neuronal signal compared to the ALFF [203], also fractional SD (fSD), a normalized index of SD, is more specific and reliable to variations of the neuronal activity. Therefore, fSD was obtained as the ratio of SD for each frequency band and SD in the entire range (0-0.167 Hz), for the SFB and for both the Slow-4 and Slow-5 bands [195]. Whole-brain variability was obtained extracting the fSD values using a GM mask. The GM mask

	RR-MS (N=20)	CIS (N=17)	HS (N=27)
Roll	0.0421	0.0374	0.0055
	(-0.539; 1.5571)	(-0.298; 0.5564)	(-0.851; 0.513)
Pitch	-0.006	0.0318	-0.056
	(-0.801; 1.0829)	(-0.909; 1.0793)	(-0.728; 0.6589)
Yaw	-0.019	0.0063	0.0123
	(-0.644; 0.3828)	(-0.244; 0.2005)	(-0.398; 0.4599)
DispSup	0.0597	0.0719	0.1273
	(-0.844; 1.0892)	(-0.352; 0.7036)	(-0.856; 1.2101)
DispLeft	0.0203	0.0204	-0.013
	(-0.302; 0.9746)	(-0.196; 0.626)	(-0.758; 0.3371)
DispPost	-0.006	-0.012	0.0006
	(-0.237; 0.2913)	(-0.231; 0.1305)	(-0.194; 0.2195)

Table 3.1: Mean and range of the 6 motion parameters per each group.
Roll, pitch and yaw are expressed in degrees CCW. DispSup, DispLeft and DispPost are expressed in mm. The average value and the range of values are reported for each group.
DispSup= displacement in the superior direction
DispLeft= displacement in the left direction
DispPost= displacement in the posterior direction

was obtained by averaging the partial volume estimates of GM (output of FAST, part of FSL) for each subject and then thresholded at 0.2. To test differences in variability at a whole-brain level, voxel-wise statistics were performed in AFNI, using ANOVA (among RR-MS, CIS and HS) in SFB, Slow-4 and Slow-5, with age, gender and the estimated head motion parameters as covariates. The results were thresholded at a corrected p-value=0.05 an alpha=0.05 using a Montecarlo simulation via 3dClustSim in AFNI, with the autocorrelation function. Whole-brain variability analysis revealed significant differences between HS and CIS at the level of left intraparietal sulcus within Slow-5 and between HS and RR-MS patients at the level of the posterior cingulate cortex (PCC) within Slow-5 (see Results and Fig.1).

Post hoc analysis

Based on whole-brain variability results we chose to:

1. perform subsequent analyses focusing on the default mode network (DMN) and the dorsal attentional network (DAN) within Slow-5 and SFB. These two networks were chosed because intraparietal sulcus and PCC are part of the DAN and DMN, respectively. Moreover, since the differences were found only within Slow-5, analysis within Slow-4 was discarded, while the analysis within SFB was kept in order to compare results with previous findings in literature.

2. validate the results of the variability analysis at a whole-brain level, performing the analysis at a network level. Therefore, using AFNI, the fSD values in Slow-5 and SFB were extracted from the nodes of DMN (as defined by [204] e.g. including the PCC, precuneus, ventral anterior cingulate cortex (vACC), medial prefrontal cortex (MPFC), right and left inferior parietal lobule (r-IPL and l-IPL, respectively), left middle frontal gyrus (l-MFG) and left and right middle temporal gyrus (l-MTG and r-MTG respectively)) and of the DAN (as defined by [205] e.g. left and right frontal eye field (l-FEF and r-FEF respectively), left and right posterior intraparietal sulcus (lp-IPS and rp-IPS), left and right anterior intraparietal sulcus (la-IPS and ra-IPS), r-MTG and l-MTG); then, the values for each network were compared among the three groups with ANOVA (using SPSS, version 22.0). Prior to ANOVA analysis, the normality of distributions and homogeneity of variances were verified with Shapiro-Wilk test and Levene's Test, respectively. The Sidak correction was applied when evaluating factors interactions

3. Correlations between variability values extracted from the two networks

and T2LV, EDSS or SDMT scores were tested using partial nonparametric correlation, adding age and gender as covariates. The statistical analysis was performed with SPSS (version 22.0)

4. Lastly, the consistency of the signal variability within the two networks was evaluated in HS, CIS and RR-MS patients [197]. A Pearson correlation analysis between the variability values of each different regions of interest (ROI) of the networks was performed and r values were represented on a correlation matrix plot. Moreover, Pearson correlation values were transformed to z-scores using Fisher's r-to-z transformation and significant differences between HS and both RR-MS or CIS were assessed.

The time-series obtained from the ventral anterior cingulate cortex (vACC) (ROI of the DMN) were discarded from all subsequent analysis because signal drop was detected in 11 out of 64 subjects.

rs-FC analysis For the rs-FC a seed-based analysis was used, considering the DMN and DAN, based on the results from the variability analysis at whole-brain level. Spheres of 6 mm radius were used as ROI in the nodes of the DMN and of the DAN, as previously defined. Mean time-series for each seed-ROI were calculated by averaging the time-series of all voxels within the sphere. Correlation analysis was performed between each seed-ROI and all other brain voxels for the SFB and Slow-5. Fisher's r-to-z transform was used to obtain spatial z-maps with each voxel's intensity representing its correlation strength with the seed-ROI.

To test differences in rs-FC at a whole-brain level, voxel-wise statistics were performed in AFNI, using ANOVA (among RR-MS, CIS and HS) in SFB and Slow-5, with age, gender and the estimated head motion parameters as covariates.

In RR-MS and CIS patients, voxel-wise correlations between rs-FC and both 1) variability values extracted from DAN and DMN (in the respective frequency

ranges) and 2) T2LV, were performed in AFNI, with age, gender and the estimated head motion parameters as covariates. The results were thresholded at a corrected p-value=0.01 an alpha=0.05 (using a Montecarlo simulation via 3dClustSim in AFNI, with the autocorrelation function). Talaraich altas in AFNI was used to anatomically label the results.

3.3 Results

Demographics, clinical and conventional MRI data of RR-MS, CIS and HS, are summarized in Table 3.2.

	RR-MS(N=20)	CIS(N=17)	HS(N=27)	p
Age°	39.10 ± 9.45	35.53 ± 8.16	32.41 ± 7.7	0.013
Gender†	11 F; 9 M	10 F; 7 M	15 F; 12 M	0.969
Disease duration (months)‡	27.80 ± 15.45	14.12 ± 8.20	-	0.022
EDSS (median; range)‡	1.5; 1.0-3.5	1.0; 0.0-2.0	-	0.008
SDMT°	54.20 ± 15.02	58.94 ± 10.74	60.46 ± 11.00	0.136
T2LV (mL)‡	7.45 ± 8.03	1.81 ± 1.75	-	0.005
T1LV (mL)‡	3.07 ± 3.68	0.45 ± 0.50	-	0.005

Table 3.2: Demographic and clinical data of the RR-MS, CIS and HS groups. Results are reported as average±standard deviation unless otherwise specified. °Kruskal Wallis test was used: $\chi^2(2) = 8,76$ $p = 0.01$ and $\chi^2(2) = 3,99$ $p = 0.14$ for age and SDMT respectively. Post hoc pairwise comparison revealed a significant different for age between HS and RR-MS ($p = 0.02$)
† Chi square test was used. $\chi^2(2) = 0.064$.
‡ Mann Whiney U test was used.
Abbreviations: EDSS expanded disability status scale; SDMT: symbol digit modalities test;T2 LV: T2 lesion volume; T1 LV: T1 lesion volume.

Whole brain variability within SFB, Slow-4 and Slow-5

When compared to HS, CIS patients showed one cluster of significant increased

variability at the level of the left parietal region (peak in x= 26, y= 68, z= 36, Talaraich coordinates), while RR-MS patients presented increased variability at the level of the PCC (peak in x= 7, y= 50, z=12, Talaraich coordinates), both within Slow-5 (Figure 3.1). No statistically significant differences were found when CIS and RR-MS patients were compared in any of the frequency bands. Based on these results a subsequent analysis focusing on the DAN and DMN was performed.

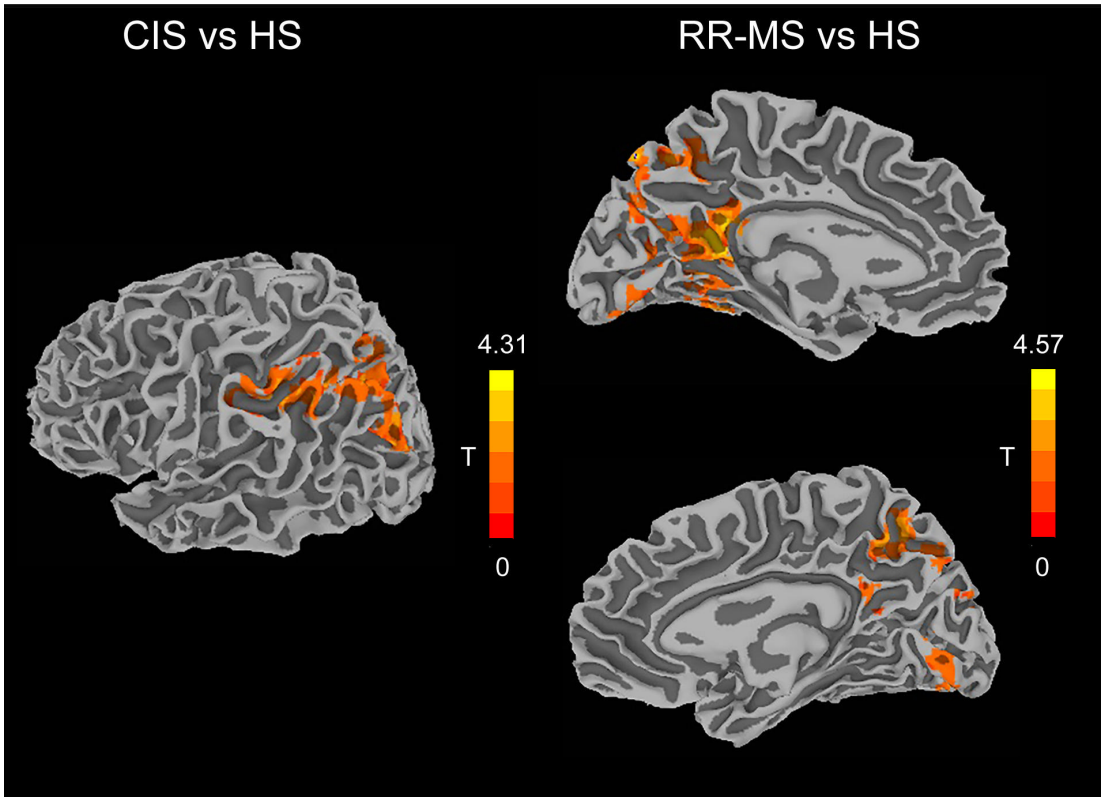

Figure 3.1: Results of the comparisons among the three groups within Slow-5 at the whole-brain level. When compared to HS, CIS patients showed one cluster of significant increased variability at the level of the left parietal region (peak in x= 26, y= 68, z= 36, Talaraich coordinates), while RR-MS patients presented increased variability at the level of the PCC (peak in x= 7, y= 50, z=12, Talaraich coordinates).

Variability within DAN and DMN in Slow-5 and SFB

Based on the results from the whole brain analysis we chose to focus on the fSD values extracted from DAN and DMN ROI in Slow-5.

With regard to the DAN, ANOVA analysis revealed a significant difference for the l-FEF ($F(2,59)=5.57$, p¡0.01), l-MTG ($F(2,59)=3.41$, $p=0.04$) and r-MTG ($F(2,59)=3.96$, $p=0.02$) and the whole network ($F(2,59)=4.03$, $p=0.02$. Post-hoc pairwise comparisons revealed a significant difference for l-FEF between both RR-MS ($p<0.01$) and CIS ($p=0.048$) when compared to HS, for l-MTG between RR-MS and HS ($p=0.04$) and for r-MTG between CIS and HS ($p=0.02$). Finally, the whole DAN significantly differed between CIS and HS ($p=0.04$) with a trend between RR-MS and HS ($p=0.07$).

With regard to the DMN, only the fSD values extracted from the PCC seed, were significantly higher in RR-MS compared to HS ($F(2,59)=3.71$, $p<0.05$, post-hoc analysis $p=0.04$). In all cases both groups of patients showed higher fSD compared to HS.

No significant differences were found among fSD values extracted from both DAN and DMN regions within SFB.

Correlations between variability and clinical parameters

The following significant correlations were found between clinical measures and fSD values within Slow-5 in the MS patients (results are reported in Table 3.3):

- The SDMT positively correlated with the whole DAN, l-FEF, r-FEF, rp-IPS, la-IPS and ra-IPS in the RR-MS group and with l-MTG in the CIS group. No significant correlations were found between DAN and EDSS in both groups.

- Regarding the DMN, SDMT negatively correlated with variability values within the precuneus in CIS but positively with the whole network, r-IPL

and l-IPL and l-MTG in the RR-MS group. Moreover, the EDSS negatively correlated with the whole network, r-IPL and l-IPL in the RR-MS group.

No correlations were found between both SDMT and EDSS with fSD values of DAN or DMN regions within SFB, except for l-FEF and SDMT in RR-MS group (r=0.619, p=0.006). No correlations were found between SDMT and fSD values of the DAN or DMN regions in HS.

SDMT			
		RRMS	CIS
DAN		r=0.491, p=0.039	-
	l-FEF	r=0.641, p=0.004	-
	r-FEF	r=0.569, p=0.014	-
	rp-IPS	r=0.502, p=0.034	-
	la-IPS	r=0.561, p=0.015	-
	ra-IPS	r=0.569, p=0.014	-
	l-MTG	-	r= 0.539, p=0.038
DMN		r=0.511, p=0.30	-
	Precuneus	-	r= -0.683, p=0.005
	r-IPL	-	r=0.566, p=0.014
	l-IPL	-	r=0.601, p=0.008
	l-MTG	-	r=0.475, p=0.046
EDSS			
		RRMS	CIS
DMN		r= -0.475, p=0.046	-
	r-IPL	r= -0.511, p=0.030	-
	l-IPL	r=-0.559, p=0.016	-

Table 3.3: Partial correlations between fSD of the DAN and DMN with SDMT and EDSS within Slow5.
Abbreviations: l-MTG: left middle temporal gyrus; l-IPL: left inferior posterior lobule; r-IPL: right inferior posterior lobule; r-FEF: right frontal eye field; l-FEF: left frontal eye field; rp-IPS: right posterior intraparietal sulcus; ra-IPS: right anterior intraparietal sulcus; la-IPS: left anterior intraparietal sulcus.

Consistency of the variability signal within each network

HS exhibited a better correlation of the signal variability within different ROI of

the DMN, compared to CIS and RR-MS patients, in Slow-5 and SFB. Correlation coefficients resulted significantly different when both RR-MS and HS or CIS and HS were compared, especially regarding MPFC, parietal and temporal regions, in both SFB and Slow-5 (Figure 3.2). No significant differences were found for the DAN.

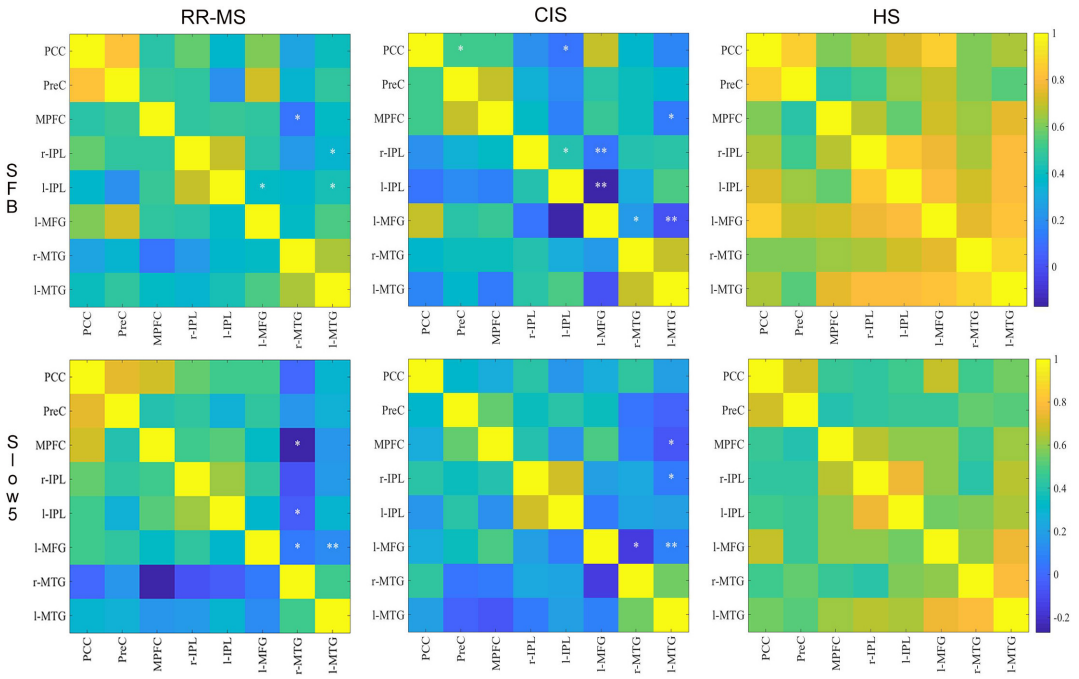

Figure 3.2: Matrix plots representing the r values of the correlation analysis between the ROIs of DMN in the three groups in both SFB and Slow5 * $p < 0.05$ compared to HS ** $p < 0.01$ compared to HS Abbreviations: PCC: posterior cingulate cortex; PreC: precuneus; MPFC: medial prefrontal cortex; r-IPL: right inferior posterior lobule; l-IPL: left inferior posterior lobule; MFG: middle frontal gyrus; r-MTG: right middle temporal gyrus; l-MTG: left middle temporal gyrus.

Functional connectivity within SFB and Slow-5

RR-MS patients showing reduced rs-FC in the nodes of the DMN (in both SFB and Slow-5) and DAN (SFB), compared to HS. CIS patients also showed lower rs-FC when compared to HS, of the posterior, frontal and temporal areas of the

DMN (SFB and Slow-5). Compared to CIS, RR-MS patients presented reduced connectivity of regions of the two networks in SFB, with the exception of an increased connectivity of the frontal areas of the DMN (Table 3.4).

	Seed ROI	Size	*Coordinates* (x,y,z)	Target	T
SFB					
CIS vs HS			DMN		
	Precuneus	334	-55,22,41	r-Postcentral	-4.65
	MPFC	362	34,6,4	l-Insula	-5.12
		214	-34,13,20	r-Insula	-3.95
	r-MTG	249	22,-12,8	l-LN	-5.23
	l-MTG	157	22,-12,9	l-LN	-4.57
RR-MS vs HS			DMN		
	PCC	183	1,73,5	l-Cuneus	-4.65
	MPFC	366	-1,64,-30	r-Uvula	-4.97
	r-IPL	697	55,4,11	l-Precentral	-5.65
		211	-61,-1,17	r-Precentral	-5.21
	l-IPL	195	37,-1,14	r-Insula	-4.72
	l-MFG	420	-4,64,-6	r-Culmen	-4.31
		178	-55,10,8	r-STG	-4.00
		158	28,16,-12	l-ParaHip	-4.38
	r-MTG	573	25,1,11	l-LN	-5.30
		428	7,64,-12	l-Declive	-4.53
		238	-55,31,20	r-Insula	-4.70
		181	-31,37,-30	r-CerebTonsil	-5.79
	l-MTG	279	28,-1,5	l-LN	-4.23

		223	-43,46,-24	r-Culmen	-5.79
		185	10,55,-12	l-Declive	-4.46
			DAN		
	r-FEF	169	22,7,2	l-LN	-4.03
	lp-IPS	392	7,55,-15	l-Culmen	-4.77
RR-MS vs CIS			DMN		
	r-IPL	342	52,22,32	l-Postcentral	-5.16
	l-MFG	329	-43,-22,29	r-MFG*	6.33
			DAN		
	l-FEF	380	49,7,8	l-Precentral	-4.58
	r-MTG	190	40,4,44	l-Precentral	-4.69
Slow5					
CIS vs HS			DMN		
	r-MTG	167	-7,46,-15	r-Culmen	-4.88
RR-MS vs HS			DMN		
	Precuneus	225	7,91,-3	l-LG	-3.97
	l-MFG	211	4,73,5	l-LG	-4.54
	r-MTG	480	25,-1,8	l-LN	-5.28
	l-MTG	323	30,2,14	l-Insula	-4.94
		195	-10,46,-18	r-Culmen	-4.95

Table 3.4: Functional connectivity differences among the three groups in SFB and Slow5.
ANOVA analysis, with age, gender and motion parameters added as covariates. Both CIS and RR-MS patients showed reduced connectivity, compared to HS, and RR-MS a reduced connectivity compared to CIS patients from all seed ROIs if not otherwise specified. Abbreviations: PCC: posterior cingulate cortex; MPFC: medial prefrontal cortex; l-Cuneus: left cuneus; l-MTG: left middle temporal gyrus; r-MTG: right middle temporal gyrus; l-IPL: left inferior posterior lobule; r-IPL: right inferior posterior lobule; r-FEF: right frontal eye field; lp-IPS: left posterior intraparietal sulcus; l-Insula: left insula; r-Insula: right insula; l-MFG: left middle frontal gyrus; r-MFG: right middle frontal gyrus; l-LN: left lentiform nucleus; r-Uvula: right cerebellar uvula; l-Precentral: left precentral gyrus; r-Precentral: right precentral gyrus; l-Postcentral: left postcentral gyrus; r-Postcentral: right postcentral gyrus r-STG: right superior temporal gyrus; l-ParaHip: left parahippocampal gyrus; l-Declive: left declive; r-CerebTonsil: tight cerebellar tonsil; l-Culmen: left culmen; r-Culmen: right culmen; l-LG: left lingual gyrus. * clusters showing increased connectivity with the seed regions in RR-MS compared to CIS patient

Correlation between FC and variability within the DAN and the DMN in SFB, and Slow-5

Significant inverse correlations between rs-FC and global variability within the SFB, and Slow-5 were found, in particular within DMN regions, in the RR-MS group. In the CIS group clusters of positive correlations were found within areas of the DAN in both SFB and Slow-5 (Table 3.5). Finally, in the HS group no significant correlations were found between FC and variability in the two networks in all frequency bands.

Correlation between FC or variability and T2LV in SFB and Slow-5

T2LV correlated negatively with rs-FC of frontal regions of the DAN in CIS and RR-MS patients and with rs-FC of DMN regions in CIS patients (Table 3.6). No significant correlations were found between T2LV and variability values within

	Seed ROI	Size	Talaraich Coordinates (x,y,z)	Target Cluster	T
			SFB		
CIS	DAN	178	28,68,29	l-MTG∘	7.20
RR-MS	DMN	533	-53,23,27	r-IPL	-7.92
		153	50,34,32	l-IPL	-4.92
			Slow5		
CIS	DAN	145	32,68,39	l-MTG∘	5.70
RR-MS	DMN	175	-50,34,30	r-IPL	-6.08

Table 3.5: Correlations between FC and fSD within the DAN and the DMN in SFB and Slow5.
Correlations adjusted for age, gender and motion parameters, corrected for multiple comparisons at $p<0.01$. Abbreviations: l-MTG: left middle temporal gyrus; r-MTG: right middle temporal gyrus; l-IPL: left inferior posterior lobule; l-IPL: right inferior posterior lobule.
∘ clusters showing positive correlation

the DAN or DMN.

3.4 Discussion

To our knowledge this is the first study that characterizes the pattern of variability of the BOLD signal in patients with CIS and RR-MS. The results indicate that patients present increased variability of the BOLD signal within the Slow-5 band in regions of the DAN and DMN, which is associated with the clinical performance.

The most novel findings of this study are related to the analysis of BOLD signal variability, investigated by means of the fSD in the standard- and low-frequency ranges, in a cohort of CIS and RR-MS patients. We found that CIS and RR-MS patients exhibited higher variability values, compared to HS, within the DAN and in the PCC of the DMN respectively, when the Slow-5 frequency

	Seed ROI	Size	Talaraich Coordinates (x,y,z)	Target Cluster	T
SFB					
CIS	DMN				
	l-MFG	150	-25,-37,-9	r-MFG	-6.21
	r-MTG	225	-17,22,59	r-Precentral	-8.27
		175	-46,34,14	r-STG	-5.41
	DAN				
	r-FEF	235	28,88,-9	l-IOG	-5.20
Slow5					
CIS	DAN				
	r-FEF	181	-43,28,32	r-Postcentral	-7.84
RR-MS	DAN				
	ra-IPS	150	31,58,50	l-SPL	-4.89

Table 3.6: Correlations between FC and T2LV within SFB and Slow5.
Correlations adjusted for age, gender and motion parameters, corrected for multiple comparisons at $p < 0.01$. Abbreviations: l-MFG: left middle frontal gyrus; r-MFG: right middle frontal gyrus; r-MTG: right middle temporal gyrus; r-Precentral: right precentral gyrus; r-STG: right superior temporal gyrus; r-FEF: right frontal eye field; ra-IPS: right anterior intraparietal sulcus; l-IOG: left inferior occipital gyrus; r-Postcentral: right postcentral gyrus; l-SPL: left superior parietal lobule.

range was considered. As shown in previous studies in HS, the temporal variability of the BOLD signal within low-frequency range has a higher specificity and sensitivity in detecting neuronal activity at a grey matter level [197]. The only previous study on variability in MS, on a cohort of progressive patients, revealed increased variability in patients compared to HS, in particular at the level of the frontal and temporal regions of the DAN. Indeed, we found increased fSD in CIS patients, within the low-frequency band Slow-5, at the level of left intraparietal sulcus and in the whole DAN, including frontal and temporal areas. Moreover, higher values of fSD were detected also at the level of the PCC in RR-MS patients who, interestingly, presented a reduced rs-FC within the DMN and an inverse correlation, coherent among both SFB and Slow-5, between rs-FC

of this network and the fSD. Conversely, in CIS patients, a positive relationship between connectivity and variability was found in the temporal areas of the DAN.

In line with previous studies, a reduced large-networks rs-FC in MS patients compared to HS was observed [129; 131; 143; 206]. In particular, in this study, a decreased rs-FC of the areas of DMN in all frequency bands in both groups of patients was found, and, only in the RR-MS group, a decreased rs-FC of areas of the DAN in SFB, when compared to the HS group. The trend of a reduced rs-FC in patients was consistent among SFB and the low-frequency range, Slow-5, previously not investigated in MS patients at the early stages of disease. Moreover, FC inversely correlated with the T2 lesion load in particular at the level of the frontal and parietal areas of the DAN in both CIS and RR-MS patients and in frontal and temporal areas of DMN in CIS patients.

The interpretation of the relationship between rs-FC and variability is uncertain [207] and whether the differences in the variability affect the connectivity of two brain regions is still a matter of discussion [5]. Based on our findings, we could speculate that, in MS patients, a decoupling occurs between fSD and rs-FC. Whether the increase in variability precedes or is a consequence of the reduced connectivity or whether they occur simultaneously is difficult to establish, especially in a structurally damaged brain. However, the relationships between FC and T2LV, at the level of the frontal and parietal areas of DAN in Slow-5, could suggest that the increase in variability could compensate for disruption of FC caused by structural damage, at least in the very early stages. On the other hand, in RR-MS patients, the functional disruption affects more deeply the functional organization and in particular the DMN, possibly interfering with its interplay with other networks and, at this stage, the compensating mechanisms could result insufficient.

In this work we also found a reduced consistency of the fSD values within

the different regions of the DMN in both CIS and RR-MS patients, while HS exhibited a better correlation between the fSD values within DMN. In particular, the lower consistency seemed to interest more the temporal regions of the DMN in Slow-5 in both RR-MS and CIS groups; interestingly the same brain areas showed a reduced rs-FC in the same group of patients, underlining a further possible relation between rs-FC and variability.

Another novelty of our study regards the association between variability values and clinical parameters. In fact, we found that a higher variability in specific resting-state networks is associated with a better clinical performance, in terms of SDMT and, regarding RR-MS patients, also EDSS. This is in contrast with the findings in patients in a progressive and more advanced phase of the disease [141].

Cognitive impairment is present since the early stages of the disease, and SDMT has been provided to be a reliable method of assessing the processing speed in MS [208]. In the MS population of this study, the performance at the SDMT did not differ compared to the HS group and correlated with increased BOLD signal variability in both DAN and DMN, especially in RR-MS. The increase in fSD could reflect the attempt of the brain to respond to the disease, by increasing the efficiency in specific regions, especially in the very early stages. Interestingly, the only negative correlation between SDMT and variability was found when the fSD values of the precuneus were considered. Posterior regions of the DMN have been already associated with cognitive impairment in MS [131] and a functional reorganization within DMN regions could be hypothesized, with a compensatory role of the parietal regions, at least for processing speed.

Altogether these results suggest that increased signal variability could reflect the capability of the brain to overcome the structural damage in order to allow a normal functional performance. This, at least in the early stages of MS disease,

could represent a successful compensatory mechanism, which becomes less efficient in the more advanced phase of the disease, where an increase in variability does not result in a better clinical performance [141].

This study is not without limitations such as the small sample size and the lack of analysis of WM microstructural damage. Moreover, in our work we investigated variability as a measure of the changes of the BOLD signal magnitude over time, calculated as SD. It is noteworthy that this is only one of the possible methods to measure variability and results obtained with different procedures and pipelines should be compared with caution, as suggested also by [209].

However, this is the first study exploring the variability of the BOLD signal in a group of patients with early MS, revealing the differences with respect to HS and the relationships with clinical measures. Moreover, the relation with rs-FC and the finding of a disrupted consistency of the variability within different areas of the DMN suggest a role for BOLD signal variability in the functional reorganization occurring in the early stage of MS. Therefore, the investigation of the variability of the BOLD signal could improve the understanding of the reorganization subsequent to the structural damage in MS disease, by providing complementary information about the functional efficiency of different brain regions.

3. BOLD SIGNAL VARIABILITY IN EARLY MULTIPLE SCLEROSIS

Chapter 4

Behavioral and neural correlates of position sense at the lower limbs in early multiple sclerosis

Summary

Here are presented the rationale and methods of the study of the position sense in patients with Multiple Sclerosis at the early stage of the disease, the results and their interpretation.

4.1 Introduction

The ability to identify the position of lower limb in space is critical for ambulation1 and balance control [210; 211]. Since proprioception results from a complex process of integration of sensory inputs from different peripheral receptors, involving the central nervous system (CNS) at different levels [212], it is likely to be affected in a spatially disseminated disease such as multiple sclerosis (MS).

4. BEHAVIORAL AND NEURAL CORRELATES OF POSITION SENSE AT THE LOWER LIMBS IN EARLY MULTIPLE SCLEROSIS

MS is a chronic demyelinating disease of the CNS, causing neurological disability, especially in young adults [213]. Sensory deficits are predominant in patients with MS and, among them, proprioceptive impairment is the most common, involving the lower more than the upper limbs [214; 215]. Moreover, patients with MS frequently have an impaired control of ankle motion [216], which is necessary for maintaining standing posture and during gait [156]. Taken all together, these observations suggest that the sensori-motor impairment at the level of the ankle may be a primary factor that determines mobility and balance impairment in people with MS. However, the role of proprioception impairment in determining disability is often underestimated, due to the limited sensitivity and reproducibility of the conventional clinical measures [217]. Furthermore, in MS patients, the investigation of proprioception at the level of the lower limb and specifically at the level of the ankle joints, has received little attention so far, especially in terms of neural correlates. Indeed, previous works focused on brain functional activity during active or passive motor tasks, including both upper limb and ankle movements [162; 218; 219].

It has been also reported that position sense at the level of the ankle, in terms of either behavioral outcome or neural activity, correlates with balance performance, in both healthy subjects (HS) [80; 81] and patients with neurological diseases [220]. Although balance impairment characterizes MS since its early stages[221] and it has been extensively investigated[146; 146; 222], none of these studies explored the specific relationship between the proprioceptive-related brain activity and the balance ability during quiet standing, in MS patients.

Lastly, both the performance of sensory tasks requiring an inter-hemispheric transfer of information and the postural control rely on the integrity of the corpus callosum (CC)[146; 223]. The anterior part and mid-body of the CC connect higher order sensory and primary/secondary somatosensory areas respectively,

and CC integrity is required during bimanual coordination movements[224]. The CC is affected since the early stages of MS23 and its microstructural disruption has been associated with a poor postural control [225]. However, there are no studies that examined the relationship between the microstructural integrity of the CC and the proprioceptive impairment during bilateral sensory tasks with the lower limbs or during quiet standing, in patients at the early stages of the disease.

Against this background, we planned this study with three specific aims. The first aim was to assess the distal lower limb proprioception, in terms of both behavioral performance and neural activity, in patients with early Relapsing-Remitting MS (eRR MS). Specifically, we investigated the proprioceptive-related brain activity using functional MRI (fMRI) during ipsilateral and contralateral matching tasks [66] performed with the lower limb. The second aim of our study was to determine whether, in eRR MS subjects, the functional neural correlates of proprioception and the behavioral performance during the matching tasks were related to postural control during quiet standing, thus investigating the impact of proprioceptive deficits on balance. Finally, as a third aim, we tested the hypothesis that the structural damage in the CC could affect the performance during the proprioceptive matching task requiring bilateral coordination and during quiet standing, since the early stages of the disease. We focused on matching tasks for the following reasons: a) they are best suited and extensively employed to study position sense[66; 226]; b) they have been already employed in subjects with stroke, [227; 228]R; c) they involve different aspects of sensori-motor control that can be affected in MS [229].

4.2 Materials and methods

Participants. Outpatients with eRR MS and gender- and age-matched HS were prospectively enrolled. The inclusion criteria were: (i) right or mixed foot dominance (Waterloo inventory score > -6 [78]); (ii) no previous history of musculoskeletal injuries at the lower limb level; (iii) no previous intense performance of sport activities that involved extensively the lower limbs; (iv) no other neurological or psychiatric disorder. eRR MS subjects were selected according to McDonald's criteria 2017 [108] and with the following additional inclusion criteria: (v) disease duration of less than 5 years and (vi) no relapses in the three months previous to the examination. We screened 34 eRR MS patients. However, five patients were excluded because they were left-footed and three of them because they had suffered a relapse in the three months before the examination. Two out of the 26 patients were excluded from the analysis: the first one because she did not complete the MRI scan, the second one because of the poor image quality due to motion artifacts. Thus, the final sample size of our study included 48 subjects, 24 eRR MS and 24 age and gender matched HS. Patients with eRR MS underwent clinical evaluation including Expanded Disability Status Scale (EDSS) and the assessment of the upright standing ability by means of a WII balance board, within two days of the MRI acquisition. The study conforms to the standard of the declaration of Helsinki and was approved by the local ethical committee (CER Liguria, n. 222REG2017). All subjects provided written informed consent prior to participation in the study.

fMRI experimental setup and protocol. For all subjects the distal lower limb proprioception inside the MR-environment was evaluated, by using the MR-compatible setup described in [230] (see Figure 4.1 A-B for further details). Subjects were asked to perform ipsilateral and contralateral matching tasks with the

right foot during fMRI. In addition, subjects performed ipsilateral and bilateral active motor tasks involving the same dorsi-plantar flexion movements needed to perform the matching tasks. In both the active motor tasks and the matching tasks, we used a block fMRI design with 4 blocks of rest (30 s each) alternated with 4 blocks of foot movements for the motor task and 6 blocks of rest alternated with 6 blocks of position matching for the proprioceptive task. All subjects performed the following tasks (Figure 4.1 D):

- Unilateral and bilateral active motor tasks (ACTIVE-UNILAT and ACTIVE-BILAT, respectively). Subjects actively moved in the sagittal plane the right foot, during ACTIVE-UNILAT, or both feet in phase, during ACTIVE-BILAT, by synchronizing with a metronome set at 1 Hz.

- Ipsilateral matching task with the right dominant foot (IMA-R), consisting in matching the target position with the same foot (right one); in each of the six blocks of this task (30 s), the operator presented three target positions, thus subjects performed 18 ipsilateral matching (3 targets 3×6 blocks). Each target position was reached at least 4 times and the order of the targets' presentation was pseudo-random. The operator passively moved the foot from the starting position (Figure 4.1 C, BAS) to one of the four target positions (Figure 4.1 C) and then back to the BAS position. Subsequently, subjects had to reach the target position with the same foot and then return to the BAS position.

- Contralateral matching task with the right-dominant foot (CMA-R). An operator moved the left non-dominant foot to one of the same four positions as in IMA-R task. The subject had to reach the selected position with the contralateral right-dominant foot and go back to the BAS location with both feet. During the matching tasks subjects were required to keep their

eyes closed. For all the matching tasks, the subjects were asked to perform the matching trial with a single movement, without corrections while approaching the target. Once the participants reached the intended matching position, they were asked them to maintain it for 1 second before coming back to the baseline position. The order of presentation of the tasks was balanced across the subject population to minimize potential order effects. The number of times each target was presented was the same in CMA-R and IMA-R tasks. To familiarize with the task-fMRI experiment, all subjects performed the motor and matching tasks within 2 days before MRI acquisition. The entire fMRI experimental session was performed outside the MR room with the same setup used in the MRI setting. During this familiarization session, we checked for the absence of voluntary contractions during the passive movements of the matching tasks by analyzing surface electromyographic activity.

Foot positions during matching tasks. Subject had to match four different foot positions spanning the plantar-dorsiflexion range: DF7, REF, PF7, PF14. These four positions corresponded to four equally spaced rotations (7°) of the foot platform: in the REF position the foot platform was orthogonal to the leg, in DF7 it was rotated by 7° in the dorsiflexion range, in PF7 and PF14 it was rotated respectively of 7° and 14° in the plantar-flexion range. Each trial started with both feet on a baseline resting position (baseline, BAS). The range spanned between the BAS position and the furthest position in the dorsi-flexion range (DF7) was 35°.

Behavioral analysis of the matching performance. As an indicator of the matching performance we computed the constant error (CE) that is the difference between the position reached by the matching foot and the target position,

both measured in terms of angular rotations of the foot platforms. The values computed for each trial were averaged across repetitions and across targets, obtaining a single measure of the overall performance to correlate with the fMRI data in each task (IMA-R and CMA-R), with the structural damage of the corpus callosum as well as with the parameter assessing the balance performance. This measure indicates a systematic error: a negative value corresponds to an undershoot of the target positions, a positive value to an overshoot; if the CE is zero, there is no systematic error.

Assessment of the upright standing ability of eRR MS patients. The WII balance board is a low cost instrument used in several studies to measure the variation of the centre of pressure during quite standing with different subjects populations [231; 232; 233], for a review, see [234] including Multiple Sclerosis [235; 236; 237].

In this experiment all subjects were assessed with the same WBB device, following the recommendations of [233]. During the neurological examination, all eRR MS patients underwent also a test aiming at evaluating their standing balance. They stand upright and barefoot on a Nintendo WII Balance Board (WBB, Nintendo, Kyoto, Japan), with the arms relaxed along the sides of the body, the heels separated by about 2 cm, and the feet abducted at 20° [238] (see Figure 4.1 E-F). They were asked to remain as still as possible for three trials, each lasting 40 s. We asked subjects to keep their eyes closed during the three testing trials to increase reliance on proprioception and to eliminate visual cues [80; 222].

Data acquired from the four load cells of the WBB were transferred via Bluetooth to a laptop using a custom modification of the software ([1] (Figure 4.1 E, F). The signals from the four load cells of the WBB were sampled at 40 Hz.

[1] `https://www.colorado.edu/neuromechanics/research/wii-balance-board-project`

The offset recorded during unloaded condition was subtracted to the signal of each load cell [235] before computing the two components of the CoP trajectory [233]. The CoP coordinates were low-pass filtered with a 5th order Butterworth filter with cut-off frequency 10 Hz and the mean value from both signals was subtracted [239]. Then, for each trial we estimated the Root Mean Square of the Antero Posterior oscillations of the center of pressure (RMSAP [mm]). We chose this parameter because it is influenced by the responses of the muscle spindle and thus, it is strictly related to proprioceptive information; an increment of this parameter reflects poor balance performance [80]. Moreover, RMSAP has been indicated among the most reliable parameters when using a WBB in HS and patients with MS [235]. No learning effects were observed across the three trials, as already described in a previous study [238], thus we averaged the obtained values.

MRI acquisition and image processing. All subjects underwent MRI at 1.5 T Signa Excite (Signa Excite General Electric Healthcare, WI, USA) with 8-channels phased-array head coil. The protocol included: High resolution Fast Spoiled Gradient Echo (FGPR) 3D T1-weighted sequence: $voxelsize = 1.2x1.2x1.2\ mm^3$, repetition time (TR)/echo time (TE)/inversion time (TI)= 9.7/4.1/500 ms). Spin-echo dual-echo proton density-weighted and T2-weighted sequence: voxel size= $0.94x0.94x0.94\ mm^3$, $TR/TE1/TE2 = 2120/38.2/102$ ms for lesions identification. Single-shot echo-planar imaging (EPI) sequence for task fMRI: $voxelsize = 3.75x3.75x4\ mm^3$, $TR/TE = 3000/60$ ms. Axial single-shot spin echo diffusion tensor imaging sequence: $voxelsize = 0.94x0.94x2.5\ mm^3$; $TR/TE = 14000/95.7$ ms; flip angle= 90°; with 30 non-collinear diffusion directions with $b = 1000$ s/mm2 and 5 $b = 0$ s/mm2.

fMRI preprocessing and first level analysis. fMRI data processing.

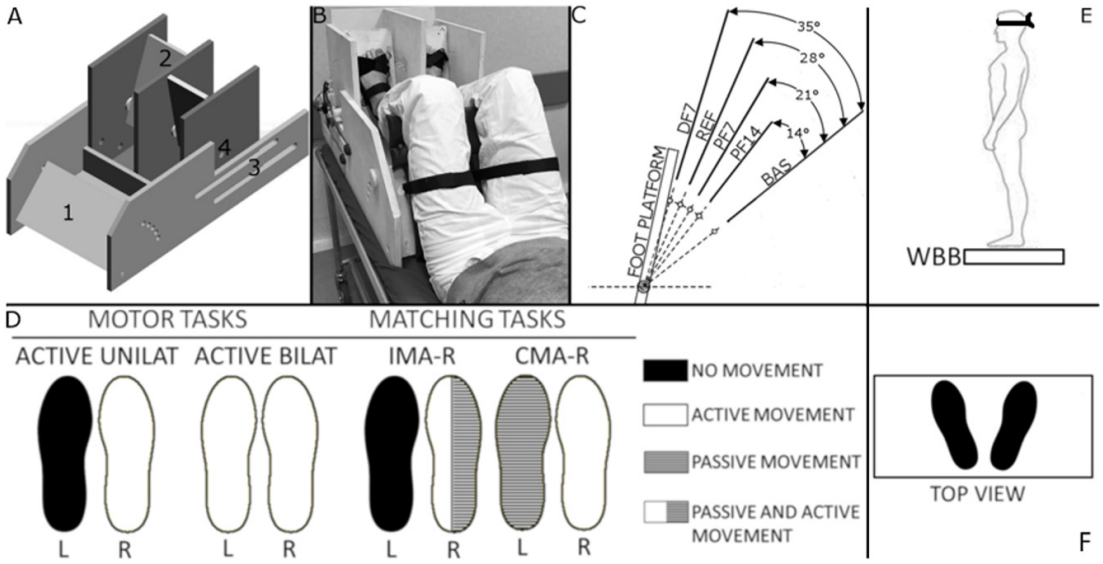

Figure 4.1: Figure 1. (A) Custom-made MR compatible passive device employed during the MRI experimental protocol. The numbers indicate (1) the adjustable tight platform; (2) the foot platforms that allow for each foot independent one degree-of-freedom movement in the sagittal plane; (3) the two rails (two per each side) that allow the thigh platform and the foot platforms to slide relative to one another to fit different subjects' anthropometries; (4) the MR compatible optical encoder was attached to each platform axis of rotation. (B) An overview of a subject outside the MR environment. The thighs and the feet were firmly strapped to the corresponding platform with velcro straps. (C) The four presented platform positions (PF14, PF7, REF, and DF7) that the subjects were required to match during each matching tasks. The angle values on the right show the rotation values of the platform with respect to the BAS position from which each trial started. (D) Task-fMRI protocols during motor and matching tasks. Rest and block duration were 30 s each. Tasks were randomized across subjects. (E-F) Overview of the subject and of the feet position during balance control task.

Firstly, the T1-weighted images of eRR MS patients underwent a lesion in-painting procedure prior to the brain extraction and anatomical structures' segmentation. The in-painting procedure was needed to avoid failure of the segmentation procedure since, without it, the white matter (WM) lesions would have been considered as gray matter by FAST (part of FSL) [202]. These T1 and T2 WM lesions were identified by neurologists on the T2/Proton Density-weighted

and T1-weighted, using a semi-automated technique based on user-supervised local thresholding (Jim version 6; Xinapse Systems, [1]. Initial pre-processing step of despiking (detection and reduction of extreme time series outliers by fitting a smooth curve insensitive to extreme outliers to the data) were performer in AFNI [2] [240]. Non-brain removal was performed with FreeSurfer skull stripping [241]. All other pre-processing steps were performed using FSL (FMRIB's Software Library, [3]) [242; 243] as implemented in FEAT [244; 245], including: removal of the first 3 volumes, motion correction using MCFLIRT [4] [242], slice-timing correction for regular ascending acquisition (using Fourier-space time series phase-shifting), spatial smoothing (Gaussian kernel, FWHM=6 mm), grand-mean intensity normalization of all volumes by a single multiplicative factor, and high-pass temporal filtering (Gaussian-weighted least-squares straight line fitting, sigma = 30 s). Nuisance signal from white matter (WM) and cerebrospinal fluid (CSF) was calculated by segmenting T1-weighted images with FAST [246], then registering the resulting WM and CSF masks to functional space and averaging the raw time series within each mask. To detect task-related activity, one explanatory variable (EV) was defined to model the On-Off periods of the task for each run (ACTIVE-UNILAT and ACTIVE-BILAT motor tasks, IMA-R, and CMA-R tasks) and convolved with the hemodynamic response function. The 24 motion parameters calculated during motion correction were added as confound EVs. Mean CSF and WM signals were added to the general linear model as covariates of no interest. Boundary-based registration BBR [247] was used to register each individual functional data to the corresponding T1-weighted brain image. Then, linear affine with twelve degree of freedom registration was performed to register each subject's T1-weighted brain to the standard space (MNI152 brain template,

[1] http://www.xinapse.com)
[2] (https://afni.nimh.nih.gov/)
[3] https://fsl.fmrib.ox.ac.uk/fsl/fslwiki
[4] (https://fsl.fmrib.ox.ac.uk/fsl/fslwiki/MCFLIRT)

voxel size: $2x2x2$ mm3) [242].

In order to model mean activation per group, one-sample t-test was used per each task (4 group mean activation in total, one per each of the task performed, 2 motor and 2 matching tasks). To investigate differences in the neural correlates of the matching tasks within the same group, the IMA-R and CMA-R tasks performed with the right foot using two-sample paired t-tests (IMA-R vs CMA-R) were compared. Anatomical localization of the peaks of activation were computed with the SPM anatomical toolbox [248].

DTI processing. Data were processed using FMRIB's Diffusion Toolbox (part of FSL). First, we corrected for motion and eddy currents artifacts and then standard DTI metrics of fractional anisotropy (FA) and mean diffusivity (MD) were computed. The region of interest (ROI) of the CC was extracted from the JHU DTI based white matter atlas (ICBM-DTI-81 white-matter labels [249] and co-registered to the diffusion images of each subject using a combination of linear and non-linear registration (FLIRT [1] and FNIRT [2] [242; 250]. Mean FA and MD values were extracted from the ROI of CC in both eRR MS patients and HS groups.

Statistical analysis. The statistical analysis was performed with SPSS (Version 20.0), except for the fMRI section, performed with FSL. Prior to all statistical testing, we tested (Kolmogorov-Smirnov test) the hypothesis that the demographic, behavioral and DTI data were normally distributed. We used Levene's and Mauchly' tests to verify, respectively, the homogeneity of variances for all the above-mentioned independent measures and the sphericity assumption for the behavioral indicator (CE) computed during the matching task.

[1] `https://fsl.fmrib.ox.ac.uk/fsl/fslwiki/FLIRT`
[2] `https://fsl.fmrib.ox.ac.uk/fsl/fslwiki/FNIRT`

Demographic and clinical data. Differences in age and gender between the two groups were assessed with the unpaired t-test and chi-square tests, respectively.

Proprioceptive matching performance. To investigate significant difference during matching tasks we performed a repeated measures ANOVA with one between-subjects factor 'group' (eRR MS vs HS) and two within-subject factors i.e. 'task' (CMA-R and IMA-R) and 'positions' (DF7, REF, PF7 and PF14). When the sphericity assumption was rejected, we applied the Greenhouse-Geisser correction. Then, based on the ANOVA results, we used a Tukey's HSD post-hoc test to further investigate significant differences among the four target positions and an unpaired t-test to investigate specific difference between the two groups of HS and eRR MS subjects in each task. A Pearson correlation coefficient was used to assess the relationship between CE during CMA-R and RMSAP within the eRR MS group.

fMRI. To strictly investigate position sense related activity, we chose to contrast the matching tasks neural response with the purely active motor neural response, using two sample paired t-tests (IMA-R>ACTIVE-UNILAT, CMA-R>ACTIVE-BILAT), as performed in a previous study [230]. Results were converted to Z-values and then a threshold of $Z \geq 3.1$ for cluster formation was applied, followed by with a significance threshold of $p = 0.0001$ (cluster corrected using Gaussian Random Field Theory (GRFT)). In all the different group level analyses, we added age and gender as covariates for the HS group while age, gender and disease duration for the eRR MS group. To compare the activity during IMA-R and CMA-R between the HS and eRR MS group, we used unpaired t-test. A threshold of $Z \geq 2.3$ for cluster formation and a significance threshold of $p = 0.01$ (cluster corrected using GRFT). The correlations between brain activations of eRR MS patients (IMA-R and CMA-R) and the behavioral

measure CE during the two matching tasks were modeled separately with age, gender and disease duration as covariates. A threshold of $Z \geq 2.3$ for cluster formation was applied, followed by with a significance threshold of $p = 0.01$ (cluster corrected using GRFT). We performed the same correlation analysis for the HS group, using age and gender as covariates. In addition, to test the a-priori hypothesis that there is a correlation between the balance parameter during quiet standing (RMSAP) and the proprioceptive-related brain activity in the eRR MS group, we used the same correlation analysis as above (for the CE). We selected the brain activity measured during CMA-R, since for both fulfilling this task and maintaining balance during quiet standing, the proprioceptive representation of both legs is needed.

DTI METRICS AND BEHAVIORAL PARAMETERS. Unpaired t-test was used to assess differences in Fractional anisotropy (FA) and mean diffusivity (MD) values of the CC between HS and eRR MS. Moreover, partial correlation between the DTI metrics and CE during CMA-R was assessed in the two groups separately and in the HS+eRR MS group, adding age and gender as covariates, using Pearson correlation coefficient. The latter test was used also to assess the relationship between diffusion metrics and the quiet standing parameter (RMSAP), in eRR MS group.

4.3 Results

Participants. Demographic and clinical characteristics of all subjects included in the analysis are reported in Table 4.1. The median sensory functional system score (s-FSS) in eRR MS group was 0 (range: 0-2). The demographic data as well as the behavioral and DTI parameters were normally distributed ($p > 0.05$ in all cases). Age and gender did not significantly differ between the two groups:

t(46)= -1.05, p=0.298 and $\chi(1)$=0.375 , p=0.540, for age and gender, respectively.

	Patients (N=24)	HS (N=24)
Age	32.50 ± 6.76	30.75 ± 4.54
Gender	17 females; 7 males	15 females; 9 males
Waterloo scale score	7.5 ± 7.9	11.82 ± 4.91
Disease Duration (months)	38.17 ± 24.77	-
EDSS (median; range)	1 (0-3.5)	-
s-FSS (median; range)	0 (0-2)	-
CE CMA-R (°)	10.89 ± 4.56	8.38 ± 2.96
CE IMA-R (°)	6.33 ± 2.53	6.59 ± 2.69
RMSAP (mm)	4.96 ± 1.73	-
T2-LV (mL)	2.43 ± 2.65	-
T1-LV (mL)	1.89 ± 1.85	-
CC FA	0.64 ± 0.03	0.66 ± 0.03
CC MD ($\times 10 - 3 mm^2 s^{-1}$)	0.77 ± 0.02	0.75 ± 0.02

Table 4.1: Demographic, clinical and behavioral data.
Mean± standard deviation are reported if not otherwise specified. Abbreviations: s-FSS: sensory functional system score; EDSS: expanded disability status scale; CE: constant error; CMA-R: contralateral matching task executed with the right foot; IMA-R: ipsilateral matching task executed with the right foot; RMSAP: root mean square of the antero-posterior direction; T2-LV: lesion volume in T2-weighted sequence; T1-LV: lesion volume in T1-weighted sequence.

Behavioral performance during matching tasks and during quiet standing. The sphericity assumption was verified for both the group and task factors ($p > 0.05$), but not for the positions factor ($\chi^2(2) = 66.78$, $p < 0.001$). Thus, for the latter case, we adopted the Greenhouse-Geisser correction ($\eta = 0.54$). Both populations systematically overshot the target position. eRR MS patients had a greater CE than HS during the CMA-R task while, during the IMA-R task, the two groups showed similar performance (Figure 4.2): group × task effect, F(1,46)=7.26, p=0.010, group effect F(1,46)=1.98, p=0.170. Mean and standard

deviation CE values during CMA-R were $10.89 \pm 4.56°$ and $8.38 \pm 2.96°$ for eRR MS and HS respectively, with the unpaired t-test highlighting a significant difference (t=2.26, p=0.029). Mean and standard deviation CE values during IMA-R were 6.33±2.53° and 6.59±2.69° for eRR MS and HS respectively (unpaired t-test t=-0.35, p=0.730). The CE in CMA-R was greater than IMA-R for both populations (task effect: F(1,46)=38.31, $p < 0.001$). The ANOVA highlighted also a position effect (F(1.61,73.96)=9.79; $p < 0.001$; $\eta = 0.54$, Greenhouse-Geisser corrected). Specifically, as revealed by the post-hoc analysis, the error was greater in plantarflexion than in dorsiflexion or in the REF position (post-hoc analysis: $p < 0.002$ for all comparisons among positions with the exception of the comparison between DF7 and REF ($p > 0.05$)). In addition, we found an interaction group × task × position (F(3,138)=2.96; p=0.035) due to the fact that for eRR MS patients the CE in the CMA-R task had a monotonic increase from dorsi-flexion to plantar-flexion, while this effect was not present neither in the IMA-R for both population nor in the CMA-R for the HS subjects. The performance of eRR MS related to postural control during quiet standing, i.e. the root mean square of the antero-posterior direction (RMSAP), is reported in Table 4.1. RMSAP significantly correlated with CE during CMA-R (r=0.510, p=0.015).

Brain activations during matching and motor tasks in eRR MS patients and HS.

Single-group analysis: brain activity for both eRR MS patients and HS groups is reported in Table 4.2 and Table 4.3 for matching and motor tasks, respectively.

IMA-R. eRR MS patients activated at the level of left paracentral lobule, postero-medial frontal cortex (PMFC), right supramarginal gyrus (SMG) and bilateral cerebellum. The same areas were involved also in HS group with addi-

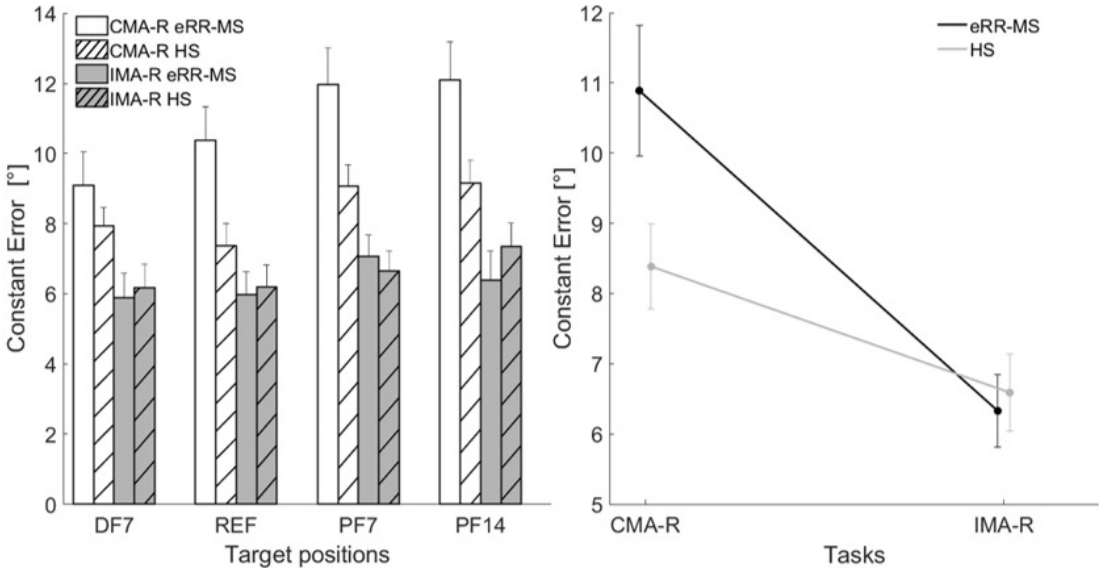

Figure 4.2: On the left: Constant Error for the four target angular positions (DF7, REF; PF14, and PF7) presented during the matching tasks. Error bars represent the standard error (mean± SE). On the right: Mean group differences (eRR MS vs HS, black and gray lines, respectively) in constant error for the two matching tasks (CMA-R and IMA-R). Filled circles and bars indicate mean and standard errors.

tional activity at the level of right inferior and bilateral middle frontal gyrus, and the right inferior and superior parietal lobule (IPL and SPL, respectively).

CMA-R. eRR MS patients activated at the level of the bilateral paracentral lobule, right middle frontal gyrus and PMFC, left inferior frontal gyrus, right postcentral gyrus and SMG and bilateral cerebellum. HS presented additional activation at the level of the right insula, left superior temporal gyrus, IPL and SMG.

ACTIVE-UNILAT. eRR MS group activated at the level of the bilateral premotor and left primary motor cortex, bilateral IPL, bilateral parietal operculum, left putamen and right cerebellum. Instead, HS activated at the level of left paracentral and posterior medial frontal cortex, left parietal operculum, bilateral rolandic operculum, bilateral cerebellum, bilateral putamen and right IPL.

ACTIVE-BILAT. eRR MS patients' group activations were found at the level of bilateral primary motor, cerebellum, supramarginal gyrus, rolandic operculum and putamen and right IPL. HS activations were detected at the level of the right primary motor cortex, bilateral IPL, bilateral cerebellum and right putamen.

Location	Cytoarchitetonic location	MNI coordinates X Y Z	Z score	Side
eRR MS IMA-R				
Paracentral Lobule	Area 6	-4 -18 68	7.85	L
Paracentral Lobule	Area 4a	-6 -34 68	7.45	L
Posterior-Medial Frontal	Area 6	8 -2 70	7.29	R
Cerebellum (III)	Lobule I IV	10 -42 -18	6.59	R
Cerebellum (VIII)	Lobule VIIb	-30 -64 -54	6.51	L
Cerebellum (VII)	Lobule VIIa	-22 -72 -46	6.2	L
Cerebellum (VI)	Lobule VI	28 -58 -22	6.13	R
Vermis (4/5)	Lobule I IV	4 -46 -12	6.02	
Vermis (4/5)	Lobule V	2 -56 -4	5.79	
SupraMarginal Gyrus	Area PFop	56 -22 28	7.31	R
SupraMarginal Gyrus	Area PF	64 -32 26	6.66	R
SupraMarginal Gyrus	Area PFcm	54 -34 26	6.45	R
SupraMarginal Gyrus	Area PFt	56 -30 36	6.07	R
eRR MS CMA-R				
Paracentral Lobule	Area 4a	6 -38 66	7.92	R
Paracentral Lobule	Area 6	-2 -22 70	7.6	L
Postcentral Gyrus	Area 3b	12 -40 68	7.41	R
Middle Frontal Gyrus		34 -2 54	7.26	R
SupraMarginal Gyrus	Area PFcm	60 -28 30	7.23	R
Posterior-Medial Frontal	Area 6	10 2 58	6.88	R

Cerebellar Vermis (4/5)	Lobule I IV	-2 -48 -12	6.19	
Cerebellum (IV-V)	Lobule V	-18 -38 -24	6.04	L
Cerebellum (IV-V)	Lobule I IV	-4 -46 -8	5.76	L
Cerebellum (III)	Lobule I IV	14 -38 -24	5.71	R
Cerebellum (VI)	Lobule VI	-32 -56 -26	5.5	L
Cerebellum (VII)	Lobule VIIb	-12 -74 -44	5.5	L
Precentral Gyrus	Area 44	-54 6 14	5.37	L
Inferior frontal gyrus	Area 44	-46 12 0	5.06	L
HS IMA-R				
Paracentral Lobule	Area 4a	-6 -32 64	7.48	L
Inferior frontal gyrus	Area 44	48 10 12	7.23	R
Paracentral Lobule	Area 6	-6 -18 70	7	L
Posterior-Medial Frontal	Area 6	-10 -12 66	6.91	L
Cerebellum (IV-V)	Lobule V	16 -38 -22	6.77	R
Middle Frontal Gyrus		-26 -8 52	6.72	L
SupraMarginal Gyrus		56 -30 38	6.42	R
SupraMarginal Gyrus	Area PF	58 -32 42	6.38	R
SupraMarginal Gyrus	Area PFcm	56 -34 26	6.35	R
SupraMarginal Gyrus		48 -26 24	5.76	R
SupraMarginal Gyrus	Area Pfop	62 -24 24	5.76	R
Inferior Parietal Lobule	Area PF	56 -30 52	5.7	R
Cerebellum (VI)	Lobule VI	-34 -64 -24	5.88	L
Cerebellum (VIII)	Lobule VIIIa	-28 -64 -54	5.54	L
Cerebellum (VIII)	Lobule VIIb	-40 -48 -56	4.49	L
Middle Frontal Gyrus		36 48 24	5	R
Cerebellum (VIII)	Lobule VIIIb	20 -48 -52	5.27	R
Cerebellum (VIII)	Lobule VIIIa	22 -62 -50	4.32	R

Cerebellum (IX)	Lobule VIIIb	12 -52 -60	4.23	R
Cerebellum (IX)	Lobule IX	10 -58 -56	4.05	R
Cerebellum (IX)	Lobule IX	10 -58 -52	3.9	R
Vermis 8	Lobule VIIIb	0 -68 -44	3.85	
Superior parietal lobule	Area 5L	18 -50 74	4.5	R
Superior parietal lobule	Area 7A	18 -68 64	4.18	R
Superior parietal lobule	Area 7P	16 -68 54	3.7	R
HS CMA-R				
Paracentral Lobule	Area 4a	6 -30 70	7.11	R
Paracentral Lobule	Area 4a	-4 -24 72	6.38	L
Paracentral Lobule	Area 4a	8 -38 72	6.29	R
Insula Lobe		42 20 2	6.18	R
Vermis (4/5)	Lobule I IV	0 -48 -12	6.6	
Cerebellum (IV-V)	Lobule I IV	-4 -48 -16	6.32	L
Cerebellum (VI)	Lobule VI	-28 -66 -26	6.1	L
Cerebellum (III)	Lobule I IV	16 -36 -24	5.87	R
Cerebellum (VIII)	Lobule VIIIb	-20 -54 -52	5.65	L
Superior Temporal Gyrus	Area OP1	-52 -30 18	5.8	L
SupraMarginal Gyrus Area	PFcm	-52 -36 24	4.89	L
Superior Temporal Gyrus	Area PFcm	-56 -36 22	4.88	L
Inferior Parietal Lobule	AreahIP2	-48 -36 36	4.69	L
SupraMarginal Gyrus		-46 -34 32	4.55	L
Inferior Parietal Lobule	Area hIP3	-42 -42 42	4.51	L
Middle Frontal Gyrus		36 46 30	5.33	R

Table 4.2: Brain activations during matching tasks in eRR MS patients and HS

Location	Cytoarchitetonic location	MNI coordinates X Y Z	Z score	Side
eRR MS ACTIVE-UNILAT				
Paracentral Lobule	Area 6	-4 -22 68	7.11	L
Paracentral Lobule	Area 4a	-8 -34 68	6.66	L
Rolandic Operculum	Area OP2	-36 -28 16	6.41	L
Superior temporal Gyrus	Area PFcm	-48 -32 20	6.38	L
SupraMarginal Gyrus	Area OP1	-46 -30 24	6.34	L
Putamen		-28 -8 12	5.98	L
Vermis (4/5)	Lobule I IV	0 -50 -6	6.31	
Vermis (4/5)	Lobule V	4 -54 -12	6.22	
Cerebellum (III)	Lobule I IV	14 -36 -22	5.89	R
Cerebellum (IV-V)	Lobule V	22 -30 -26	5.13	R
Cerebellum (VI)	Lobule VI	28 -56 -24	4.7	R
Superior temporal Gyrus	Area PFcm	56 -34 22	6.05	R
Superior temporal Gyrus	Area PF	66 -30 22	5.35	R
SupraMarginal Gyrus	Area OP1	64 -18 18	5.08	R
Postcentral gyrus	Area PFop	58 -12 26	4.73	R
Precentral Gyrus	Area 6	54 0 48	5.91	R
Precentral Gyrus	Area 44	58 6 26	4.13	R
Postcentral Gyrus		-50 -8 54	5.81	L
Precentral Gyrus	Area 6	-40 -14 56	4.76	L
Cerebellum (IX)	Lobule VIIIb	16 -48 -52	4.65	R
Cerebellum (VIII)	Lobule VIIIa	28 -58 -52	4.64	R
Cerebellum (IX)	Lobule IX	16 -54 -50	4.53	R
eRR MS ACTIVE-BILAT				

Paracentral Lobule	Area 4a	-6 -36 70	7.37	L
Cerebellar Vermis (4/5)	Lobule V	4 -52 -8	6.87	
Cerebellum (IV-V)	Lobule V	-20 -36 -22	6.54	L
Cerebellum (VI)	Lobule VI	28 -58 -20	5.94	R
Cerebellum (IV-V)	Lobule I IV	-8 -44 -18	5.86	L
Rolandic Operculum		44 -30 22	5.82	R
Superior Temporal Gyrus	Area PFcm	54 -34 20	5.21	R
Putamen		30 -8 6	5.15	R
SupraMarginal Gyrus		50 -32 32	5.14	R
Rolandic Operculum	Area OP1	-48 -28 20	6.72	L
SupraMarginal Gyrus		-44 -36 24	6.18	L
Putamen		-28 2 6	5.64	L
Precentral Gyrus	Area 6	40 -6 50	4.9	R
HS ACTIVE-UNILAT				
Paracentral lobule		-8 -36 66	7.41	L
Posterior-Medial frontal		0 -4 64	6.24	L
Postcentral gyrus	Area 5L	-20 -42 70	5.94	L
Putamen		-28 -4 12	6.26	L
SupraMarginal gyrus	Area OP1	-54 -26 20	6.12	L
Rolandic operculum	Area OP2	-36 -28 18	5.35	L
Cerebellum (III)	Lobule I IV	10 -40 -22	7	R
Vermis (4/5)	Lobule I IV	-2 -50 -6	6.39	
Cerebellum (VI)	Lobule VI	28 -60 -20	5.82	R
Putamen		28 0 12	5.59	R
Insula lobe		44 4 4	5.25	R
Rolandic operculum	Area PFcm	48 -30 20	5.46	R

SupraMarginal gyrus	Area Pfop	56 -24 26	5.28	R
Rolandic operculum	Area TE 1.1	40 -30 16	5.22	R
Cerebellum (VI)	Lobule VI	-30 -56 -26	6.06	L
Cerebellum (IV-V)	Lobule V	-28 -38 -30	4.15	L
Fusiform gyrus	Area FG4 -42	-54 -24	3.91	L
Cerebellum crus 1	Area FG2	-40 -64 -22	3.83	L
Cerebellum (VIII)	Lobule VIIIa	24 -58 -54	5.23	R
Cerebellum (IX)	Lobule IX	12 -52 -52	4.64	R
Cerebellum (VIII)	Lobule VIIIb	18 -50 -54	4.36	R
HS ACTIVE-BILAT				
Precuneus	Area 3a	-10 -40 68	7.84	L
Paracentral Lobule	Area 4a 8	-28 66	7.45	R
Posterior-Medial Frontal		8 -18 70	6.99	R
Superior Temporal gyrus	Area Pfop	-52 -32 22	6.32	L
Rolandic operculum	Area Pfop	56 -24 22	6.31	R
Rolandic operculum	Area OP1	50 -26 22	6.27	R
SupraMarginal gyrus		-54 -32 26	5.81	L
Putamen		30 -2 12	5.73	R
Vermis (4/5)	Lobule I IV	-2 -50 -12	7.67	
Cerebellum (III)	Lobule I IV	14 -38 -22	6.77	R
Cerebellum (IV-V)	Lobule V	-20 -38 -22	6.64	L
Cerebellum (IV-V)	Lobule I IV	-20 -34 -26	6.27	L
Cerebellum (VIII)	Lobule VIIIb	20 -58 -54	5.11	R
Cerebellum (VIII)	Lobule VIIIb	-22 -50 -56	4.8	L
Cerebellum (VIII)	Lobule VIIIa	-22 -64 -54	4.53	L

Table 4.3: Brain activations during motor tasks in eRR MS patients and HS

Within-group analysis in eRR MS patients:

1) IMA-R > ACTIVE-UNILAT: the activation clusters involved the bilateral frontal areas, superior and inferior parietal lobule (SPL and IPL, respectively), primary somatosensory cortex (S1), right supramarginal gyrus (SMG), and left precuneus (Figure 4.3, Table 4.4); 2) CMA-R > ACTIVE-BILAT: the contrast revealed several clusters covering parietal and frontal areas, in particular the bilateral postero-medial frontal cortex, right SPL, SMG and S1, while the precuneus was activated bilaterally (Figure 4.3, Table 4.4); 3) IMA-R > CMA-R: cortical activations of the left paracentral lobule and of IPL were observed; 4) CMA-R > IMA-R: a cluster of greater activation was observed at the level of the right paracentral lobule (Table 4.5).

Location	Cytoarchitetonic location	MNI coordinates X Y Z	Z score	Side
IMA-R>ACTIVE-UNILAT				
Superior parietal lobule	Area 7A	18 -70 62	6.23	R
Inferior parietal lobule	Area hIP2	42 -40 48	5.34	R
Inferior parietal lobule	Area PFt	54 -34 50	5.12	R
Superior parietal lobule	Area 5L	20 -54 68	4.84	R
SupraMarginal gyrus	Area PFm	54 -36 44	4.82	R
Postcentral gyrus	Area 1	40 -44 66	4.75	R
Superior parietal lobule	Area 7A	-20 -64 54	5.72	L
Inferior parietal lobule	Area hIP3	-38 -46 46	5.1	L
Inferior parietal lobule	Area 2	-42 -42 54	5	L

Precuneus		-14 -52 58	4.99	L
Postcentral gyrus	Area 2	-40 -42 58	4.89	L
Middle frontal gyrus		32 0 56	5.89	R
Mid-cingulate cortex		8 16 44	5.11	R
Inferior frontal gyrus	Area 44	52 8 16	4.64	R
Middle frontal gyrus		-24 -6 48	5.82	L
Superior frontal gyrus		-24 -2 56	5.03	L
Posterior-Medial frontal		-16 -4 62	4.74	L
CMA-R>ACTIVE-BILAT				
Precuneus		8 -56 56	6.2	R
Precuneus	Area 7A	8 -64 58	5.94	R
Superior Parietal lobule	Area 5L	20 -52 60	5.44	R
Precuneus	Area 5L	6 -58 62	5.37	R
Precuneus	Area 5M	-10 -54 56	5.25	L
Superior frontal gyrus		28 -2 60	5.46	R
Precentral Gyrus	Area 6	34 -2 50	4.74	R
Posterior-Medial frontal	Area 6	14 14 60	3.52	R
Posterior-Medial frontal	Area 6	-24 -4 62	5.12	L
SupraMarginal gyrus	Area PFm	60 -42 34	4.99	R
SupraMarginal gyrus	Area PF	60 -36 36	4.49	R
Postcentral gyrus	Area 1	56 -24 52	4.07	R
Postcentral gyrus	Area 2	46 -24 42	3.64	R
SupraMarginal gyrus	Area PFt	56 -28 42	3.61	R

Table 4.4: Brain activations during matching tasks vs motor tasks in eRR MS

Between-group analysis for matching tasks. Motor tasks: no dif-

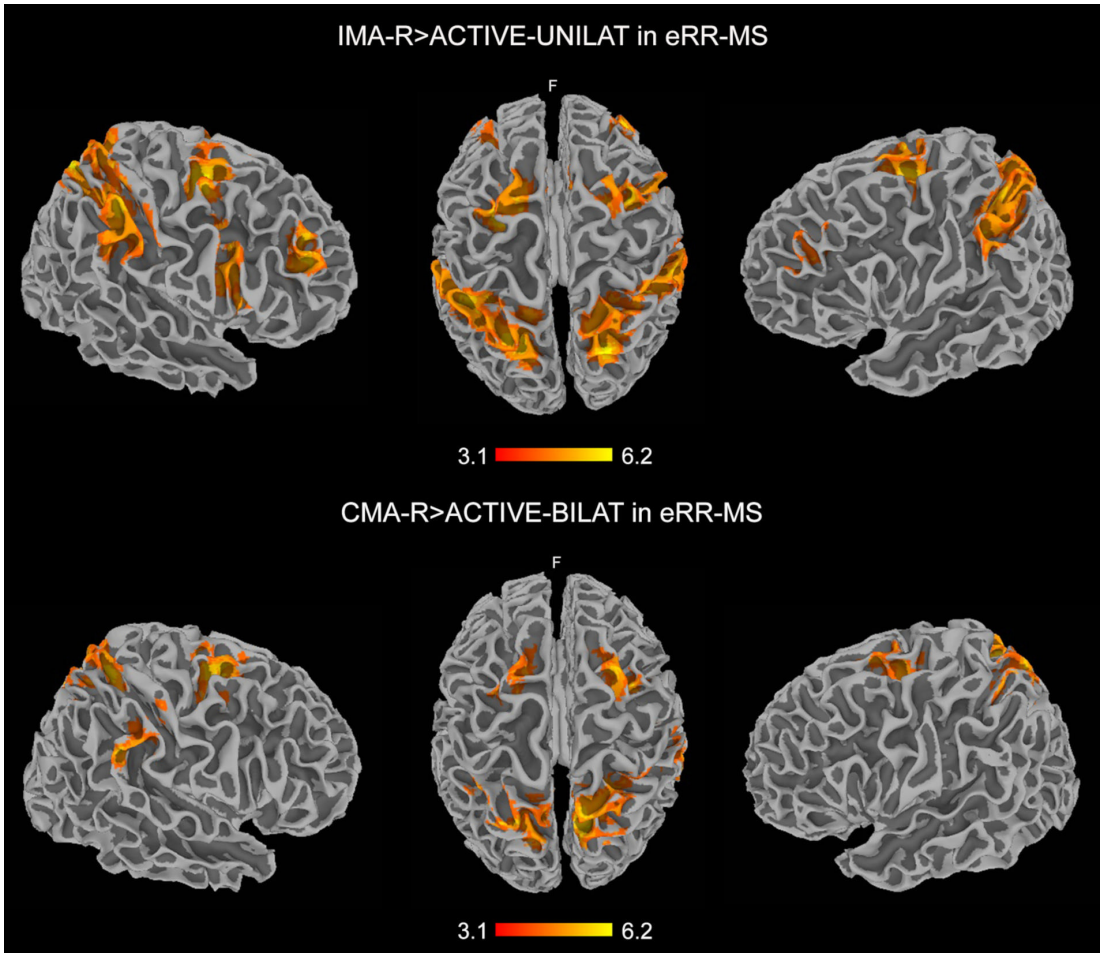

Figure 4.3: Clusters of activations resulting from the contrasts IMA-R>ACTIVE-UNILAT (top) and CMA-R>ACTIVE-BILAT (bottom), thus reflecting position sense neural correlates without the motor component of the task, in eRR MS group. The results are cluster corrected for multiple comparisons ($Z \geq 3.1$, $p < 0.0001$) and are shown in MNI space. Note the cortical activity in the bilateral fronto-parietal areas, more widespread during IMA-R>ACTIVE-UNILAT.

ferences were detected between eRR MS patients and HS during bilateral motor task; on the contrary, when performing motor task with the right foot, eRR MS patients had a greater activation, compared to HS, in the left MTG and SMG (Table 4.6). Matching tasks: differences between eRR MS patients and HS were detected between cortical activations during IMA-R but not CMA-R. (Table 4.7,

Location	Cytoarchitetonic location	MNI coordinates X Y Z	Z score	Side
IMA-R>CMA-R				
Paracentral Lobule	Area 4a	-8 -30 74	5.68	L
Precentral gyrus		-36 -2 64	4.83	L
IPL	Area hIP3	-34 -48 48	4.33	L
IPL	Area 7A	-40 -56 60	3.91	L
CMA-R>IMA-R				
Paracentral Lobule	Area 4a	8 -30 68	6.85	R
Postcentral gyrus	Area 5L	14 -40 70	6.36	R

Table 4.5: Contrast IMA-R vs CMA-R and CMA-R vs IMA-R in eRR MS patients

Figure 4.4).

Location	Cytoarchitetonic location	MNI coordinates X Y Z	Z score	Side
eRR MS patients>HS				
Middle temporal gyrus	Area PGp	-54 -62 16	4.56	L
Supramarginal gyrus	Area PFm	-56 -48 32	3.41	L

Table 4.6: Differences in brain activation during unilateral motor task (ACTIVE-UNILAT) between eRR MS and HS

Brain-behavior correlations. In eRR MS, during IMA-R, CE negatively correlated with brain activity at the level of the right S1 and SPL, while it positively correlated with brain activity at the level of the right frontal areas (Table 4.8, Figure 4.5 A-B). Instead, the CE during CMA-R positively correlated with an activation cluster at the level of the left motor and premotor area and S1 (Table 4.8, Figure 4.5 C). Moreover, the RMSAP inversely correlated with cortical activation during CMA-R, in particular with activity at the level of the right SPL and IPL and primary motor cortex (Table 4.8, Figure 4.5 D). No cortical or subcortical activation related to CE was found during either IMA-R

Location	Cytoarchitetonic location	MNI coordinates X Y Z	Z score	Side
eRR MS patients>HS				
IPL	AreahIP3	-38 -50 56	3.94	L
IPL	Area hIP2	-50 -38 42	3.35	L
PostCg	Area 1	-30 -42 66	3.2	L
HS>eRR MS patients				
MCC		-4 -40 38	4.67	L
MCC		2 -30 44	3.51	R

Table 4.7: Differences in brain activation during IMA-R between eRR MS and HS
Abbreviations: IPL: inferior parietal lobule; PostCg: Postcentral gyrus; MCC: mid-cingulate cortex.

or CMA-R in HS group.

Location	Cytoarchitetonic location	MNI coordinates X Y Z	Z score	Side
IMA-R(Negative)				
Superior parietal lobule	Area 5L	20 -46 72	5.26	R
Postcentral gyrus	Area 5L	16 -46 70	4.76	R
Superior parietal lobule	Area 7PC	22 -50 58	4.13	R
Postcentral gyrus	Area 2	28 -42 62	3.56	R
IMA-R (Positive)				
Middle frontal gyrus		36 36 48	4.52	R
Superior frontal gyrus		26 40 34	3.81	R
Inferior frontal gyrus		40 16 36	2.82	R
CMA-R (Positive)				
Postcentral gyrus	Area 4p	-44 -14 40	3.66	L
Postcentral gyrus	Area OP4	-64 -8 14	3.6	L

Precentral gyrus	Area 6	-28 -14 58	3.59	L
Postcentral gyrus	Area 3a	-44 -14 32	3.38	L
Postcentral gyrus	Area 3b	-52 -14 40	3.31	L
RMSAP (Negative)				
Inferior Parietal Lobule	Area hIP1	36 -50 40	4.17	R
Superior Parietal Lobule	Area 7PC	26 -46 46	3.95	R
Superior Parietal Lobule	Area 5L	18 -46 70	3.89	R
Superior Parietal Lobule	Area 7A	24 -66 52	3.72	R
Paracentral Lobule	Area 4a	6 -44 70	3.68	R

Table 4.8: Correlations between CE and the relative matching task activations; correlations between the behavioral parameter during quiet standing (RMS_{AP}) and brain activations during CMA-R

CC diffusion tensor metrics and relationship with behavioral performance during CMA-R and during quiet standing. Mean FA and MD values extracted from CC (reported in Table 4.1) resulted significantly different between eRR MS and HS (unpaired t-test, t(46)=3.015, p=0.004 and t(46)=-3.522, p=0.001, respectively). Moreover, when considering both eRR MS patients and HS, the FA and MD of CC correlated with behavioral performance in terms of CE during CMA-R (r=-0.298, p=0.044 and r=0.335, p=0.023, respectively), but no significant correlation was found when the two groups were considered separately. No significant correlations were found between FA or MD of the CC and RMSAP for the eRR MS group.

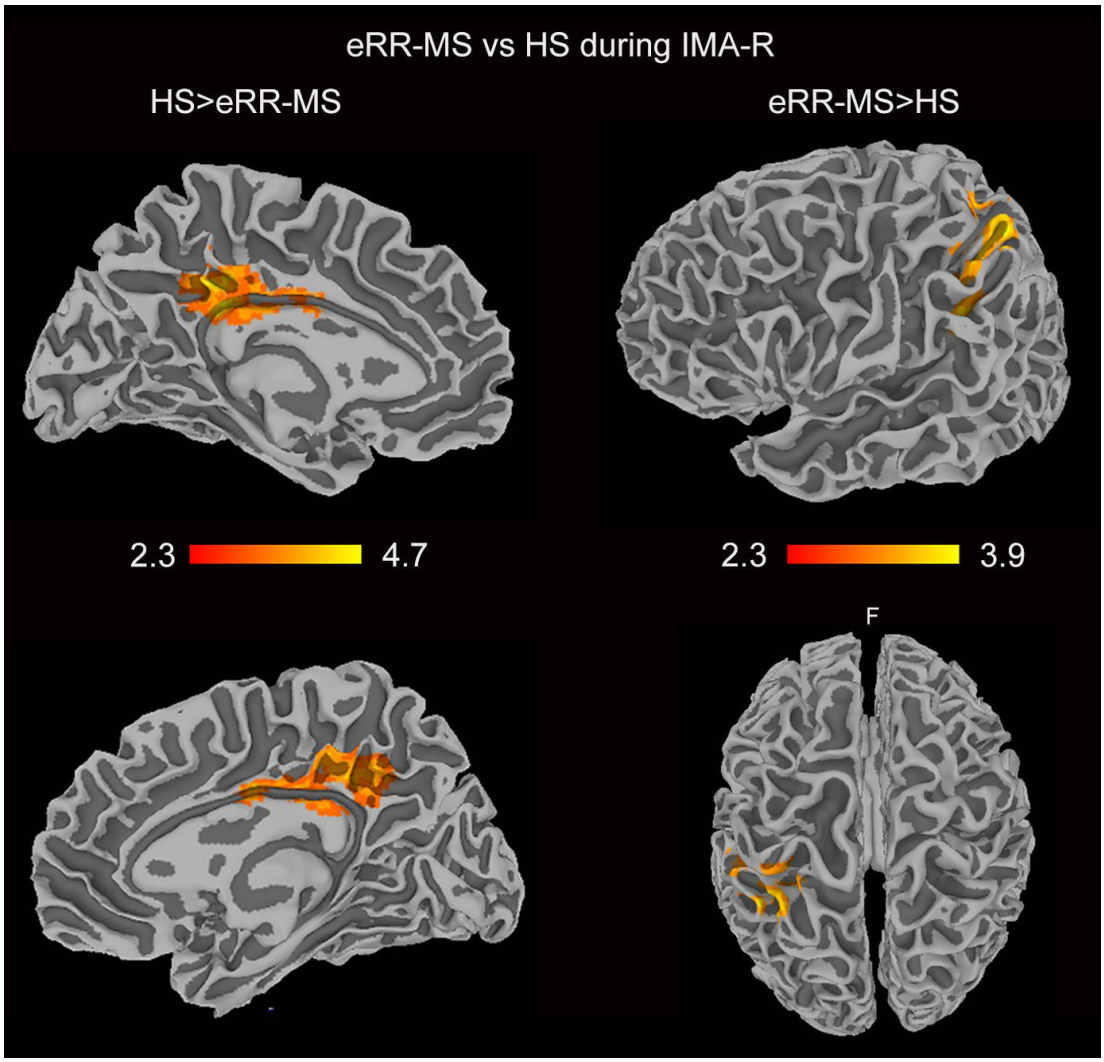

Figure 4.4: Clusters resulting from the comparison between eRR MS patients and HS brain activity during IMA-R. The results are cluster corrected for multiple comparisons ($Z \geq 2.3$, $p<0.01$) and are shown in MNI space. Note the greater activation in the mid-cingulate cortex in HS vs eRR MS and in the left parietal cortex in eRR MS vs HS.

4.4 Discussion

In this work, we describe the behavioral and neural correlates of the lower limbs position sense in eRR MS patients, as well as their relationship with balance per-

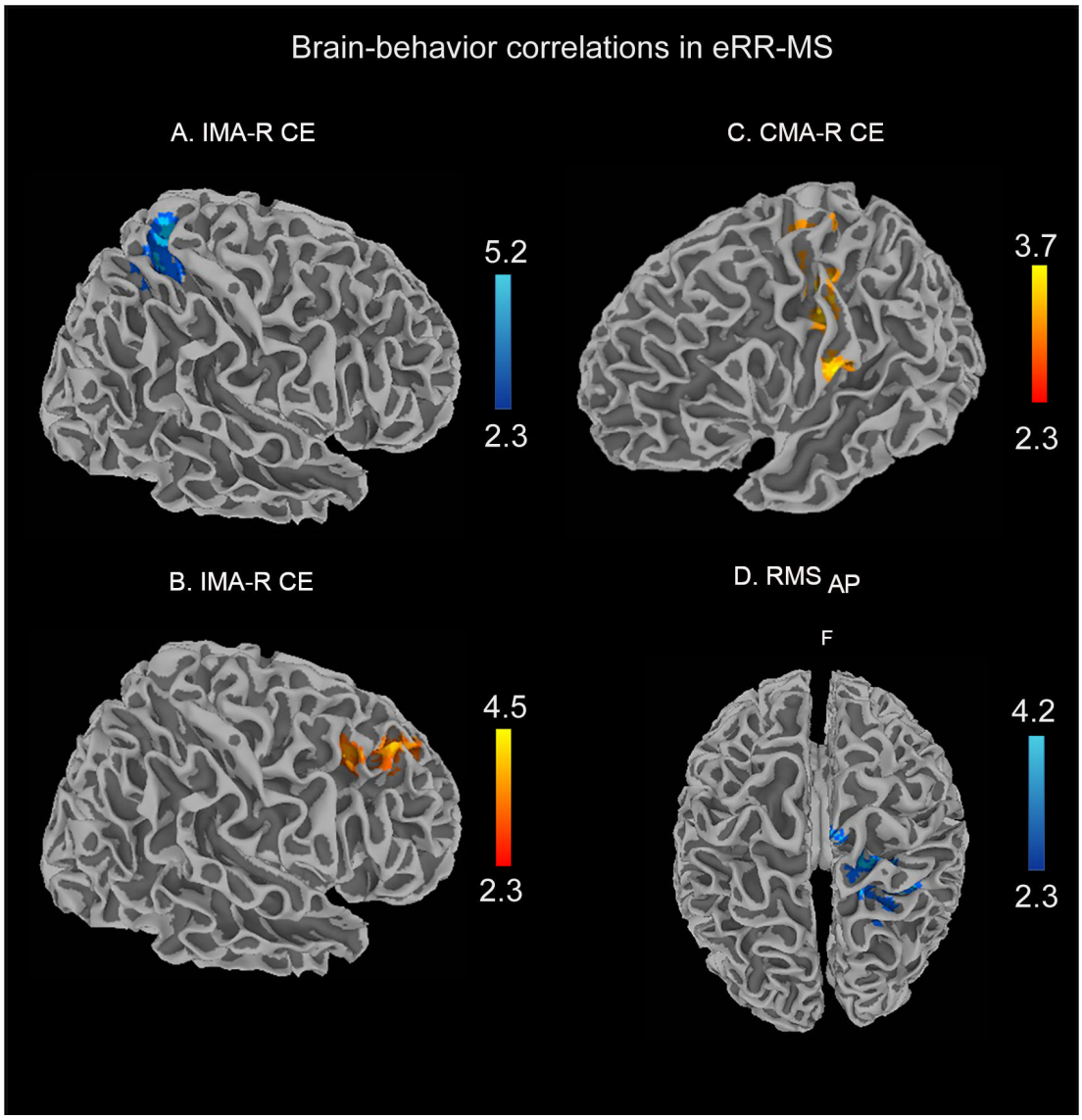

Figure 4.5: Clusters resulting from the correlation between BOLD signal and behavioral parameters during matching tasks (CMA-R and IMA-R CE) and during quiet standing (RMSAP) in eRR MS patients group. The results are cluster corrected for multiple comparisons ($Z \geq 2.3$, $p < 0.01$) and are shown in MNI space. Brain activity during IMA-R presented both negative and positive correlations with the CE (A and B, respectively) while during CMA-R only a negative correlation was found (C). RMSAP negatively correlated with brain activity during CMA-R task (D).

formance during quiet standing. In summary, eRR MS patients presented a worse systematic matching error than controls during contralateral but not during ipsilateral task. However, compared to HS, eRR MS patients showed a functional reorganization involving the parietal areas during the ipsilateral matching task, while no differences between the two groups were found during CMA-R. Moreover, both the behavioral metrics and the neural activity during CMA-R correlated with the performance during quiet standing. Lastly, the worse performance during the contralateral task correlated with the damage at the level of the CC.

Position sense deficits and their neural correlates during lower limb matching tasks. In our study, both groups had a greater error during the contralateral than during the ipsilateral matching tasks and this may be explained by the greater complexity of the former, that is associated to a higher likelihood of error [66; 230]. Moreover, eRR MS patients had worse proprioceptive performance than HS during the contralateral but not during the ipsilateral matching task. This latter finding is relevant from a clinical point of view since it indicates that contralateral matching tasks can reveal subtle position sense deficits that are below the sensitivity of the standard clinical examination, as shown by the normal median s-FSS in our population of eRR MS patients. Moreover, this result highlights the limits of the most used rating scale for assessing disability in MS, the EDSS, in properly evaluating deep sensation deficits. In fact, in the EDSS, position sense is scored together with other somatosensory modalities, thus making its impact on disability not easy to estimate. The introduction of a quantitative measure of proprioceptive deficits in the clinical practice could help overcome this limit. Although an indirect quantitative characterization of the proprioceptive impairment in patients with MS, employing posturographic or electrophysiological measurements, has been suggested by previous studies [251; 252], matching tasks allow for a direct assessment of position sense and a

quantification of the related deficits [66].

As for the neural correlates of position sense, a predominant fronto-parietal activity was detected in eRR MS patients when the contrasts between matching tasks and pure motor tasks (IMA-R>ACTIVE-UNILAT and CMA-R>ACTIVE-BILAT) were examined. Frontal areas play a role in sensory attentional and spatially oriented processing but also in working memory processing [253; 254] while parietal regions are involved in the processing of proprioceptive information [255], reorienting,[256] recognition of a matching position during visually guided tasks [257] and with the modulation of spinal motor output during movement preparation [258]. Another relevant and novel finding of our study is the observation of a significant increase of brain activity in patients, compared to HS, during the ipsilateral matching task. This result, in combination with the absence of significant differences in behavioral performance between the two populations for this task, suggests an efficient supplying functional reorganization occurring during the execution of a simpler task such as the ipsilateral matching task. Conversely, during the contralateral matching task, the modulation of functional activity was not accomplished or not sufficient, resulting in a compromised behavioral performance. We found further evidence in support of the occurring functional reorganization. In fact, in eRR MS we found a negative correlation between CE during IMA-R and activity in the right parietal areas, but a positive correlation with right frontal areas. This result could further support a fronto-parietal functional reorganization, at the level of the right hemisphere, underlying the lower rate of proprioceptive errors. Moreover, the positive correlation between CE during IMA-R and the right frontal cortex activation could imply the role of the spatial attention [259] in the execution of the task. On the contrary, we could speculate that the positive correlation found between post and precentral gyrus activation and CE during CMA-R represents an inefficient attempt to improve

the task performance. No correlations were found in the HS group between brain functional activity and behavioral parameters during the matching tasks, further suggesting that the findings in eRR MS group are indicative of mechanisms of functional plasticity.

Correlations with behavioral parameters during quiet standing. In eRR MS patients, the amplitude of the antero-posterior oscillations of the center of pressure (RMSAP) during quiet standing correlated positively with the errors (CE) during CMA-R, suggesting that the position sense deficits, measured with matching tasks, affect balance during quiet standing. The amplitude of the postural sway displayed also an inverse correlation with activations in different brain areas, and specifically at the level of the right parietal lobe, suggesting that a deterioration of balance performance due to proprioceptive deficits is associated with an increased activity in the brain area processing position sense.

Behavioral performance during matching tasks and CC diffusion tensor metrics. The behavioral performance during CMA-R was significantly associated with the mean FA and MD values of the CC, leading us to speculate that during a bilateral task, such as the contralateral matching task, structural damage at the level of the CC prevents an efficient interhemispheric transfer of information as well as a functional cortical reorganization to compensate and guarantee a normal behavioral performance. Interestingly, results from previous studies seem to support this interpretation. In fact, a correlation between sensori-motor cortex functional connectivity and structural alterations of the CC, measured by means of DTI parameters, has already been reported in patients with eRR MS [260]. Likewise, in a DTI study on HS, bimanual task performance in absence of augmented visual feedback was significantly correlated with CC structural properties [261].

This study has a few limitations. First of all, the relatively small sample size

of our patients' group that included only subjects in the early stage of the disease. Although our approach and our findings are novel, they will have to be confirmed in larger populations of patients and at different stages of the disease. Admittedly, the lack of availability of postural control parameters in our controls' group limits the interpretation of the relationship observed between quiet standing behavioral measures and brain activity during matching tasks. However, the measurement of patients' postural control parameters has been instrumental to the assessment of the impact of our findings on balance. Moreover, our MRI protocol did not include sequences for the structural and functional assessment of spinal cord integrity thus precluding the investigation of the contribution of spinal cord abnormalities to proprioception processing. Lastly, although we performed this analysis on patients with low disability, the assessment of position sense by matching tasks on a sample of patients with moderate or severe disability could be influenced by their cognitive abilities, in particular in terms of attention. Therefore, cognitive assessment would be useful to exclude patients with attention impairment or to correct the results accordingly. At moderate or severe stages of the disease, other methods of proprioception assessment, such as the active movement extent discrimination apparatus, which requires less memory and attention [64], would be more appropriate.

Chapter 5

Functional connectivity in patients with progressive multiple sclerosis

Summary

Here are presented the rationale and methods of the study of the functional connectivity in patients with progressive multiple sclerosis, the results and their interpretation.

5.1 Introduction

Progressive multiple sclerosis is characterized by a compartmentalised and a lower burden of inflammation associated to neurodegeneration, with axonal and neuronal loss. However, a brain adaptation and reactive changes to damage occur even at this stage and could account, at least in part, for the gap between conventional imaging features and clinical disability. In fact, it's still debated whether

changes detected with both structural and functional imaging reflect an adaptive or a maladaptive response. Nonetheless, both a compensatory and a maladaptive modulation could occur at the same time.

Previous studies on patients with progressive MS revealed reduced functional activation within the default mode network (DMN) in both PP MS and SP MS compared to healthy controls, although the reduction was observed in different areas [262]. During task fMRI, cognitively impaired PP MS patients revealed an increased functional activity during the performance of a cognitive task, which inversely correlated with the cognitive status and increased activity within the motor network during a motor task [140; 263]. A recent study showed in patients with progressive MS increased FC after a rehabilitation training of the upper limbs, which correlated with the motor improvement [264]. Although task fMRI could reveal changes related to a specific treatment, is more influenced by the task itself since the performance would be more affected in more clinically impaired patients. rs-fMRI analysis doesn't suffer from this disadvantage and could offer a more straightforward insight on the mechanisms subtending the clinico-radiological gap observed also in the advanced stages of the disease.

While resting state functional reorganization has been largely investigated in patients with CIS and RR MS, by means of connectivity and graph metrics, studies on the global functional remodulation occurring at the progressive stage of the disease are still missing.

5.2 Materials and methods

Participants.

Forty-seven patients with either PP or SP MS and 27 healthy controls (HC) were recruited. Diagnosis of PP or SP MS was made according to McDonald's

criteria 2010 [201]. All subjects underwent MRI and, on the same day, patients with MS underwent clinical and neuropsychological evaluation. The study was approved by the institutional review board of the Icahn School of Medicine at Mount Sinai and all the subjects gave written informed consent to participate.

Clinical and neuropsychological assessment. Patients with PP or SP MS underwent neurological examination including expanded disability status scale (EDSS), timed 25-foot walking (T25FW) test, 9-hole peg test (9HPT) and neuropsychological assessment including symbol digit modalities test (SDMT), California verbal learning test second edition (CVLT-II, considering the first five recall trials) and the brief visuospatial memory test revised (BVMT-R, considering the first three recall trials [265]). Raw scores were transformed into z-scores according to [266].

MRI acquisition. All the participants underwent MRI on a 3.0 T scanner (Siemens Magnetom Skyra, Erlangen, Germany) with a protocol including the following sequences: a) T2-weighted sequence: voxel size 0.5x0.5x3 mm^3, repetition time (TR) 8000 ms, echo time (TE) 95ms; b) 3D T1-weighted sequence: voxel size:0.8x0.8x0.8 mm^3, TR 3000 ms, TE 2.47 ms, flip angle 7°, inversion time 1000 ms); c) echo planar imaging (EPI) sequence for the resting state: voxel size: 2.1x2.1x2.1 mm^3, TR 1000 ms, TE 35 ms, multi-band acceleration factor 7, flip angle 60°, 400 volumes. During resting state fMRI subjects were asked to rest with their eyes closed.

Structural MRI analysis. T2 and T1 lesion load were computed on the T2-weighted and the 3D-T1-weighted images respectively, using a semi-automated technique (Jim version 7; Xinapse Systems, http://www.xinapse.com). A lesion mask obtained on the 3D-T1-weighted images was obtained for each patient and

used to fill-in the T1-hypointense lesions [202].

Functional resting state MRI analysis. RS fMRI data were preprocessed using custom made MATLAB scripts and SPM8 (FIL, UCL, UK). Preprocessing steps included: realignment and discarding of the first 10 volumes, resulting in 390 time points. T1 images were co-registered to the individual functional space and segmented into white matter (WM), grey matter (GM) and cerebrospinal fluid (CSF). The average WM and CSF signals were obtained from standard WM and ventricular masks mapped to the subject's space and masked with the subjects' WM and CSF masks. Regression of the nuisance variables, including WM and CSF signals and the six motion parameters, was then performed using DPARSF toolbox. Framewise displacement according to Power et al. [267] was computed and subjects with a FDPower >0.5 mm in more than 25% of the volumes were discarded from the analysis [268]. In all other subjects, scrubbing was applied with contaminated volumes (FDPower>0.5mm) censored and replaced with average of the surrounding volumes. Lastly, despiking and band-pass filtering (0.01-0.15) were applied. From the initial sample of 74 subjects, 4 were excluded for issues in the structural/functional co-registration and 13 (1 HC, 8 SP MS patients and 4 PP MS patients) were excluded after motion scrubbing because more than 25% of volumes in their scans had a framewise displacement above the threshold of 0.5 mm. T1 images were processed using FreeSurfer software to obtain cortical surphace for each subject [269; 270] and registered to a the Schaefer atlas using the 100 parcels and 17 networks atlas [271]. The parcellation using FreeSurfer was preferred to a co-registration of the atlas to the individual space since the representation of the cortical thickness was more reliable.

Functional connectivity. The FC was assessed using a non parametric estimator called "accordance" e.g. a measure, range 0-1, that reflects coupling

between two ROIs. The co-activations and co-deactivations between regions are obtained by thresholding the normalized fMRI signal at positive and negative thresholds, respectively. The threshold used was the 80% quantile of the normal distribution [272]. Therefore, for each subject two matrices based on the accordance (including co-activations and co-deactivations) and discordance (reflecting the activation-disactivation between timecourses) were obtained. A Fisher's Z-transformation was further applied to the accordance and discordance matrices to improve the normality of the measure.

Graph properties. The brain connectivity toolbox ([1]) [22] was used to compute the graph measures on accordance matrices. For each region were obtained the following metrics:

- nodal strength for weighted undirected graphs
- eigenvector centrality for weighted unndirected graphs [273]
- clustering coefficient for weightes undirected graphs according to [274]
- local efficiency for weighted graphs according to [275]
- betweenness centrality for weighted graphs [276]

Statistical analysis. Chi-square test and analysis of variance (ANOVA) were used to assess differences among the three groups in gender and age, respectively. Two sempled t-test or non-parametric Mann Whitney U test were used to compare the clinical parameters between the two groups, if the condition of normality of the single variable per group was or not satisfied, respectively. Analysis of covariance (ANCOVA) was used to test differences in accordance and

[1] `http:/www.brain-connectivity-toolbox.net`

discordance and in graph metrics between HS, PP MS and SP MS patients, with age and gender as covariates. The false discovery rate (FDR) method was applied to correct for multiple comparisons across regions. To verify relationship between functional connectivity and clinical measures a partial least squares correlation (PLSC) analysis was performed [277]. Two analysis were performed: i) for the first PLSC analysis EDSS score and the pyramidal, sensory and mental functional system scores were included, ii) in the second one the T25FW test and the 9HPT (using the averaged score between the dominant and non dominant hand); were included as measures of motor disability, iii) in the third one the SDMT, BVMT T1-3 and CVLT T1-5 as measures of cognitive disability. The correlation components obtained with singular value decomposition underwent permutation testing (300 permutations) and bootstrapping (300 bootstrap samples) to assess, respectively, the significance and stability of behavior and brain weights. Only the accordance measure of FC was tested as brain variable. We discarded the cerebellar, visual, bladder/bowel and brainstem functional system scores of the EDSS since these score can be considerably affected by damage at the level of the spinal cord, the cerebellum or the brainstem.

5.3 Results

Demographic and clinical characteristics. Demographic data for the three groups and clinical data for the patients with MS are reported in Table 1. HC, SP MS and PP MS patients did not show significant differences in gender ($\chi(1)$=2.882, p=.237) or age (F(2,27)=1.462, p=.241). See Table 5.1

Functional connectivity. ANCOVA analysis among the three groups revealed differences in functional coupling, defined by the accordance metric, be-

	HS(N=25)	PPMS(N=18)	SPMS(N=14)	p
Age	47.28 ± 8.74	49.39 ± 10.42	52.64 ± 9.16	0.241
Gender	10 F; 15 M	11 F; 7 M	9 F; 5 M	0.237
Disease duration (years)	-	9.17 ± 4.76	23.36 ± 13.83	<0.001
EDSS° (median; range)	-	5.0; 1.0-6.5	6.0; 3.0-6.5	0.565
SDMT°	-	45.47 ± 16.62	49.71 ± 11.49	0.462
BVMT-R T1-3	-	17.24 ± 8.98	16.92 ± 8.18	0.922
CVLT-II T1-5	-	58.78 ± 13.52	49.64 ± 11.29	0.051
T25FW°	-	7.28 ± 2.24	9.78 ± 4.96	0.320
9HPT-Avg°	-	30.99 ± 10.17	31.56 ± 8.62	0.578
9HPT-D°	-	27.64 ± 9.15	29.52 ± 6.18	0.295
9HPT-ND°	-	32.11 ± 10.55	33.61 ± 12.82	0.721
years of education	-	16.61 ± 2.64	16.57 ± 2.14	0.964

Table 5.1: Demographic and clinical data. °: tested with non parametric Mann-Whitney U test. Abbreviationa: EDSS: expanded disability status scale; SDMT: symbol digit modalities test; CVLT-II: California verbal learning test second edition; BVMT: brief visuospatial memory test revised; T25FW: timed 25 foot walking test; 9HPT-Avg: average of the 9-hole peg test of the dominant and non dominant hand; 9HPT-D: 9-hole peg test of the dominand hand; 9HPT-ND: 9-hole peg test for the non dominant hand

tween regions of the visual network, salience, default mode, dorsal attention, control and temporo-parietal networks. However, no connections survived after correction for multiple comparison. Instead, discordance showed anticoupling between regions of the default, control, salience and temporoparietal networks. The anticoupling between precuneus and parahippocampal cortex survided multiple comparison correction, with a posthoc comparison revealing a reduced discordance in SP MS patients. No significant differences were found between PP MS and SP MS patients (Figure 5.1).

Graph Properties. No differences were in graph metrics survived multiple comparison correction.

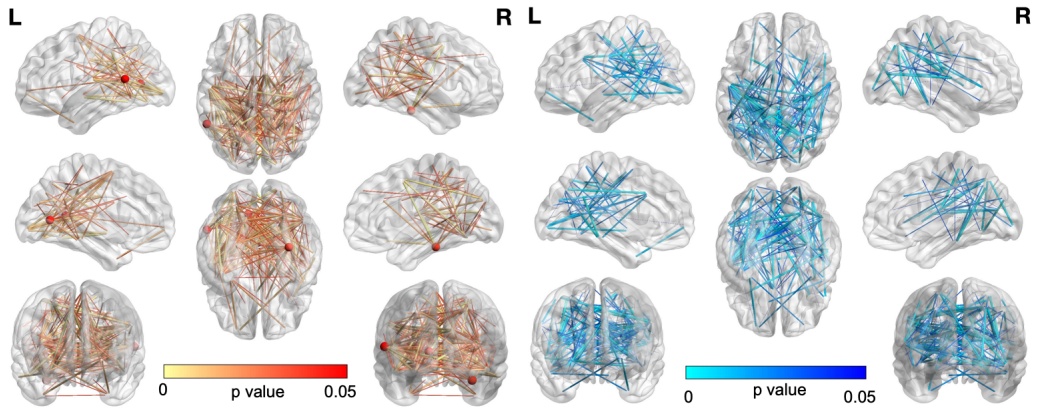

Figure 5.1: Differences between HS and MS patients in nodal strength and accordance (left) and in discordance (right) measures. Both nodal strength and coupling/anticoupling are thresholded at $p<0.01$ for visualization purposes.

Correlations with clinical disability. The PLSC analysis revealed two significant association between FC, expressed with accordance and clinical parameters: the first with EDSS ($p=0.003$), and the second one ($p=0.033$) with motor disability, expressed by both TF25TW and 9HPT scores. The third PLSC did not show any significant correlations between FC and cognitive test scores. In the significant correlation component of the first PLSC analysis a FC pattern including connections mainly between areas of the DMN (in particular the posterior cingulate cortex (PCC) and the temporal and retrosplenial cortices) and the precuneus with regions of the dorsal attention, salience end sensorimotor networks correlated with the global EDSS for both PP and SP MS groups. This FC pattern correlated also with EDSS functional system scores: with the sensory functional system score for the PP MS patients and with the pyramidal functional system score for both groups but in opposite directions (a direct weak correlation for SP MS group and a stronger negative correlation for PP MS group) (Figure 5.2). Regarding the second PLSC analysis, the correlation was driven mainly by the T25FW scores of SP MS patients and mainly involved connections of the

prefrontal regions of the DMN with sensori-motor network regions (positive correlation) and between sensori-motor regions, post central and fronto-medial areas and of the postcentral areas (negative correlation). The results in the first PLSC analysis were mainly driven by the PP MS group, while in the second by SP MS group (Figure 5.3).

5.4 Discussion

The first novelty of this work is the analysis of the functional connectivity expressed by both a coupling and anticoupling between timecourses in patients with progressive Multiple Sclerosis. The results indicate that patients with progressive MS, compared to HS, showed a different functional coupling and anti-coupling among multiple network but the greatest difference was captured by anti-coupling, suggesting this could be a novel measure to include in further studies.

The study of the functional reorganization in progressive MS is quite intriguing: the motor task fMRI studies have consistently showed an increased activation in SP and PP MS patients compared to controls and RR MS patients [142; 263; 278]. Cognitive task fMRI studies revealed a greater activity in the cognitively impaired group of patients [140] and in SP MS group compared to patients with clinically isolated syndrome [143]. On the contrary, there is a relative lack of resting state fMRI studies, with the few available focusing on specific networks [141; 262].

Resting state fMRI in the inflammatory phase of the disease has instead received a larger attention, with most of the studies on patients with RR MS or CIS, showing an increase in functional connectivity. Previous studies also indicate that the functional reorganization is related to white matter structural general

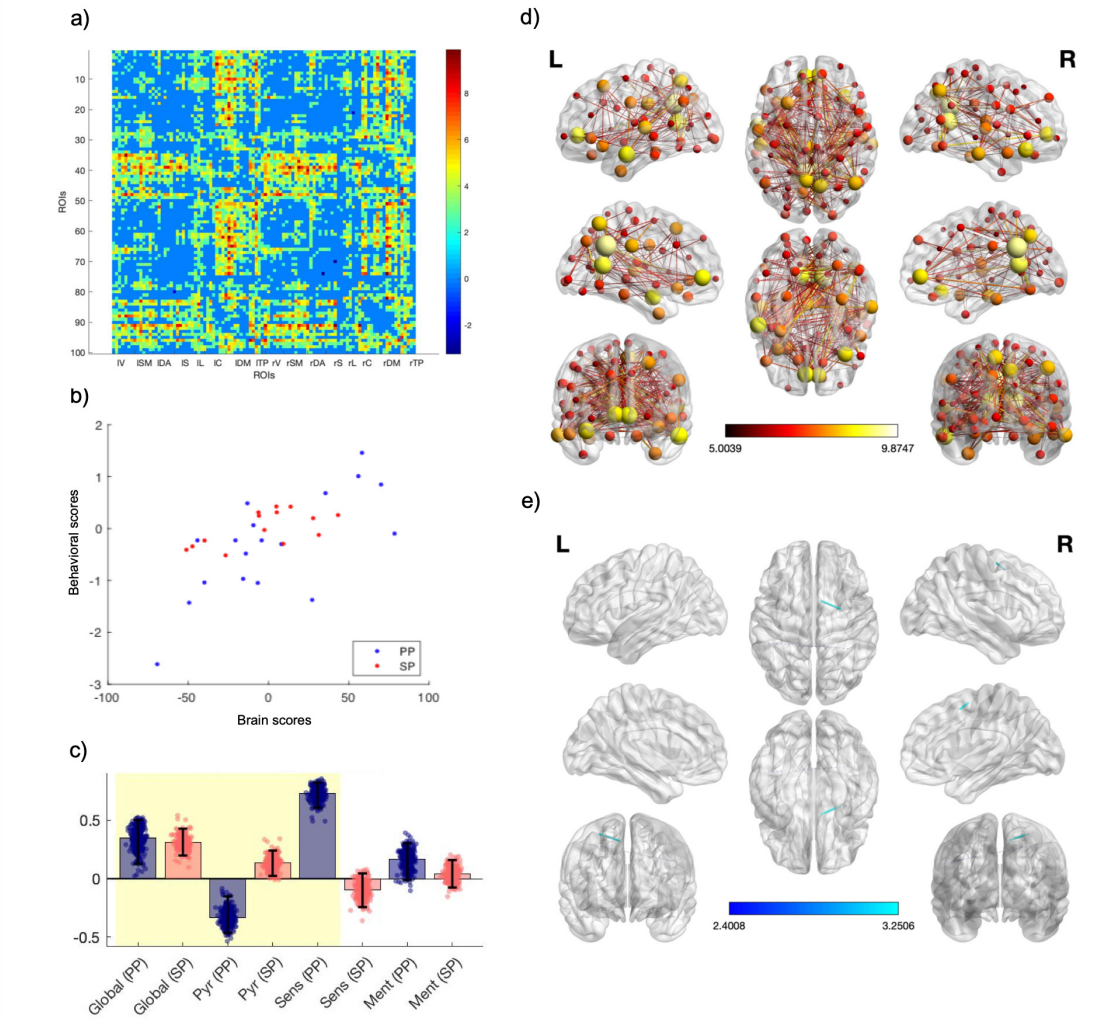

Figure 5.2: a) bootstrap ratio results, indicating pattern of ROIs positively and negatively correlated with disability score (global EDSS score, pyramidal, sensory and mental functional system scores); networks are indicating on x axis and the ROIs number on y axis; b) correlation between behavior and brain scores as resulting from the significant latent variable; c) design saliences, showing the strong effect of the PP MS subgroup; d) nodal strength of positive weights in the 100 ROIs with edges representing the bootstrap scores, indicating positive correlation and corresponding to positive values in A; e) nodal strength of negative weights in the 100 ROIs with edges representing the bootstrap scores, indicating negative correlation and corresponding to negative values in A). lV: left visual network, lSM: left somatomotor network, lDA: left dorsal attention network, lS: left salience network, lL: left limbic network, lC: left executive control network, lDM: left default mode network, lTP: left temporo-parietal network, rV: right visual network, rSM: right somatomotor network, rDA: right dorsal attention network, rS: right salience network, rL: right limbic network, rC: right executive control network, rDM: right default mode network, rTP: right temporo-parietal network.

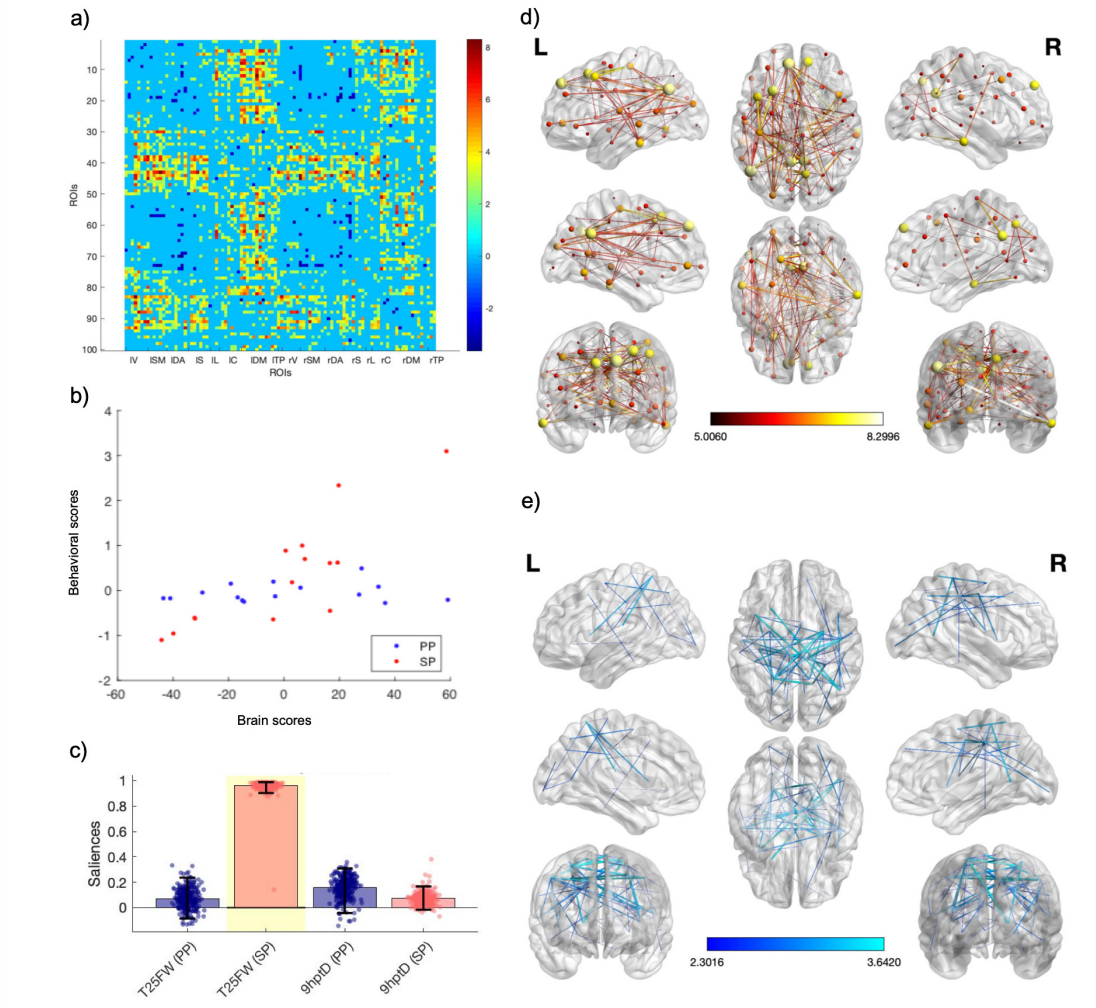

Figure 5.3: a) bootstrap ratio results, indicating pattern of ROIs positively and negatively correlated with motor disability score (T25FW and 9HPT); networks are indicating on x axis and the ROIs number on y axis; b) correlation between behavior and brain scores as resulting from the significant latent variable; c) design saliences, showing the strong effect of the SP MS subgroup; d) nodal strength of positive weights in the 100 ROIs with edges representing the bootstrap scores, indicating positive correlation and corresponding to positive values in A; e) nodal strength of negative weights in the 100 ROIs with edges representing the bootstrap scores, indicating negative correlation and corresponding to negative values in A). lV: left visual network, lSM: left somatomotor network, lDA: left dorsal attention network, lS: left salience network, lL: left limbic network, lC: left executive control network, lDM: left default mode network, lTP: left temporo-parietal network, rV: right visual network, rSM: right somatomotor network, rDA: right dorsal attention network, rS: right salience network, rL: right limbic network, rC: right executive control network, rDM: right default mode network, rTP: right temporo-parietal network.

dysruption [122; 123] and to focal lesions [279]. However, in the progressive stages of the disease focal inflammation phenomena are more rare while diffuse neurodegenerative processes become predominant. Observing the course of functional modulation occurring in other neurological diseases resulting in focal and acute damage could help in the interpretation. A longitudinal study on patients with stroke showed that the asymmetry in resting state FC between ipsi- and contra-lesional motor area was larger in patients compared to healthy controls at onset and one month after the stroke but no differences were found after 3 and 6 months [280].

We could speculate that during the inflammatory stages of MS the acute damage in the white matter would result in a more evident modulation of FC while in the progressive stages changes are more subtle. Recently a novel definition of the clinical course in patients with MS has been proposed, implying a subdivision of clinical phenotypes based on disease activity and disease progression based on the assumption that they reflect an ongoing inflammatory or neurodegenerative process, respectively, with a different impact on the prognosis, therapeutic decisions and trials outcome [90]. A future direction for the study of functional connectivity in patients at the progressive stage would be the exploration of differences between patients with active disease, expressed in terms of both clinical relapses and the detection of new lesions on MR imaging.

Nonetheless, in this work we found that functional connectivity explains motor and global disability. In particular, the global EDSS score in PP and SP MS groups and the sensory functional score in PP MS were associated to a stronger spread connectivity between regions of the posterior DMN, mainly the PCC, and of the precuneus with other networks such as the dorsal attention, salience and sensori-motor networks. A greater functional connectivity between regions of the DMN and sensori-motor regions explained also the worse score of the T25WT in

patients with SP MS. Altogether these results indicate that a stronger coupling between regions of the DMN and other networks associates with a greater disability in patients with progressive MS. Previous studies focused on the relationship between FC and cognitive tests, revealing a positive association between cingulate and medial prefrontal cortex functional activity and a better cognitive performance [262] or a decreased FC between the executive control and attentional networks [141]. While in our study we did not find any significant association between cognitive tests and functional connectivity, we could hypothesize that a resilience in the FC of the DMN and a less fluid and dynamic could explain at least in part the clinical disability occurring at a more chronic stage of the disease. The investigation of the dynamic functional connectivity and of the relationship with the structural damage could help clarifying and extend these results.

Graph metrics did not showed significant differences between patients and controls. However, brain graph analysis present a large statistical variability [281] and in previous studies differences in functional graph metrics did not survive multiple comparison correction [118] or different methods other than FDR were used [134]. Limitations of this work include the small sample size, the lack of measures of subcortical functional connectivity and of structural damage. Altogether, the results of this work suggest that more subtle changes in resting state functional connectivity occur at the late and chronic stage of MS. Further investigation including longitudinal measures and markers of white matter damage are needed.

5. FUNCTIONAL CONNECTIVITY IN PATIENTS WITH PROGRESSIVE MULTIPLE SCLEROSIS

Chapter 6

Neural correlates of action observation in patients with Parkinson Disease

Summary

Here are presented the rationale and methods of the study of the neural correlates of action observation in patients with Parkinson disease with or without freezing of gait, the results and their interpretation.

6.1 Introduction

The observation of someone performing an action recruits brain areas that are activated also during the action execution. The physiological bases of this phenomenon rely on the mirror neuron system (MNS), firstly discovered in the ventral premotor cortex of monkeys (area F5)[179]. Further neurophysiological and brain imaging studies confirmed a mirror mechanism is also present in humans [180],

thus providing a first potential localization of the MNS.

MNS has been identified as the neural substrate for action observation (AO) training, observation plus repetition of actions, which has been proposed as a rehabilitation strategy in neurological disorders, including Parkinson's disease [282]. However, whether the MNS, and thus the efficacy of AO, is preserved or altered in patients with PD is still controversial [178] Indeed, voluntary movement imitation seems to be preserved [283] and movement observation is accompanied by bilateral beta reduction in subthalamic power and cortico-subthalamic coherence [284; 285]. On the contrary, the modulation of motor evoked potentials [286] as well as the event-related mu-rhythm desynchronization [287] during AO have been showed to be impaired in PD.

Gait disorders are frequent in PD patients but, in spite of their major effects on disability, their neural correlates remain quite unknown. Most of studies exploring the neural correlates of gait in PD patients have been performed with fMRI using a task of motor imagery, and some discrepancies have been reported when comparing patients with and without freezing of gait (FOG) [192; 288].

It has been demonstrated that AO training is effective in improving levodopa-resistant gait disturbances such as FOG [181]. In a recent study, Agosta and coworkers [289] showed that PD patients with FOG, after a 4-week training based on observation plus execution of gait, exhibited a clinical improvement and an increased recruitment of cortical areas involved in motor and attentional control. However, in this study, the Authors focused only on patients with FOG and used a specific task to emphasize FOG, while there are no data in the literature about the neural correlates of AO of gait in patients with or without FOG.

In addition, it should be considered that most previous studies have explored brain activity during gait in patients with PD in the "off" state [289; 290]. Although this may unveil the functional reorganization and reflect more accurately

the physiopathological substrate of the disease, it prevents the comprehension of the neural functional mechanisms underlying behavioral performance in the every-day life of PD patients. This prompted us to design a functional MRI (fMRI) study in order to evaluate the neural structures recruited during the observation of human-gait in PD patients with (FOG+) or without FOG (FOG-) while in the "on" state, and to investigate the relationship between AO-induced brain activation and gait performance.

6.2 Materials and methods

Subjects. A total of 54 subjects (33 PD subjects and 21 healthy adults) were prospectively enrolled in the study. Participants with idiopathic PD (according to the UK Brain Bank criteria [291], were recruited at the outpatient Movement Disorders clinic (Department of Neuroscience) of the University of Genova (Italy). Healthy subjects (HS) were recruited from local community groups and from caregivers and relatives of PD patients. The study was approved by the regional ethical committee and was performed according to the principles of the Declaration of Helsinki. Written informed consent was obtained from each participant prior to study entry. Participants were excluded if they had an history of neurologic disorders other than PD, if they scored ¡25/30 at the Mini-Mental State Examination (MMSE) [292], if they had visual impairments that could hinder task-fMRI acquisition and any musculoskeletal disorders that could hamper gait task, or if they needed assistance during walking. In PD subjects, severity and stage of the disease were evaluated with the MDS–Unified Parkinson Disease Rating Scale [293] and the Hoehn and Yahr stage respectively [294] . The presence of FOG was assessed according to the new FOG questionnaire [295].

Study design and procedures The study consisted of two separate experi-

mental sessions (gait evaluation and AO fMRI) performed by each participant in two different days. The first day, demographic and clinical characteristics were collected, then participants were randomly assigned and underwent to either gait assessment evaluations or AO fMRI. The second day subjects performed the other part of the study protocol. Each session was scheduled at the same time for each participant. The sessions were scheduled over a period of 7 days. All PD patients were under treatment with dopaminergic therapy and clinical and instrumental evaluations took place during the "on" state ($\approx$ 1 hour after taking antiparkinsonian medications).

Gait evaluation Participants were required to walk at their comfortable speed (labeled as Normal Walking - NW); on a sensorized mat (GaitRite®, CIR Systems Inc. Clifton, US) for 1 minute. The GaitRITE ($\approx$ 7 m long) was positioned in the center of the room so that there was a minimum of 3 m of open space at either end and a minimum of 2.5 m at either side. This arrangement provided sufficient open space to minimize gait acceleration and deceleration while walking on the walkway. The Proto-Kinetics movement analysis software was use for analyzing the spatiotemporal gait parameters. Cadence (i.e. number of steps x minutes), gait velocity (GV), stride length (SL) and their coefficients of variability (CV; Standard deviation/Mean *100) were then determined. Kinematic data of gait were determined from all steps recorded during the entire task.

Action observation and fMRI Task The MRI protocol aimed to assess the functional activity during AO; we chose a block fMRI design with 30 seconds of rest (one block) followed by 30 seconds of task, 8 blocks total. After standardized verbal instructions, subjects were required to carefully watch a third-person videoclip representing human gait, inside the magnetic resonance scanner. The walker proceeded from the left to the right of the screen, on a neutral background,

so that participants watched the human gait on a sagittal plane. Participants watched the videoclip by looking at the mirror positioned on the head coil. The mirror reflected the human gait video displayed on a screen placed inside the magnet room, located $\approx$ 1 m far from the bottom of the scan. A video-projector was connected with a computer and placed outside the magnet room. A custom-made Matlab Software (Mathworks, Massachusetts, USA) synchronized videoclip onset with fMRI acquisition. Cushions were used to avoid head motion and the mirror on the head coil was carefully adjusted to ensure a clear vision of the screen to each participant.

Functional MRI image acquisition and preprocessing. Images were acquired on Signa Excite 1.5 MRI (Signa Excite General Electric Healthcare, WI, USA) with 8-channels phased array head coil. The MRI protocol included a T2-weighted sequence (TR/TE= 2340/102 ms, voxel size: $0.94x0.94x4\ mm^3$), Fast Spoiled Gradient Echo (FSPGR) 3-D T1-weighted sequence (TR/TE= 11.70/5.12, voxel size: $1x1x1\ mm^3$) and a single-shot echo-planar imaging (EPI) sequence (TR/TE = 3000/60 ms, slice thickness = 4 mm, pixel size = 3.75 mm^2) for fMRI task during action observation of gait. Initial pre-processing step included the despiking (detection and reduction of extreme time series outliers by fitting a smooth curve insensitive to extreme outliers to the data), performed in AFNI (`https://afni.nimh.nih.gov`) (Cox, 1996). Brain extraction was performed with FreeSurfer skull stripping on the T1-weighted anatomical sequence [241]. The other pre-processing steps were performed using FSL (FMRIB's Software Library, `https://fsl.fmrib.ox.ac.uk/fsl/fslwiki`) [243; 296] as implemented in FEAT [244; 245], including: removal of the first 3 volumes, motion correction using MCFLIRT (`https://fsl.fmrib.ox.ac.uk/fsl/fslwiki/MCFLIRT`) [242], slice-timing correction for regular ascending acquisition (using Fourier-space time series phase-shifting), spatial smoothing (Gaussian kernel, FWHM=6

mm), grand-mean intensity normalization of all volumes by a single multiplicative factor, and high-pass temporal filtering (Gaussian-weighted least-squares straight line fitting, sigma=30 sec). T1-weighted brain images were segmented into white matter (WM), grey matter (GM) and cerebrospinal fluid (CSF) using FAST [246]; then the WM and CSF masks were registered to the functional space and the average of the raw time-series within each mask was derived in order to obtain the nuisance signal from WM and CSF.

Statistical analysis

Demographics, clinical data and gait assessment. Analyses were performed using Statistical Package for the Social Sciences (SPSS) version 22 and means and standard deviations (SD) were calculated for all dependent variables. Gender differences among groups (PD FOG+, PD FOG- and HS) were assessed using the Chi-square procedure. For age and education group differences were assessed by the non-parametric Kruskal-Wallis test because data were not normally distributed (according to the Kolmogorov Smirnov statistical test) and group to group comparison was performed using Mann-Whitney U-test. For gait kinematic parameters, that were normally distributed, a one-way ANOVA was used to perform groups comparison. For clinical data the comparison between PD FOG+ and PD FOG- groups was done using an unpaired t-test. P values < 0.05 was considered significant.

Functional MRI. One explanatory variable (EV) was defined to model the On-Off periods of the task (action observation, AO) and convolved with the hemodynamic response function (HRF), to detect task-related activity. The 24 motion parameters calculated during motion correction were added as confound EVs together with the mean CSF and WM signals. Boundary-based registration BBR (Greve and Fischl, 2009) was used to register each individual functional data to the corresponding T1-weighted brain image. Then, linear affine 12 de-

gree of freedom registration was performed to register each subject's T1-weighted brain to the standard space (MNI152 brain template, voxel size: 2 mm^3) [242]. A one-sample t-test was used to model group mean activation for both PD patients and healthy controls. Differences between the two groups (HS and PD) were investigated using a two-sample unpaired t-test, adding age and gender as covariates. Moreover, to test for significant differences among FOG+, FOG- and HS groups, ANCOVA, with age and gender as covariates, was used. Results were converted to Z-values and then thresholded at $Z = 2.3$ for cluster formation and significance threshold corrected for multiple comparisons ($p < 0.05$). The correlations between brain activations of HS or PD patients (both FOG- and FOG+ groups) and the behavioral measures, in particular GV, SL and their CV (i.e. $GV - CV$ and $SL - CV$), were modeled separately with age and gender as covariates. $Z - maps$ were thresholded at $Z \geq 2.3$ for cluster formation, followed by with a significance threshold of p = 0.05 (cluster corrected using Gaussian Random Field Theory). Brain functional activations were labeled using the Eickhoff atlas (SPM Anatomy toolbox) [248].

6.3 Results

Demographics and clinical data. Two PD subjects could not complete the MRI examination. Moreover, two subjects were excluded from the analysis because they resulted outliers at the behavioural performance (i.e. needed assistance during gait task). Thus, results were obtained from 50 participants (29 PD and 21 HS). HS (13 females) had a mean age of 64.62 years (range 22-84 years). PD patients (8 females, mean age = 70.10 years, range 60-83 years) had mild-to-moderate symptoms as indicated by a mean Hoehn & Yahr stage of 2.02 ($SD \pm 0.56$; range 1 – 3). Motor symptoms severity (i.e. MDS-UPDRS section

III) ranged from 8 to 46 and the patients' mean score ($\pm SD$) was of 22.28±11.95. Twelve PD participants were confirmed to experience Freezing of Gait (FOG+), whereas the rest ($n = 17$) were classified as PD without FOG (FOG-). At the end of the recruitment phase, age sex and education levels were similar among the three groups (PD FOG+, PD FOG- HS; $palways > 0.05$). As expected, one way ANOVA revealed that MoCA score was different among groups ($p < 0.01$). Post hoc analysis showed that PD subjects had a lower score compared to HS participants (PD FOG+ vs HS and PD FOG- vs HS p always < 0.001), whereas no difference were seen between FOG+ and FOG- patients ($p = 0.131$). When clinical data were compared between FOG+ and FOG- PD patients, no differences emerged for Hoehn and Yahr stage, UPDRS-III motor ($p > 0.05$ for all these variables). The statistics for demographic and clinical data are reported in Table 6.1.

	HS (n=21)	PD (n=29)	p value
Demographic and clinical characteristics			
Age (years)	64.62±13.52.	70.10 ± 5.16	.08
Education (years	11.16 ± 6.37	9.22±5.17	.19
MoCA score	28.81± 1.01	25.62±2.08	<.01
Disease duration(years)	-	10.55 ± 4.79	-
H&Y (stage)	-	2.02 ± 0.56	-
MDS-UPDRS (motor score)	-	22.18 ± 11.95	-
Gait Parameters			
Gait velocity (cm/s)	132.27 ± 11.84	113.89 ± 20.56	<.01
Gait velocity CV	4.40 ± 1.81	3.46 ± 0.90	.03
Stride Length (cm)	135.78 ± 11.46	122.76 ± 15.86	<.01
Stride Length CV	2.20 ± 0.61	3.21 ± 1.18	<.01
Cadence (n steps x minD)	114.51 ± 9.17	110.98 ±12.59	.29

Table 6.1: Demographic, clinical and gait parameters of participants. Reported as mean ± SD.
Abbreviations: HS, Healthy Subjects; PD, Parkinson's disease; n, number; SD, Standard Deviation; MoCA, Montreal Cognitive Assessment; H&Y, Hoehn and Yahr; MDS–UPDRS, Movement Disorders Society - Unified Parkinson Disease Rating Scale; CV, coefficient of variability.

Gait Performance. As expected, statistical analysis revealed significant differences between the two groups (PD vs HS) for most of the kinematic parameters obtained during gait task. One-way ANOVA revealed that GV and SL were different among groups ($p = 0.023$ and $p = 0.038$, respectively). Post-hoc analysis showed that both FOG+ and FOG- participants had a reduced gait speed ($p = 0.10$ and $p = 0.48$ respectively) and shorter steps ($p = 0.47$ and $p = 0.35$ respectively) compared to HS. For $GV - CV$ and $SL - CV$ statistical analysis were significantly higher (i.e., worse) in patients with PD compared to HS participants ($GV - CV$ $p = 0.048$; $SL - CV$ $p = 0.003$). Post-hoc analysis revealed a higher variability in FOG+ and FOG- patients compared to HS ($GV - CV$: FOG+ vs HS, $p = 0.44$ and FOG- vs HS, $p = 0.039$; $SL - CV$: FOG+ vs HS, $p = 0.03$ and FOG- vs HS, $p = 0.006$). No significant differences were found between FOG+ and FOG- subjects related to gait parameters. Finally, statistical analysis did show any significant difference between HS and PD groups for cadence ($p = 0.56$)

Action Observation (AO) fMRI task.

PD and HS single groups activations. During the AO task, the whole PD group showed several clusters of activation at the level of the occipital and temporal regions, inferior and superior parietal lobule (IPL and SPL, respectively) and precentral gyrus, in both hemispheres. HS activated at the level of the temporal and occipital regions bilaterally, bilateral SPL and intraparietal sulcus (IPS), left pre- and post-central gyrus and superior frontal gyrus (Figure 6.1, Table 6.2).

FOG- and FOG+ single group activations. When FOG- and FOG+ groups were investigated separately, the former showed activity at the level of right temporal and frontal regions and bilateral occipito-parietal areas, while the latter activated only at the level of the occipital regions (Figure 6.1).

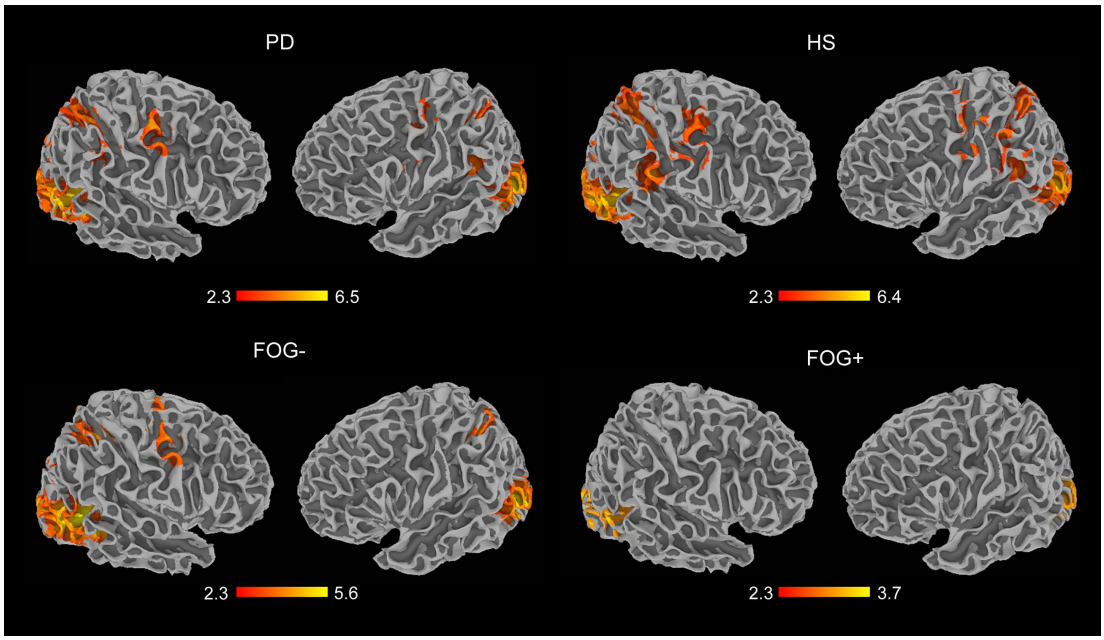

Figure 6.1: Cortical activity during AO of gait in the whole group of PD patients (top,left), in the HS group (top,right), in FOG- (bottom,left) and FOG+ (bottom,right) patients. The results are cluster corrected for multiple comparisons ($Z \geq 2.3$, $p < 0.05$) and are shown in MNI space.

PD vs HS. When the PD and the HS groups were compared, HS showed a significantly greater activation at the level of the cingulate cortex, posterior medial frontal cortex (PMFC), occipital regions and the precuneus (Table 6.3).

Subgroups comparisons. ANCOVA analysis revealed a significant difference among the three groups at the level of the left posterior-medial frontal cortex and cingulate cortex. Both FOG- and HS showed an increased activity in the bilateral PMFC, in the left IPL and in the postcentral gyrus compared to FOG+ participants. Moreover, HS showed two clusters of greater activation, compared to FOG-, at the level of the left occipital regions, right precuneus, left cingulate cortex and right pre- and post-central gyrus (Figure 6.2, Table 6.4 and Table 6.5).

Brain-behavioral correlations. When brain activations were correlated

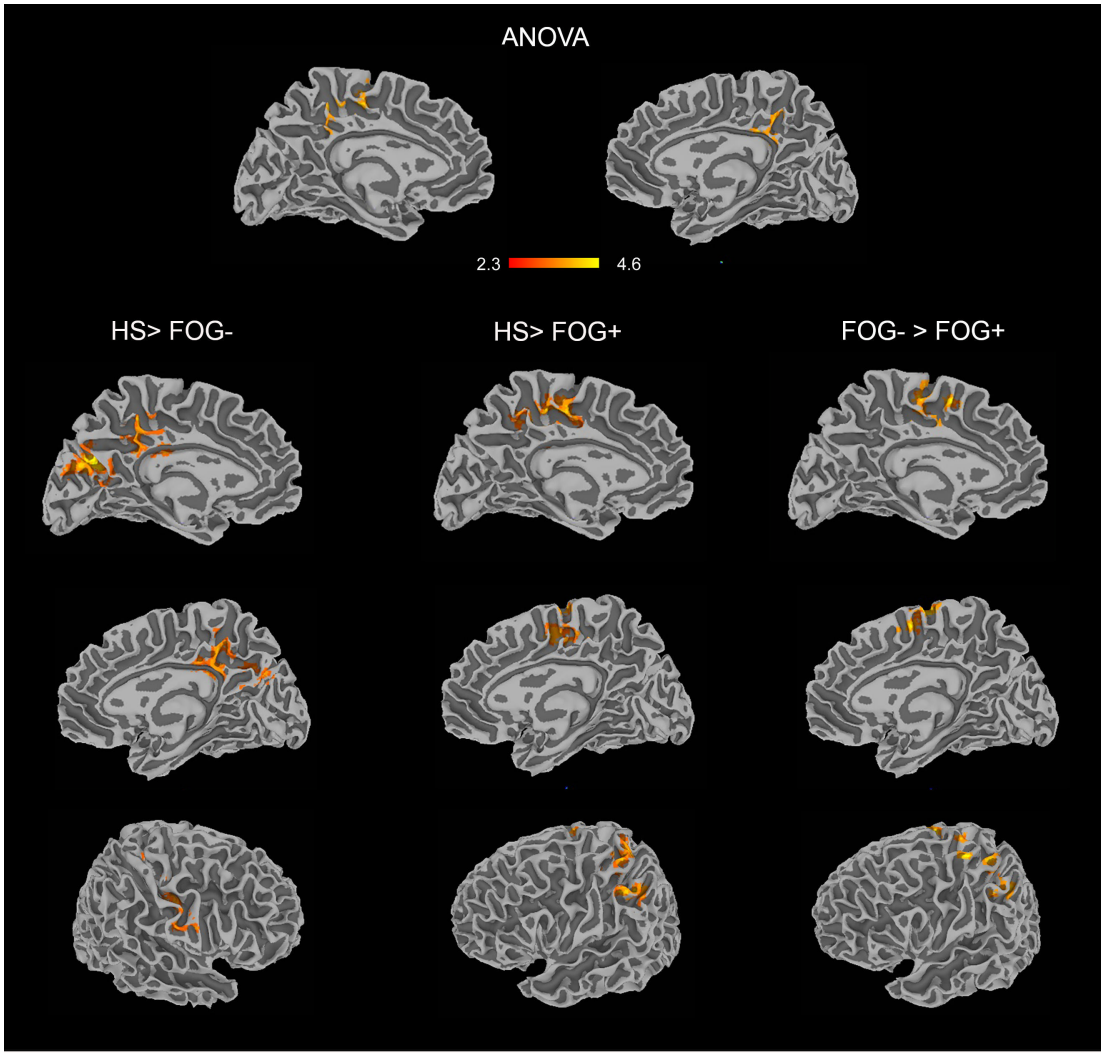

Figure 6.2: Results of the ANOVA analysis (top) and comparison between subgroups. The results are cluster corrected for multiple comparisons ($Z \geq 2.3$, $p < 0.05$) and are shown in MNI space.

with kinematic parameters obtained during normal walking task, significant correlations were found in the FOG+ group. Specifically, increased activity at the level of the precuneus cortex was associated with higher $SL - CV$ and $GV - CV$ values (Figure 6.3, Table 6.6). No significant relationships between brain activations and gait parameters were found for FOG- or HS group.

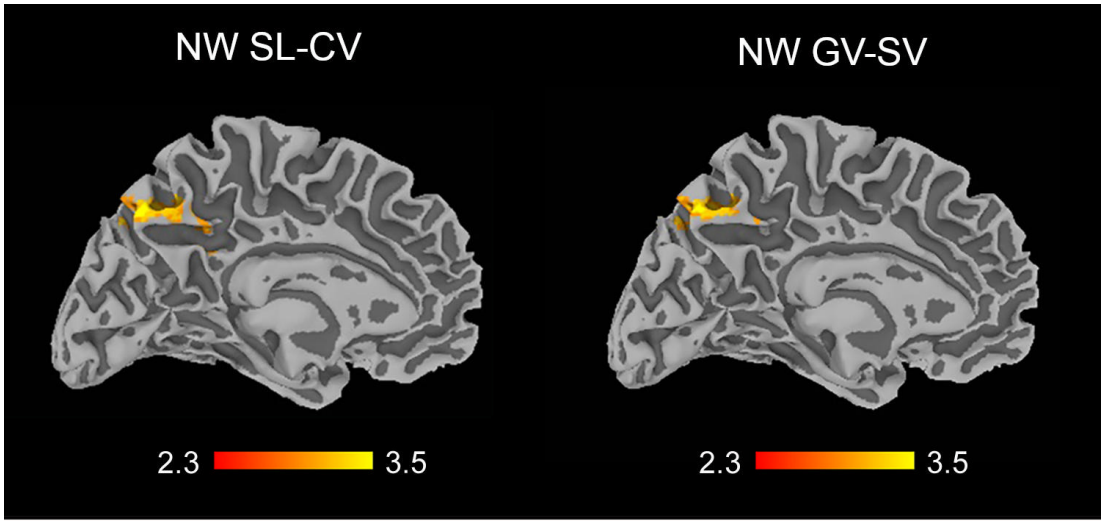

Figure 6.3: Brain-behavioral correlations, in particular correlations of brain activity during AO of gait and $SL - CV$ (left) or $GV - CV$ (right) during normal walking. The results are cluster corrected for multiple comparisons ($Z \geq 2.3$, $p < 0.05$) and are shown in MNI space

6.4 Discussion

In this study, we investigated the neural mechanisms underlying AO of gait and the possible association between brain activity and walking performance in PD patients, with and without FOG and in HS. There are two main findings: first, patients with PD present a modulation of brain activation during AO of normal walking, and that this functional reorganization occurs in both FOG- and FOG+ patients; second, in PD FOG+ participants, activity in the precuneus is associated with spatio-temporal parameters of gait.

Although AO is emerging as a tool for rehabilitation of PD symptoms, including FOG, the neural correlates of AO of gait remain unknown. Previous studies explored brain activity during real walking task [48] and imagined gait task [297] which showed a similar pattern of neural activity. One study of gait observation in HS revealed activations mainly at the level of frontal areas, particularly of

the the supplementary motor area and the dorsal premotor cortex, but also of parietal, occipital regions and parahippocampal gyrus, mostly overlapping with the activity elicited during virtual walking [298]. The similarity of activation patterns between real, imagined and observed gait and the improvement of motor performance after AO training in PD patients corroborate the hypothesis that AO could enhance motor learning and motor performance in a varied rehabilitative protocols.

In this framework, the results of this study add some novel information about the response of PD patients to AO of gait, with potential consequences on the practical application of AO in the rehabilitation training. We showed, in both HS and PD groups, a cortical activation at the level of the occipital, parietal and frontal areas during the observation of walking. In particular, the pattern of activity we found in HS is similar to the one found by [298] However, cortical activation was significantly reduced in PD patients, when compared to HS at the level of the PMFC and of regions in the posterior parietal cortex. Interestingly, both the occipital areas and the precuneus have been found to be active in HS during observation of gait [298] with precuneus being involved in spatial control of motor behavior and perspective taking of actions [299] and both areas being hypoactivated during real gait in patients with PD, compared to HS [190]. Besides, PMFC is one of the brain areas most consistently observed in studies on gait [48; 190; 298] and affected in patients with PD [190]. Thus, our results confirm the impaired functionality of fronto-parietal areas related to gait in patients with PD, even during AO of gait.

When FOG+ and FOG- patients were considered separately, the more striking result was found in the FOG+ group, showing brain activation only at the level of occipital lobes and, compared to both FOG- and HS, presenting a reduced activity at the level of association regions such as PMFC and IPL, while the main

differences between HS and FOG- was at the level occipital and primary sensorimotor cortices. Previous studies found a reduced activity in FOG+ patients, compared to FOG- [288], in particular at the level of the supplementary motor area and parietal regions [192] during imaging of gait. Similarly, the previous study on AO in PD patients with FOG [289] revealed a reduced activity in the precentral and SMA areas, in comparison with HS.

The preserved activation of PMFC we found in FOG- but not FOG+ patients adds a missing piece, confirming the involvement of this area in the functional reorganization subtending FOG [222], and suggesting that this could be a target of AO training. On the other hand, the IPL has been described to play a role in the representation of actions from sensory stimuli, including the visual input [282]. Therefore, a dysfunction in this area, resulting in an altered sensory input integration and a misrepresentation of the action could contribute to the occurrence of FOG. This could be also one of the mechanisms underlying the effectiveness of AO training in improving FOG [181]. Although L-dopa has been found to modulate brain activity during imaging of gait in FOG+ patients restoring the cortico-subcortical connectivity, in their PET study, Maillet et al. did not directly compare HS and patients with PD under the effect of medication [191]. Overall, our results confirm an impaired cortical activation in PD patients, compared to HS, even under the effects of anti-parkinsonian medication. Both PD patients with and without FOG undergo a change in the functional connectivity subtending the AO of gait, but a wider modification occurs in PD patients presenting FOG. The knowledge of the pattern of brain activity during AO of gait in their most frequent condition, i.e. under the effect of medications, could help in understanding the functional modulation shaped by AO training and therefore in designing the most appropriate rehabilitation protocols. Finally, in FOG+ patients we found a significant association between brain activity during AO of gait

and the kinematic parameters recorded during normal walking task. Precisely, the activity at the level of the precuneus correlated with a worse performance in terms of SL and GV variability during normal walking, This association was not significant both in patients PD FOG- and in healthy controls.

This current finding appear to fit with findings in HS were the activations of the precuneus was associated with the imagination of complex locomotor functions such as walking with obstacles [297], attention shift and the processing of visuo-spatial stimulus [299]. Therefore, we could speculate that the activity at the level of the precuneus is crucial in the covert action of walking, in those subjects presenting walking difficulties, such as PD patients with FOG. It would be interesting to investigate whether activity at this level might change with AO training.

This study is not without limitations, including the relatively small sample size of the FOG-/FOG+ sub-groups of patients and the lack of a control condition in the "off" state. However, this is the first study investigating neural correlates of AO of gait in a population of both FOG+ and FOG- PD patients, revealing that a functional reorganization occurs in PD patients and in particular in those presenting with FOG, which could be linked to a fronto-parietal dysfunction. Furthermore, in the latter patients, the behavioral performance during gait is associated with activity at parietal level (in particular, the precuneus) suggesting that these regions could have a role in AO rehabilitation of gait in FOG+ patients. Exploring the neural correlates of AO of gait and the differences between FOG+ and FOG- patients, this study would be helpful in designing and assessing the efficacy of rehabilitation protocols including AO training as a potential resource for improving the motor performance.

Side	Location	Cytoarchitetonic location	PD patients		HS	
			MNI coord (x y z)	Z score	MNI coord (x y z)	Z score
R	MTG	-	46 -60 0	6.35	-	
R	ITG	Area FG2	44 -64 -12	5.93	44 -70 -10	5.82
L	STG	Area PFcm	-48 -34 22	5.1	-	
R	IOG	Area h0c4v	36 -80 -8	4.73	-	
R	IOG	Area h0c4lp	-		36 -84 -4	5.75
L	IOG	Area h0c4lp	-		-36 -96 -4	5.26
L	IOG	Area h0c5	-44 -72 -6	4.94	-	
R	MOG/V5	Area h0c5	-		46 -68 4	6.41
L	MOG/V5	Area h0c5	-44 -74 2	6.57	-	
R	MOG	Area h0c3d	30 -92 12	4.95	30 -98 12	5.19
L	MOG	Area h0c4la	-42 -86 0	5.5	-46 -76 2	5.38
L	MOG	Area h0c4d	-22 -90 10	4.21	-	
L	MOG	Area h0c4lp	-44 -86 16	4.06	-40 -88 -6	4.58
L	MOG	Area h0c3d	-		-22 -98 0	5.02
L	FG	Area FG2	-40 -72 -18	4.09	-	
R	IPL	Area 2	40 -38 54	4.79	32 -42 46	3.58
R	IPL	Area hIP3	38 -44 54	4.79	36 -44 52	4.16
R	SPL	Area 7A	32 -56 58	4.1	-	
R	SPL	Area 7PC	-		36 -46 58	4.13
R	SPL	Area 5L	-		16 -56 74	3.65
L	SPL	Area hIP3	-22 -60 52	3.61	-40 -50 60	4.17
L	SPL	Area 7A	-26 -68 64	2.8	-24 -64 62	3.46
L	SPL	Area 5L	-		-18 -56 72	3.34
R	SMG	Area 2	32 -40 46	3.55	-	
R	SMG	Area PF	-		64 -26 28	4.31
L	SMG	-	-50 -40 28	4.21	-	
R	MFG	-	48 2 52	4.82	-	
R	PrecG	Area 44	56 4 40	3.4	-	
L	PrecG	-	-44 -8 54	3.24	-52 -6 52	4.54
L	PostG	-	-52 -8 54	3.44	-62 -6 36	3.38
L	SFG	-	-		-34 -4 66	3.41

Table 6.2: Clusters of brain activation in PD patients (whole group) and HS. Abbreviations: R: right; L: left; MTG: middle temporal gyrus; ITG: inferior temporal gyrus; STG: superior temporal gyrus; IOG: inferior occipital gyrus; MOG: middle occipital gyrus; FG: fusiform gyrus; IPL: inferior parietal lobule; SPL: superior parietal lobule; SMG: supramarginal gyrus; MFG: middle frontal gyrus; SFG: superior frontal gyrus; PrecG: precentral gyrus; PostG: postcentral gyrus

Side	Location	Cytoarchitetonic location	MNI coordinates X Y Z	Z score
L	SOG	-	-14 -72 28	4.41
L	CG	-	-16 -66 14	3.95
R	Prec	-	12 -68 30	4.16
L	Prec	-	-4 -46 28	4.66
R	MCC	Area 5Ci	6 -38 46	3.54
L	MCC	Area 5M	-4 -36 50	3.97
R	PMFC	-	10 -8 50	3.34

Table 6.3: Comparison between HS and PD patients.
Abbreviations: R: right; L: left; SOG: superior occipital gyrus; CG: calcarine gyrus; Prec: precuneus; MCC: midcingulate cortex; PMFC: posteromedial frontal cortex;

Side	Location	Cytoarchitetonic location	$HS > FOG-$		$HS > FOG+$	
			MNI coord (x y z)	Z score	MNI coord (x y z)	Z score
L	SOG	-	-14 -72 28	4.69	-	
L	Cuneus	-	-4 -76 28	4.56	-	
L	CG	-	-16 -66 16	4	-	
R	Prec	-	12 -68 30	3.99	-	
L	IPL	Area PFt	-		-56 -30 42	3.7
L	IPL	Area PF	-		-54 -40 44	3.28
L	MCC	-			-8 -22 40	3.47
L	ParaG	Area 5M	-4 -38 50	3.69	-4 -32 50	3.4
R	PMFC	-	-		6 -12 68	3.45
L	PMFC	-	-		-4 -18 50	4.28
R	PrecG	-	50 -12 46	3.14	-	
R	PostG	Area 3a	44 -12 32	3.16	-	
R	PostG	Area4p	50 -12 32	3.08	-	
L	PostG	Area 1	-		-34 -40 64	3.75

Table 6.4: Comparison between HS versus FOG+ and FOG- patients.
Abbreviations: R: right; L: left; SOG: superior occipital gyrus; CG: calcarine gyrus; Prec: precuneus; IPL: inferior parietal lobule; MCC: midcingulate cortex; PMFC: posteromedial frontal cortex; MFG: middle frontal gyrus; PrecG: precentral gyrus; PostG: postcentral gyrus; ParaG: paracentral gyrus.

Side	Location	Cytoarchitetonic location	MNI coordinates X Y Z	Z score
L	IPL	Area PFt	-54 -32 42	3.48
L	IPL	Area hIP2	-50 -46 38	3.35
L	IPL	Area hIP1	-46 -50 44	3.31
R	PMFC	-	6 -12 68	3.92
L	PMFC	-	-2 4 54	3.7
L	PrecG	-	-44 -16 60	3.72
L	PostG	Area 1	-46 -30 60	3.42

Table 6.5: Comparison between FOG+ and FOG- patients.
Abbreviations: R: right; L: left; IPL: inferior parietal lobule; PMFC: posteromedial frontal cortex; PrecG: precentral gyrus; PostG: postcentral gyrus.

Side	Location	Cytoarchitetonic location	MNI coordinates X Y Z	Z score
$GV - CV$ during normal walking				
L	Prec	Area 7P	-2 -78 50	3.46
L	SOG	-	-14 -78 44	3.18
L	Prec	Area 7A	-6 -64 48	3.13
$SL - CV$ during normal walking				
L	Prec	Area 7P	-2 -78 50	3.52
L	Prec	Area 7A	-6 -64 48	3.14
L	SOG	-	-14 -78 44	3.07

Table 6.6: Correlations between functional activity and behavioral data

Chapter 7

Conclusions

Functional magnetic resonance imaging is a powerful tool in investigating plasticity occurring in brain and, when applied to patients with neurological disease, in understanding how the functional changes are related to clinical disability. The work of these three years aimed at moving few steps forward in the process of understanding the functional reorganization occurring in multiple sclerosis and Parkinson's disease, with a focus, for the two diseases, on topics useful to design strategies for the rehabilitation of gait, in particular position sense at the lower limbs and action observation training.

Within this frame, studies were performed, using both resting state fMRI and task fMRI in patients with multiple sclerosis and in patients with Parkinson's disease. We aimed at i) exploring the pattern of BOLD signal variability, a measure reflecting the brain functional flexibility, in patients with multiple sclerosis at the early stage of the disease, ii) investigating the deficits of position sense at the lower limbs and the underlying brain functional patterns, considering the major role position sense plays in balance and gait, in patients with early multiple sclerosis, iii) characterizing the functional connectivity in patients with multiple sclerosis at the late stages of the disease, since functional changes in this phase have received less attention so far, despite the relative lack of disease modifying

drugs for these patients and thus the increased importance of rehabilitation, iv) identifying the neural correlates of action observation of gait in patients with Parkinson's disease, which would be the starting point for the comprehension of plasticity changes occurring during action observation training.

Patients with clinically isolated syndrome and RR MS presented with an increased variability which was related to a better clinical performance. A possible interpretation of this finding is a compensatory response, revealing functional variability as a measure related to plastic changes occurring in the brain. Moreover, patients with early MS presented also deficits of position sense, which were not detectable with the standard neurological examination, and that were associated to changes in brain functional connectivity, mainly interesting the frontoparietal regions, and to altered diffusion metrics of the corpus callosum. The position sense deficits affected balance at the early stages of the disease and this would provide a main contribution for further therapeutic rehabilitative approaches in these patients. A future development of this study would be the definition of the role of position sense during gait, in the same population of subjects. This work also showed that changes of resting state functional connectivity were more subtle in the late stages of multiple sclerosis, but still reflecting clinical disability. A more integrated approach to the study of functional changes in the chronic phase of multiple sclerosis is needed and would be a topic for further investigations. Lastly, patients with Parkinson's disease presented with a different functional pattern underlying action observation compared to controls, with these changes becoming more prominent when freezing of gait was present. The knowledge of such differences would allow a better insight in planning the inclusion of action observation training in rehabilitative protocols for gait disorders.

Altogether, there results offer an better insight into the pathophysiological functional mechanisms underlying disability in patients with multiple sclerosis

both a the early and late stages and provide evidence for a reorganization of the neural network underlying action observation in patients with PD. This work is intended to be a basis for a better understanding of the brain plasticity that occurs during rehabilitation. In fact, the characterization of the "baseline" changes in response to brain injury would lay the groundwork to properly select the best rehabilitation strategy and the patients who would benefit for a specific treatment.

References

[1] D. O. Hebb, *The organization of behavior; a neuropsychological theory.* Oxford, England: Wiley, 1949. 1, 6

[2] G. Berlucchi and H. A. Buchtel, "Neuronal plasticity: Historical roots and evolution of meaning," *Experimental Brain Research*, vol. 192, no. 3, pp. 307–319, 2009. 6

[3] S. J. Cooper, "Donald O. Hebb's synapse and learning rule: A history and commentary," *Neuroscience and Biobehavioral Reviews*, vol. 28, no. 8, pp. 851–874, 2005. 6

[4] M. Lövdén, L. Bäckman, U. Lindenberger, S. Schaefer, and F. Schmiedek, "A Theoretical Framework for the Study of Adult Cognitive Plasticity," *Psychological Bulletin*, vol. 136, no. 4, pp. 659–676, 2010. 6

[5] R. J. Zatorre, R. D. Fields, and H. Johansen-Berg, "Plasticity in gray and white: Neuroimaging changes in brain structure during learning," *Nature Neuroscience*, vol. 15, no. 4, pp. 528–536, 2012. 6

[6] D. V. Buonomano and M. M. Merzenich, "CORTICAL PLASTICITY: From Synapses to Maps," *Annual Review of Neuroscience*, vol. 21, no. 1, pp. 149–186, 1998. 6

[7] P. Schneider, M. Scherg, H. G. Dosch, H. J. Specht, A. Gutschalk, and

A. Rupp, "Morphology of Heschl's gyrus reflects enhanced activation in the auditory cortex of musicians." *Nature neuroscience*, vol. 5, no. 7, pp. 688–694, jul 2002. 6

[8] E. A. Maguire, D. G. Gadian, I. S. Johnsrude, C. D. Good, J. Ashburner, R. S. Frackowiak, and C. D. Frith, "Navigation-related structural change in the hippocampi of taxi drivers." *Proceedings of the National Academy of Sciences of the United States of America*, vol. 97, no. 8, pp. 4398–4403, apr 2000. 6

[9] I. Gauthier, P. Skudlarski, J. C. Gore, and A. W. Anderson, "Expertise for cars and birds recruits brain areas involved in face recognition," *Nature Neuroscience*, vol. 3, no. 2, pp. 191–197, 2000. [Online]. Available: https://doi.org/10.1038/72140 6

[10] B. Draganski, C. Gaser, V. Busch, G. Schuierer, U. Bogdahn, and A. May, "Neuroplasticity: changes in grey matter induced by training." *Nature*, vol. 427, no. 6972, pp. 311–312, jan 2004. 6

[11] Y. Yu, L. Huber, J. Yang, D. C. Jangraw, D. A. Handwerker, P. J. Molfese, G. Chen, Y. Ejima, J. Wu, and P. A. Bandettini, "Layer-specific activation of sensory input and predictive feedback in the human primary somatosensory cortex." *Science advances*, vol. 5, no. 5, p. eaav9053, may 2019. 7

[12] D. Tombari, I. Loubinoux, J. Pariente, A. Gerdelat, J.-F. Albucher, J. Tardy, E. Cassol, and F. Chollet, "A longitudinal fMRI study: in recovering and then in clinically stable sub-cortical stroke patients." *NeuroImage*, vol. 23, no. 3, pp. 827–839, nov 2004. 7

[13] C. Büchel, J. T. Coull, and K. J. Friston, "The predictive value of changes

in effective connectivity for human learning," *Science*, vol. 283, no. 5407, pp. 1538–1541, 1999. 7

[14] R. J. Nudo, "Adaptive plasticity in motor cortex: implications for rehabilitation after brain injury." *Journal of rehabilitation medicine*, no. 41 Suppl, pp. 7–10, may 2003. 7

[15] I. Lipp and V. Tomassini, "Neuroplasticity and motor rehabilitation in multiple sclerosis," *Frontiers in Neurology*, vol. 6, no. March, pp. 1–3, 2015. 7, 40

[16] S. Ogawa, D. W. Tank, R. Menon, J. M. Ellermann, S. G. Kim, H. Merkle, and K. Ugurbil, "Intrinsic signal changes accompanying sensory stimulation: Functional brain mapping with magnetic resonance imaging," *Proceedings of the National Academy of Sciences of the United States of America*, vol. 89, no. 13, pp. 5951–5955, 1992. 7

[17] B. R. Buchbinder, *Functional magnetic resonance imaging*, 1st ed. Elsevier B.V., 2016, vol. 135. [Online]. Available: http://dx.doi.org/10.1016/B978-0-444-53485-9.00004-0 8, 13

[18] P. T. Fox, M. E. Raichle, M. A. Mintun, and C. Dence, "Nonoxidative glucose consumption during focal physiologic neural activity." *Science (New York, N.Y.)*, vol. 241, no. 4864, pp. 462–464, jul 1988. 14

[19] A.-L. Lin, P. T. Fox, J. Hardies, T. Q. Duong, and J.-H. Gao, "Nonlinear coupling between cerebral blood flow, oxygen consumption, and ATP production in human visual cortex." *Proceedings of the National Academy of Sciences of the United States of America*, vol. 107, no. 18, pp. 8446–8451, may 2010. 14

[20] B. Biswal, F. Zerrin Yetkin, V. M. Haughton, and J. S. Hyde, "Functional connectivity in the motor cortex of resting human brain using echo-planar mri," *Magnetic Resonance in Medicine*, vol. 34, no. 4, pp. 537–541, oct 1995. [Online]. Available: http://dx.doi.org/10.1002/mrm.1910340409 14, 57

[21] H. Lv, Z. Wang, E. Tong, L. M. Williams, G. Zaharchuk, M. Zeineh, A. N. Goldstein-Piekarski, T. M. Ball, C. Liao, and M. Wintermark, "Resting-state functional MRI: Everything that nonexperts have always wanted to know," *American Journal of Neuroradiology*, vol. 39, no. 8, pp. 1390–1399, 2018. 15

[22] M. Rubinov and O. Sporns, "Complex network measures of brain connectivity: Uses and interpretations," *NeuroImage*, vol. 52, no. 3, pp. 1059–1069, 2010. [Online]. Available: http://dx.doi.org/10.1016/j.neuroimage.2009.10.003 15, 117

[23] J. S. Damoiseaux, S. A. R. B. Rombouts, F. Barkhof, P. Scheltens, C. J. Stam, S. M. Smith, and C. F. Beckmann, "Consistent resting-state networks across healthy subjects." *Proceedings of the National Academy of Sciences of the United States of America*, vol. 103, no. 37, pp. 13 848–13 853, sep 2006. 15

[24] J. Gonzalez-Castillo and P. A. Bandettini, "Task-based dynamic functional connectivity: Recent findings and open questions," *NeuroImage*, vol. 180, no. May 2017, pp. 526–533, 2018. [Online]. Available: https://doi.org/10.1016/j.neuroimage.2017.08.006 15

[25] J. M. Soares, R. Magalhães, P. S. Moreira, A. Sousa, E. Ganz, A. Sampaio, V. Alves, P. Marques, and N. Sousa, "A Hitchhiker's guide to func-

tional magnetic resonance imaging," *Frontiers in Neuroscience*, vol. 10, no. November, pp. 1–35, 2016. 15

[26] D. D. Garrett, G. R. Samanez-Larkin, S. W. MacDonald, U. Lindenberger, A. R. McIntosh, and C. L. Grady, "Moment-to-moment brain signal variability: A next frontier in human brain mapping?" *Neuroscience and Biobehavioral Reviews*, vol. 37, no. 4, pp. 610–624, 2013. [Online]. Available: http://dx.doi.org/10.1016/j.neubiorev.2013.02.015 17, 58

[27] D. D. Garrett, N. Kovacevic, A. R. McIntosh, and C. L. Grady, "Blood Oxygen Level-Dependent Signal Variability Is More than Just Noise," *Journal of Neuroscience*, vol. 30, no. 14, pp. 4914–4921, 2010. [Online]. Available: http://www.jneurosci.org/cgi/doi/10.1523/JNEUROSCI.5166-09.2010 17, 58

[28] C. L. Grady and D. D. Garrett, "Brain signal variability is modulated as a function of internal and external demand in younger and older adults," *NeuroImage*, vol. 169, no. December 2017, pp. 510–523, 2018. [Online]. Available: https://doi.org/10.1016/j.neuroimage.2017.12.031 17

[29] L. Grady, C Cheryl and D. D. Garrett, "Understanding variability in the BOLD signal and why it matters for aging." *Brain imaging and behavior*, vol. 8, no. 2, pp. 274–283, jun 2014. 17

[30] J. S. Nomi, T. S. Bolt, C. E. Chiemeka Ezie, L. Q. Uddin, and A. S. Heller, "Moment-to-moment BOLD signal variability reflects regional changes in neural flexibility across the lifespan," *Journal of Neuroscience*, vol. 37, no. 22, pp. 5539–5548, 2017. 17

[31] C. Chang and G. H. Glover, "Time-frequency dynamics of resting-state

brain connectivity measured with fMRI." *NeuroImage*, vol. 50, no. 1, pp. 81–98, mar 2010. 18

[32] D. S. Bassett, N. F. Wymbs, M. A. Porter, P. J. Mucha, J. M. Carlson, and S. T. Grafton, "Dynamic reconfiguration of human brain networks during learning." *Proceedings of the National Academy of Sciences of the United States of America*, vol. 108, no. 18, pp. 7641–7646, may 2011. 18

[33] R. A. Poldrack, T. O. Laumann, O. Koyejo, B. Gregory, A. Hover, M.-Y. Chen, K. J. Gorgolewski, J. Luci, S. J. Joo, R. L. Boyd, S. Hunicke-Smith, Z. B. Simpson, T. Caven, V. Sochat, J. M. Shine, E. Gordon, A. Z. Snyder, B. Adeyemo, S. E. Petersen, D. C. Glahn, D. Reese Mckay, J. E. Curran, H. H. H. Goring, M. A. Carless, J. Blangero, R. Dougherty, A. Leemans, D. A. Handwerker, L. Frick, E. M. Marcotte, and J. A. Mumford, "Long-term neural and physiological phenotyping of a single human." *Nature communications*, vol. 6, p. 8885, dec 2015. 18

[34] E. Tagliazucchi, P. Balenzuela, D. Fraiman, P. Montoya, and D. R. Chialvo, "Spontaneous BOLD event triggered averages for estimating functional connectivity at resting state." *Neuroscience letters*, vol. 488, no. 2, pp. 158–163, jan 2011. 18

[35] X. Liu, N. Zhang, C. Chang, and J. H. Duyn, "Co-activation patterns in resting-state fMRI signals," *NeuroImage*, vol. 180, no. February, pp. 485–494, 2018. [Online]. Available: https://doi.org/10.1016/j.neuroimage.2018.01.041 18

[36] F. I. Karahanoglu and D. Van De Ville, "Transient brain activity disentangles fMRI resting-state dynamics in terms of spatially and temporally

overlapping networks." *Nature communications*, vol. 6, p. 7751, jul 2015. 18

[37] M. G. Preti, T. A. Bolton, and D. Van De Ville, "The dynamic functional connectome: State-of-the-art and perspectives." *NeuroImage*, vol. 160, pp. 41–54, oct 2017. 18

[38] L. J. O'Donnell and C.-F. Westin, "An introduction to diffusion tensor image analysis." *Neurosurgery clinics of North America*, vol. 22, no. 2, pp. 185–96, viii, apr 2011. 19

[39] J. D. Tournier, "Diffusion MRI in the brain – Theory and concepts," *Progress in Nuclear Magnetic Resonance Spectroscopy*, vol. 112-113, pp. 1–16, 2019. [Online]. Available: https://doi.org/10.1016/j.pnmrs.2019.03.001 19

[40] P. Mukherjee, J. I. Berman, S. W. Chung, C. P. Hess, and R. G. Henry, "Diffusion tensor MR imaging and fiber tractography: Theoretic underpinnings," *American Journal of Neuroradiology*, vol. 29, no. 4, pp. 632–641, 2008. 19

[41] S. Mori and J. Zhang, "Principles of Diffusion Tensor Imaging and Its Applications to Basic Neuroscience Research," *Neuron*, vol. 51, no. 5, pp. 527–539, 2006. 20, 21

[42] E. P. Zehr, "Neural control of rhythmic human movement: the common core hypothesis." *Exercise and sport sciences reviews*, vol. 33, no. 1, pp. 54–60, 2005. 22

[43] T. Drew, S. Prentice, and B. Schepens, "Cortical and brainstem control of locomotion." *Progress in brain research*, vol. 143, pp. 251–261, 2004. 22

[44] K. G. Pearson, "Proprioceptive regulation of locomotion." *Current opinion in neurobiology*, vol. 5, no. 6, pp. 786–791, dec 1995. 22

[45] S. Grillner, "The motor infrastructure: from ion channels to neuronal networks." *Nature reviews. Neuroscience*, vol. 4, no. 7, pp. 573–586, jul 2003. 22

[46] G. E. Loeb, M. J. Bak, and J. Duysens, "Long-term unit recording from somatosensory neurons in the spinal ganglia of the freely walking cat." *Science (New York, N.Y.)*, vol. 197, no. 4309, pp. 1192–1194, sep 1977. 23

[47] S. Rossignol, R. Dubuc, J.-P. Gossard, and J. Dubuc, "Dynamic Sensorimotor Interactions in Locomotion," *Physiological Reviews*, vol. 86, pp. 89–154, 2006. 23

[48] I. Miyai, H. C. Tanabe, I. Sase, H. Eda, I. Oda, I. Konishi, Y. Tsunazawa, T. Suzuki, T. Yanagida, and K. Kubota, "Cortical mapping of gait in humans: A near-infrared spectroscopic topography study," *NeuroImage*, vol. 14, no. 5, pp. 1186–1192, 2001. 23, 138, 139

[49] A. Presacco, R. Goodman, L. Forrester, and J. Contreras-Vidal, "Neural decoding of treadmill walking from noninvasive electroencephalographic signals," *Journal of Neurophysiology*, vol. 106, pp. 1875–1887, 2011. 23

[50] H. Fukuyama, Y. Ouchi, S. Matsuzaki, Y. Nagahama, H. Yamauchi, M. Ogawa, J. Kimura, and H. Shibasaki, "Brain functional activity during gait in normal subjects: a SPECT study," *Neuroscience Letters*, vol. 228, pp. 183–186, 1997. 23

[51] J. T. Gwin, K. Gramann, S. Makeig, and D. P. Ferris, "Electrocortical activity is coupled to gait cycle phase during treadmill walking," *NeuroImage*, 2011. 23

[52] B. H. Dobkin, A. Firestine, M. West, K. Saremi, and R. Woods, "Ankle dorsiflexion as an fMRI paradigm to assay motor control for walking during rehabilitation," *NeuroImage*, 2004. 23, 30, 31

[53] C. Sahyoun, A. Floyer-Lea, H. Johansen-Berg, and P. M. Matthews, "Towards an understanding of gait control: Brain activation during the anticipation, preparation and execution of foot movements," *NeuroImage*, 2004. 23

[54] E. Kapreli, S. Athanasopoulos, M. Papathanasiou, P. Van Hecke, N. Strimpakos, A. Gouliamos, R. Peeters, and S. Sunaert, "Lateralization of brain activity during lower limb joints movement. An fMRI study," *NeuroImage*, 2006. 23

[55] S. Francis, X. Lin, S. Aboushoushah, T. P. White, M. Phillips, R. Bowtell, and C. S. Constantinescu, "fMRI analysis of active, passive and electrically stimulated ankle dorsiflexion," *NeuroImage*, 2009. 23, 30

[56] O. Ciccarelli, A. T. Toosy, J. F. Marsden, C. M. Wheeler-Kingshott, C. Sahyoun, P. M. Matthews, D. H. Miller, and A. J. Thompson, "Identifying brain regions for integrative sensorimotor processing with ankle movements." *Experimental brain research*, vol. 166, no. 1, pp. 31–42, sep 2005. 23, 30, 49

[57] L. Jaeger, L. Marchal-Crespo, P. Wolf, R. Riener, L. Michels, and S. Kollias, "Brain activation associated with active and passive lower limb stepping," *Frontiers in Human Neuroscience*, vol. 8, 2014. 23

[58] G. P. Jacobson and N. T. Shephard, *Balance Function Assessment and Management, Second Edition*. Plural Publishing, Incorporated, 2014.

[Online]. Available: https://books.google.ch/books?id=nmxyDgAAQBAJ 24

[59] K. Iqbal, "Mechanisms and models of postural stability and control," in *2011 Annual International Conference of the IEEE Engineering in Medicine and Biology Society*, 2011, pp. 7837–7840. 24

[60] P. A. Forbes, A. Chen, and J. S. Blouin, "Sensorimotor control of standing balance," *Handbook of Clinical Neurology*, vol. 159, pp. 61–83, 2018. 25

[61] R. Fitzpatrick and D. I. McCloskey, "Proprioceptive, visual and vestibular thresholds for the perception of sway during standing in humans." *The Journal of physiology*, vol. 478 (Pt 1, pp. 173–186, jul 1994. 25

[62] C. S. Sherrington, "On the proprio-ceptive system, especially in its reflex aspect," *Brain*, vol. 29, no. 4, pp. 467–482, 1907. 25

[63] H. C. Dijkerman, "Somatosensory processes subserving perception and action," *The behavioral and brain Sciences*, pp. 189–239, 2007. 25

[64] J. Han, G. Waddington, R. Adams, J. Anson, and Y. Liu, "Assessing proprioception: A critical review of methods," pp. 80–90, 2016. 26, 112

[65] D. J. Goble and S. H. Brown, "Upper limb asymmetries in the matching of proprioceptive versus visual targets." *Journal of neurophysiology*, vol. 99, no. 6, pp. 3063–3074, 2008. 28

[66] D. J. Goble, "Proprioceptive acuity assessment via joint position matching: from basic science to general practice." *Physical therapy*, vol. 90, no. 8, pp. 1176–1184, 2010. 28, 29, 81, 109, 110

[67] K. Yasuda, Y. Sato, N. Iimura, and H. Iwata, "Allocation of Attentional Resources toward a Secondary Cognitive Task Leads to Compromised Ankle Proprioceptive Performance in Healthy Young Adults." *Rehabilitation research and practice*, vol. 2014, p. 7, 2014. 28

[68] D. J. Goble, Æ. C. A. Lewis, and Æ. S. H. Brown, "Upper limb asymmetries in the utilization of proprioceptive feedback," *Experimental Brain research*, pp. 307–311, 2006. 28

[69] D. J. Goble, B. C. Noble, and S. H. Brown, "Proprioceptive target matching asymmetries in left-handed individuals." *Experimental brain research*, vol. 197, no. 4, pp. 403–408, aug 2009. 28

[70] E. Naito, T. Nakashima, T. Kito, Y. Aramaki, T. Okada, and N. Sadato, "Human limb-specific and non-limb-specific brain representations during kinesthetic illusory movements of the upper and lower extremities," *The European Journal of Neuroscience*, vol. 25, pp. 3476–3487, 2007. 28

[71] E. Naito, P. E. Roland, C. Grefkes, H. J. Choi, S. Eickhoff, S. Geyer, K. Zilles, H. H. Ehrsson, P. E. Roland, C. Grefkes, H. J. Choi, S. Geyer, K. Zilles, and H. H. Ehrsson, "Dominance of the Right Hemisphere and Role of Area 2 in Human Kinesthesia," *Journal of Neurophysiology*, pp. 1020–1034, 2005. 28

[72] E. Ben-Shabat, T. A. Matyas, G. S. Pell, A. Brodtmann, and L. M. Carey, "The right supramarginal gyrus is important for proprioception in healthy and stroke-affected participants: A functional MRI study," *Frontiers in Neurology*, vol. 6, no. DEC, p. 248, 2015. 28

[73] R. L. Sainburg and S. Y. Schaefer, "Interlimb differences in control of move-

ment extent." *Journal of neurophysiology*, vol. 92, no. 3, pp. 1374–1383, 2004. 28

[74] R. L. Sainburg, "Evidence for a dynamic-dominance hypothesis of handedness," *Experimental Brain Research*, vol. 142, no. 2, pp. 241–258, 2002. 28

[75] A. Karni, G. Meyer, C. Rey-Hipolito, P. Jezzard, M. M. Adams, R. Turner, and L. G. Ungerleider, "The acquisition of skilled motor performance: fast and slow experience-driven changes in primary motor cortex," *Proceedings of the National Academy of Sciences*, vol. 95, no. 3, pp. 861–868, 1998. 28

[76] C. E. Han, M. A. Arbib, and N. Schweighofer, "Stroke rehabilitation reaches a threshold," *PLoS Computational Biology*, vol. 4, no. 8, 2008. 28

[77] G. S. Watson, R. L. Pusakulich, J. P. Ward, and B. Hermann, "Handedness, footedness, and language laterality: Evidence from Wada testing." *Laterality*, vol. 3, no. 4, pp. 323–330, 1998. 29

[78] L. J. Elias, M. P. Bryden, and M. B. Bulman-Fleming, "Footedness is a better predictor than is handedness of emotional lateralization." *Neuropsychologia*, vol. 36, no. 1, pp. 37–43, jan 1998. 29, 82

[79] Y. Laufer, S. Hocherman, and R. Dickstein, "Accuracy of reproducing hand position when using active compared with passive movement." *Physiotherapy research international : the journal for researchers and clinicians in physical therapy*, vol. 6, no. 2, pp. 65–75, 2001. 29

[80] D. J. Goble, J. P. Coxon, A. Van Impe, M. Geurts, M. Doumas, N. Wenderoth, and S. P. Swinnen, "Brain activity during ankle proprioceptive stimulation predicts balance performance in young and older adults." *The Jour-*

nal of neuroscience : the official journal of the Society for Neuroscience, vol. 31, no. 45, pp. 16 344–16 352, nov 2011. 30, 80, 85, 86

[81] D. J. Goble, J. P. Coxon, A. V. Impe, M. Geurts, W. V. Hecke, S. Sunaert, N. Wenderoth, and S. P. Swinnen, "The Neural Basis of Central Proprioceptive Processing in Older Versus Younger Adults : An Important Sensory Role for Right Putamen," *Human Brain Mapping*, vol. 908, no. March 2011, pp. 895–908, 2012. 30, 80

[82] G. M. Goodwin, D. I. McCloskey, and P. B. Matthews, "Proprioceptive illusions induced by muscle vibration: contribution by muscle spindles to perception?" *Science (New York, N.Y.)*, vol. 175, no. 4028, pp. 1382–1384, mar 1972. 30

[83] C. Sahyoun, A. Floyer-Lea, H. Johansen-Berg, and P. M. Matthews, "Towards an understanding of gait control: brain activation during the anticipation, preparation and execution of foot movements." *NeuroImage*, vol. 21, no. 2, pp. 568–575, feb 2004. 30

[84] F. B. Horak and L. M. Nashner, "Central programming of postural movements: adaptation to altered support-surface configurations." *Journal of neurophysiology*, vol. 55, no. 6, pp. 1369–1381, jun 1986. 30

[85] J. C. E. Kempen, C. A. M. Doorenbosch, D. L. Knol, V. de Groot, and H. Beckerman, "Newly Identified Gait Patterns in Patients With Multiple Sclerosis May Be Related to Push-off Quality." *Physical therapy*, vol. 96, no. 11, pp. 1744–1752, nov 2016. 31

[86] B. L. Davies, R. M. Hoffman, K. Healey, R. Zabad, and M. J. Kurz, "Errors in the ankle plantarflexor force production are related to the gait deficits

of individuals with multiple sclerosis." *Human movement science*, vol. 51, pp. 91–98, jan 2017. 31

[87] R. a. Berenberg, J. M. Shefner, and J. J. Sabol, "Quantitative assessment of position sense at the ankle: a functional approach." *Neurology*, vol. 37, no. 1, pp. 89–93, 1987. 31

[88] H. J. Meeuwsen, T. M. Sawicki, and G. E. Stelmach, "Improved foot position sense as a result of repetitions in older adults." *Journal of gerontology*, vol. 48, no. 3, pp. 137–141, 1993. 31

[89] N. Forestier, N. Teasdale, and V. Nougier, "Alteration of the position sense at the ankle induced by muscular fatigue in humans." *Medicine and science in sports and exercise*, vol. 34, no. 1, pp. 117–122, 2002. 31

[90] F. D. Lublin, S. C. Reingold, J. A. Cohen, G. R. Cutter, P. S. Sorensen, A. J. Thompson, J. S. Wolinsky, L. J. Balcer, B. Banwell, F. Barkhof, B. J. Bebo, P. A. Calabresi, M. Clanet, G. Comi, R. J. Fox, M. S. Freedman, A. D. Goodman, M. Inglese, L. Kappos, B. C. Kieseier, J. A. Lincoln, C. Lubetzki, A. E. Miller, X. Montalban, P. W. O'Connor, J. Petkau, C. Pozzilli, R. A. Rudick, M. P. Sormani, O. Stuve, E. Waubant, and C. H. Polman, "Defining the clinical course of multiple sclerosis: the 2013 revisions." *Neurology*, vol. 83, no. 3, pp. 278–286, jul 2014. 32, 124

[91] D. S. Reich, C. F. Lucchinetti, and P. A. Calabresi, "Multiple Sclerosis," *New England Journal of Medicine*, vol. 378, no. 2, pp. 169–180, 2018. [Online]. Available: http://www.nejm.org/doi/10.1056/NEJMra1401483 32

[92] M. T. Wallin, W. J. Culpepper, E. Nichols, Z. A. Bhutta, T. T. Gebrehiwot, S. I. Hay, I. A. Khalil, K. J. Krohn, X. Liang, M. Naghavi, A. H.

Mokdad, M. R. Nixon, R. C. Reiner, B. Sartorius, M. Smith, R. Topor-Madry, A. Werdecker, T. Vos, V. L. Feigin, and C. J. Murray, "Global, regional, and national burden of multiple sclerosis 1990–2016: a systematic analysis for the Global Burden of Disease Study 2016," *The Lancet Neurology*, vol. 18, no. 3, pp. 269–285, 2019. 32, 33

[93] P. Browne, D. Chandraratna, C. Angood, H. Tremlett, C. Baker, B. V. Taylor, and A. J. Thompson, "Atlas of multiple sclerosis 2013: A growing global problem with widespread inequity," *Neurology*, vol. 83, no. 11, pp. 1022–1024, 2014. 32

[94] Msif, "Atlas of MS 2013: Mapping Multiple Sclerosis Around the World," *Multiple Sclerosis International Federation*, pp. 1–28, 2013. 32

[95] N. Koch-Henriksen and P. S. Sorensen, "The changing demographic pattern of multiple sclerosis epidemiology." *The Lancet. Neurology*, vol. 9, no. 5, pp. 520–532, may 2010. 32, 33

[96] S.-M. Orton, B. M. Herrera, I. M. Yee, W. Valdar, S. V. Ramagopalan, A. D. Sadovnick, and G. C. Ebers, "Sex ratio of multiple sclerosis in Canada: a longitudinal study." *The Lancet. Neurology*, vol. 5, no. 11, pp. 932–936, nov 2006. 33

[97] E. Kingwell, M. van der Kop, Y. Zhao, A. Shirani, F. Zhu, J. Oger, and H. Tremlett, "Relative mortality and survival in multiple sclerosis: findings from British Columbia, Canada." *Journal of neurology, neurosurgery, and psychiatry*, vol. 83, no. 1, pp. 61–66, jan 2012. 33

[98] E. Leray, S. Vukusic, M. Debouverie, M. Clanet, B. Brochet, J. de Seze, H. Zephir, G. Defer, C. Lebrun-Frenay, T. Moreau, P. Clavelou, J. Pelletier, E. Berger, P. Cabre, J.-P. Camdessanche, S. Kalson-Ray, C. Confavreux,

and G. Edan, "Excess Mortality in Patients with Multiple Sclerosis Starts at 20 Years from Clinical Onset: Data from a Large-Scale French Observational Study." *PloS one*, vol. 10, no. 7, p. e0132033, 2015. 33

[99] L. Belbasis, V. Bellou, E. Evangelou, J. P. Ioannidis, and I. Tzoulaki, "Environmental risk factors and multiple sclerosis: An umbrella review of systematic reviews and meta-analyses," *The Lancet Neurology*, vol. 14, no. 3, pp. 263–273, 2015. [Online]. Available: http://dx.doi.org/10.1016/S1474-4422(14)70267-4 34

[100] C. A. Dendrou, L. Fugger, and M. A. Friese, "Immunopathology of multiple sclerosis," *Nature Reviews Immunology*, no. August, 2015. 34, 35, 36

[101] G. C. Ebers, D. E. Bulman, A. D. Sadovnick, D. W. Paty, S. Warren, W. Hader, T. J. Murray, T. P. Seland, P. Duquette, and T. Grey, "A population-based study of multiple sclerosis in twins." *The New England journal of medicine*, vol. 315, no. 26, pp. 1638–1642, dec 1986. 34

[102] J. A. Hollenbach and J. R. Oksenberg, "The immunogenetics of multiple sclerosis: A comprehensive review." *Journal of autoimmunity*, vol. 64, pp. 13–25, nov 2015. 34

[103] M. W. Koch, Y. Ilnytskyy, A. Golubov, L. M. Metz, V. W. Yong, and O. Kovalchuk, "Global transcriptome profiling of mild relapsing-remitting versus primary progressive multiple sclerosis." *European journal of neurology*, vol. 25, no. 4, pp. 651–658, apr 2018. 35

[104] H. Lassmann, "Pathogenic mechanisms associated with different clinical courses of multiple sclerosis," *Frontiers in Immunology*, vol. 10, no. JAN, pp. 1–14, 2019. 35, 37

[105] B. D. Trapp and K.-A. Nave, "Multiple Sclerosis: An Immune or Neurodegenerative Disorder?" *Annual Review of Neuroscience*, vol. 31, no. 1, pp. 247–269, 2008. 36

[106] P. K. Stys, G. W. Zamponi, J. Van Minnen, and J. J. Geurts, "Will the real multiple sclerosis please stand up?" *Nature Reviews Neuroscience*, vol. 13, no. 7, pp. 507–514, 2012. 36

[107] D. H. Miller, D. T. Chard, and O. Ciccarelli, "Clinically isolated syndromes," *The Lancet Neurology*, vol. 11, no. 2, pp. 157–169, 2012. [Online]. Available: http://dx.doi.org/10.1016/S1474-4422(11)70274-5 38

[108] A. J. Thompson, B. L. Banwell, F. Barkhof, W. M. Carroll, T. Coetzee, G. Comi, J. Correale, F. Fazekas, M. Filippi, M. S. Freedman, K. Fujihara, S. L. Galetta, H. P. Hartung, L. Kappos, F. D. Lublin, R. A. Marrie, A. E. Miller, D. H. Miller, X. Montalban, E. M. Mowry, P. S. Sorensen, M. Tintoré, A. L. Traboulsee, M. Trojano, B. M. J. Uitdehaag, S. Vukusic, E. Waubant, B. G. Weinshenker, S. C. Reingold, and J. A. Cohen, "Position Paper Diagnosis of multiple sclerosis : 2017 revisions of the McDonald criteria," *Lancet Neurology*, vol. 17, no. February, 2018. 38, 39, 82

[109] C. Lapucci, L. Saitta, G. Bommarito, M. P. Sormani, M. Pardini, L. Bonzano, G. L. Mancardi, C. Gasperini, A. Giorgio, M. Inglese, N. De Stefano, and L. Roccatagliata, "How much do periventricular lesions assist in distinguishing migraine with aura from CIS?" *Neurology*, vol. 92, no. 15, pp. e1739–e1744, apr 2019. 39

[110] P. Sati, J. Oh, R. T. Constable, N. Evangelou, C. R. G. Guttmann, R. G. Henry, E. C. Klawiter, C. Mainero, L. Massacesi, H. McFarland, F. Nelson, D. Ontaneda, A. Rauscher, W. D. Rooney, A. P. R. Samaraweera, R. T.

Shinohara, R. A. Sobel, A. J. Solomon, C. A. Treaba, J. Wuerfel, R. Zivadinov, N. L. Sicotte, D. Pelletier, and D. S. Reich, "The central vein sign and its clinical evaluation for the diagnosis of multiple sclerosis: a consensus statement from the North American Imaging in Multiple Sclerosis Cooperative." *Nature reviews. Neurology*, vol. 12, no. 12, pp. 714–722, dec 2016. 39

[111] X. Montalban, R. Gold, A. J. Thompson, S. Otero-Romero, M. P. Amato, D. Chandraratna, M. Clanet, G. Comi, T. Derfuss, F. Fazekas, H. P. Hartung, E. Havrdova, B. Hemmer, L. Kappos, R. Liblau, C. Lubetzki, E. Marcus, D. H. Miller, T. Olsson, S. Pilling, K. Selmaj, A. Siva, P. S. Sorensen, M. P. Sormani, C. Thalheim, H. Wiendl, and F. Zipp, "ECTRIMS/EAN guideline on the pharmacological treatment of people with multiple sclerosis," *European Journal of Neurology*, no. February, pp. 215–237, 2018. [Online]. Available: http://doi.wiley.com/10.1111/ene.13536 40

[112] W. J. Brownlee, "Do spinal cord lesions matter in patients with clinically isolated syndrome and early MS?" *Multiple Sclerosis Journal*, vol. 24, no. 4, pp. 430–431, 2018. 40

[113] M. P. Wattjes, A. Rovira, D. Miller, T. A. Yousry, M. P. Sormani, M. P. de Stefano, M. Tintore, C. Auger, C. Tur, M. Filippi, M. A. Rocca, F. Fazekas, L. Kappos, C. Polman, F. Barkhof, and X. Montalban, "Evidence-based guidelines: MAGNIMS consensus guidelines on the use of MRI in multiple sclerosis–establishing disease prognosis and monitoring patients." pp. 597–606, oct 2015. 41

[114] A. Rovira, M. P. Wattjes, M. Tintore, C. Tur, T. A. Yousry, M. P. Sormani, N. De Stefano, M. Filippi, C. Auger, M. A. Rocca, F. Barkhof, F. Fazekas,

L. Kappos, C. Polman, D. Miller, and X. Montalban, "Evidence-based guidelines: MAGNIMS consensus guidelines on the use of MRI in multiple sclerosis-clinical implementation in the diagnostic process." pp. 471–482, aug 2015. 41

[115] A. Eshaghi, F. Prados, W. J. Brownlee, D. R. Altmann, C. Tur, M. J. Cardoso, F. De Angelis, S. H. van de Pavert, N. Cawley, N. De Stefano, M. L. Stromillo, M. Battaglini, S. Ruggieri, C. Gasperini, M. Filippi, M. A. Rocca, A. Rovira, J. Sastre-Garriga, H. Vrenken, C. E. Leurs, J. Killestein, L. Pirpamer, C. Enzinger, S. Ourselin, C. A. M. G. Wheeler-Kingshott, D. Chard, A. J. Thompson, D. C. Alexander, F. Barkhof, and O. Ciccarelli, "Deep gray matter volume loss drives disability worsening in multiple sclerosis." *Annals of neurology*, vol. 83, no. 2, pp. 210–222, feb 2018. 41

[116] F. Durand-Dubief, B. Belaroussi, J. P. Armspach, M. Dufour, S. Roggerone, S. Vukusic, S. Hannoun, D. Sappey-Marinier, C. Confavreux, and F. Cotton, "Reliability of longitudinal brain volume loss measurements between 2 sites in patients with multiple sclerosis: Comparison of 7 quantification techniques," *American Journal of Neuroradiology*, vol. 33, no. 10, pp. 1918–1924, 2012. 42

[117] S. D. Roosendaal, M. M. Schoonheim, H. E. Hulst, E. J. Sanz-Arigita, S. M. Smith, J. J. Geurts, and F. Barkhof, "Resting state networks change in clinically isolated syndrome," *Brain*, vol. 133, no. 6, pp. 1612–1621, 2010. 42, 59

[118] I. Koubiyr, P. Besson, M. Deloire, J. Charre-Morin, A. Saubusse, T. Tourdias, B. Brochet, and A. Ruet, "Dynamic modular-level alterations of structural-functional coupling in clinically isolated syndrome," *Brain : a journal of neurology*, vol. 142, no. 11, pp. 3428–3439, 2019. 42, 125

[119] Y. Liu, Y. Duan, H. Dong, F. Barkhof, K. Li, and N. Shu, "Disrupted Module Efficiency of Structural and Functional Brain Connectomes in Clinically Isolated Syndrome and Multiple Sclerosis." *Frontiers in human neuroscience*, vol. 12, p. 138, 2018. 42

[120] N. Shu, Y. Duan, M. Xia, M. M. Schoonheim, J. Huang, Z. Ren, Z. Sun, J. Ye, H. Dong, F. D. Shi, F. Barkhof, K. Li, and Y. Liu, "Disrupted topological organization of structural and functional brain connectomes in clinically isolated syndrome and multiple sclerosis," *Scientific Reports*, vol. 6, no. April, pp. 1–11, 2016. [Online]. Available: http://dx.doi.org/10.1038/srep29383 42

[121] N. Shu, Y. Duan, J. Huang, Z. Ren, Z. Liu, H. Dong, F. Barkhof, K. Li, and Y. Liu, "Progressive brain rich-club network disruption from clinically isolated syndrome towards multiple sclerosis," *NeuroImage: Clinical*, vol. 19, no. March, pp. 232–239, 2018. [Online]. Available: https://doi.org/10.1016/j.nicl.2018.03.034 42

[122] K. R. Patel, S. Tobyne, D. Porter, J. D. Bireley, V. Smith, and E. Klawiter, "Structural disconnection is responsible for increased functional connectivity in multiple sclerosis," *Brain Structure and Function*, vol. 223, no. 5, pp. 2519–2526, 2018. [Online]. Available: http://dx.doi.org/10.1007/s00429-018-1619-z 43, 124

[123] P. Tewarie, M. D. Steenwijk, M. J. Brookes, B. M. Uitdehaag, J. J. Geurts, C. J. Stam, and M. M. Schoonheim, "Explaining the heterogeneity of functional connectivity findings in multiple sclerosis: An empirically informed modeling study," *Human Brain Mapping*, vol. 39, no. 6, pp. 2541–2548, 2018. 43, 124

[124] S. Tommasin, L. De Giglio, S. Ruggieri, N. Petsas, C. Giannì, C. Pozzilli, and P. Pantano, "Relation between functional connectivity and disability in multiple sclerosis: a non-linear model," *Journal of Neurology*, vol. 265, no. 12, pp. 2881–2892, 2018. [Online]. Available: http://dx.doi.org/10.1007/s00415-018-9075-5 43

[125] D. Pinter, C. F. Beckmann, F. Fazekas, M. Khalil, A. Pichler, T. Gattringer, S. Ropele, S. Fuchs, and C. Enzinger, "Morphological MRI phenotypes of multiple sclerosis differ in resting-state brain function," *Scientific Reports*, vol. 9, no. 1, pp. 1–7, 2019. 43

[126] D. J. Hawellek, J. F. Hipp, C. M. Lewis, M. Corbetta, and A. K. Engel, "Increased functional connectivity indicates the severity of cognitive impairment in multiple sclerosis," *Proceedings of the National Academy of Sciences of the United States of America*, vol. 108, no. 47, pp. 19 066–19 071, 2011. 44

[127] A. Faivre, A. Rico, W. Zaaraoui, L. Crespy, F. Reuter, D. Wybrecht, E. Soulier, I. Malikova, S. Confort-Gouny, P. J. Cozzone, J. Pelletier, J.-P. Ranjeva, and B. Audoin, "Assessing brain connectivity at rest is clinically relevant in early multiple sclerosis." *Multiple sclerosis (Houndmills, Basingstoke, England)*, vol. 18, no. 9, pp. 1251–1258, sep 2012. 44

[128] Y. Liu, P. Liang, Y. Duan, X. Jia, C. Yu, M. Zhang, F. Wang, M. Zhang, H. Dong, J. Ye, H. Butzkueven, and K. Li, "Brain plasticity in relapsing-remitting multiple sclerosis: evidence from resting-state fMRI." *Journal of the neurological sciences*, vol. 304, no. 1-2, pp. 127–131, may 2011. 44, 59

[129] M. A. Rocca, P. Valsasina, V. Martinelli, P. Misci, A. Falini, G. Comi, and M. Filippi, "Large-scale neuronal network dysfunction in relapsing-

remitting multiple sclerosis." *Neurology*, vol. 79, no. 14, pp. 1449–1457, oct 2012. 44, 75

[130] B. Basile, M. Castelli, F. Monteleone, U. Nocentini, C. Caltagirone, D. Centonze, M. Cercignani, and M. Bozzali, "Functional connectivity changes within specific networks parallel the clinical evolution of multiple sclerosis," *Multiple Sclerosis Journal*, 2014. 44

[131] S. Bonavita, A. Gallo, R. Sacco, M. Della Corte, A. Bisecco, R. Docimo, L. Lavorgna, D. Corbo, A. Di Costanzo, F. Tortora, M. Cirillo, F. Esposito, and G. Tedeschi, "Distributed changes in default-mode resting-state connectivity in multiple sclerosis," *Multiple Sclerosis Journal*, vol. 17, no. 4, pp. 411–422, 2011. 44, 75, 76

[132] M. M. Schoonheim, K. A. Meijer, and J. J. Geurts, "Network collapse and cognitive impairment in multiple sclerosis," *Frontiers in Neurology*, vol. 6, no. MAR, pp. 1–5, 2015. 45

[133] M. M. Schoonheim, J. J. Geurts, O. T. Wiebenga, J. C. De Munck, C. H. Polman, C. J. Stam, F. Barkhof, and A. M. Wink, "Changes in functional network centrality underlie cognitive dysfunction and physical disability in multiple sclerosis," *Multiple Sclerosis Journal*, vol. 20, no. 8, pp. 1058–1065, 2014. 45

[134] M. A. Rocca, P. Valsasina, A. Meani, A. Falini, G. Comi, and M. Filippi, "Impaired functional integration in multiple sclerosis: a graph theory study," *Brain Structure and Function*, vol. 221, no. 1, pp. 115–131, 2016. [Online]. Available: http://dx.doi.org/10.1007/s00429-014-0896-4 45, 125

[135] V. Fleischer, A. Radetz, D. Ciolac, M. Muthuraman, G. Gonzalez-Escamilla, F. Zipp, and S. Groppa, "Graph Theoretical Framework

of Brain Networks in Multiple Sclerosis: A Review of Concepts," *Neuroscience*, vol. 403, pp. 35–53, 2019. [Online]. Available: https://doi.org/10.1016/j.neuroscience.2017.10.033 45

[136] V. C. Chirumamilla, V. Fleischer, A. Droby, T. Anjum, M. Muthuraman, F. Zipp, and S. Groppa, "Functional connectivity analysis using whole brain and regional network metrics in MS patients," *Proceedings of the Annual International Conference of the IEEE Engineering in Medicine and Biology Society, EMBS*, vol. 2016-Octob, pp. 4039–4042, 2016. 45

[137] S. P. Nejad-Davarani, M. Chopp, S. Peltier, L. Li, E. Davoodi-Bojd, M. Lu, H. Bagher-Ebadian, J. Budaj, D. Gallagher, Y. Ding, D. Hearshen, Q. Jiang, and M. Cerghet, "Resting state fMRI connectivity analysis as a tool for detection of abnormalities in five different cognitive networks of the brain in Multiple Sclerosis patients." *Clinical case reports and reviews*, vol. 2, no. 9, pp. 464–471, sep 2016. 45

[138] Á. J. Cruz-Gómez, N. Ventura-Campos, A. Belenguer, C. Ávila, and C. Forn, "The link between resting-state functional connectivity and cognition in MS patients," *Multiple Sclerosis Journal*, vol. 20, no. 3, pp. 338–348, 2014. 45

[139] T. A. Fuchs, R. H. Benedict, A. Bartnik, S. Choudhery, X. Li, M. Mallory, D. Oship, F. Yasin, K. Ashton, D. Jakimovski, N. Bergsland, D. P. Ramasamy, B. Weinstock-Guttman, R. Zivadinov, and M. G. Dwyer, "Preserved network functional connectivity underlies cognitive reserve in multiple sclerosis," *Human Brain Mapping*, vol. 40, no. 18, pp. 5231–5241, 2019. 45

[140] M. A. Rocca, G. Riccitelli, M. Rodegher, A. Ceccarelli, A. Falini, M. Falau-

tano, A. Meani, G. Comi, and M. Filippi, "Functional MR imaging correlates of neuropsychological impairment in primary-progressive multiple sclerosis," *American Journal of Neuroradiology*, vol. 31, no. 7, pp. 1240–1246, 2010. 46, 114, 121

[141] M. Petracca, C. Saiote, H. A. Bender, F. Arias, C. Farrell, P. Magioncalda, M. Martino, A. Miller, G. Northoff, and F. Lublin, "Synchronization and variability imbalance underlie cognitive impairment in primary-progressive multiple sclerosis," *Nature Publishing Group*, no. October 2016, pp. 1–12, 2017. [Online]. Available: http://dx.doi.org/10.1038/srep46411 46, 58, 76, 77, 121, 125

[142] M. A. Rocca, B. Colombo, A. Falini, A. Ghezzi, V. Martinelli, G. Scotti, G. Comi, and M. Filippi, "Cortical adaptation in patients with MS: A cross-sectional functional MRI study of disease phenotypes," *Lancet Neurology*, vol. 4, no. 10, pp. 618–626, 2005. 46, 121

[143] M. Loitfelder, F. Fazekas, K. Petrovic, S. Fuchs, S. Ropele, M. Wallner-Blazek, M. Jehna, E. Aspeck, M. Khalil, R. Schmidt, C. Neuper, and C. Enzinger, "Reorganization in cognitive networks with progression of multiple sclerosis: Insights from fMRI," *Neurology*, vol. 76, no. 6, pp. 526–533, 2011. 47, 75, 121

[144] K. Rasova, J. Krasensky, E. Havrdova, J. Obenberger, Z. Seidel, O. Dolezal, P. Rexova, and M. Zalisova, "Is it possible to actively and purposely make use of plasticity and adaptability in the neurorehabilitation treatment of multiple sclerosis patients? A pilot project." *Clinical rehabilitation*, vol. 19, no. 2, pp. 170–181, mar 2005. 47

[145] V. Tomassini, P. M. Matthews, A. J. Thompson, D. Fuglo, J. J. Geurts,

H. Johansen-Berg, D. K. Jones, M. A. Rocca, R. G. Wise, F. Barkhof, and J. Palace, "Neuroplasticity and functional recovery in Multiple Sclerosis," *Nature reviews. Neurology*, vol. 8, 2012. 47

[146] L. Prosperini, E. Sbardella, E. Raz, M. Cercignani, F. Tona, M. Bozzali, N. Petsas, C. Pozzilli, and P. Pantano, "Multiple sclerosis: white and gray matter damage associated with balance deficit detected at static posturography." *Radiology*, vol. 268, no. 1, pp. 181–189, jul 2013. 47, 80

[147] Q. van Geest, L. Douw, S. van 't Klooster, C. E. Leurs, H. M. Genova, G. R. Wylie, M. D. Steenwijk, J. Killestein, J. J. Geurts, and H. E. Hulst, "Information processing speed in multiple sclerosis: Relevance of default mode network dynamics," *NeuroImage: Clinical*, vol. 19, no. March, pp. 507–515, 2018. [Online]. Available: https://doi.org/10.1016/j.nicl.2018.05.015 47

[148] A. D'Ambrosio, P. Valsasina, A. Gallo, N. De Stefano, D. Pareto, F. Barkhof, O. Ciccarelli, C. Enzinger, G. Tedeschi, M. L. Stromillo, M. J. Arevalo, H. E. Hulst, N. Muhlert, M. Koini, M. Filippi, and M. A. Rocca, "Reduced dynamics of functional connectivity and cognitive impairment in multiple sclerosis." *Multiple sclerosis (Houndmills, Basingstoke, England)*, p. 1352458519837707, mar 2019. 47

[149] M. A. Rocca, M. Hidalgo de La Cruz, P. Valsasina, S. Mesaros, V. Martinovic, J. Ivanovic, J. Drulovic, and M. Filippi, "Two-year dynamic functional network connectivity in clinically isolated syndrome," *Multiple Sclerosis Journal*, pp. 1–14, 2019. 47

[150] C. Cordani, P. Valsasina, P. Preziosa, A. Meani, M. Filippi, and M. A. Rocca, "Action observation training promotes motor improvement and

modulates functional network dynamic connectivity in multiple sclerosis," *Multiple Sclerosis Journal*, pp. 1–8, 2019. 48

[151] M. H. Cameron and Y. Nilsagard, *Balance, gait, and falls in multiple sclerosis*, 1st ed. Elsevier B.V., 2018, vol. 159. [Online]. Available: http://dx.doi.org/10.1016/B978-0-444-63916-5.00015-X 48, 49

[152] L. Comber, R. Galvin, and S. Coote, "Gait deficits in people with multiple sclerosis: A systematic review and meta-analysis," *Gait & Posture*, vol. 51, pp. 25–35, 2017. [Online]. Available: http://www.sciencedirect.com/science/article/pii/S0966636216305884 48

[153] L. Prosperini, L. Castelli, F. De Luca, F. Fabiano, I. Ferrante, and L. De Giglio, "Task-dependent deterioration of balance underpinning cognitive-postural interference in MS," *Neurology*, vol. 87, no. 11, pp. 1085–1092, 2016. [Online]. Available: https://n.neurology.org/content/87/11/1085 48

[154] D. Cattaneo and J. Jonsdottir, "Sensory impairments in quiet standing in subjects with multiple sclerosis." *Multiple sclerosis (Houndmills, Basingstoke, England)*, vol. 15, no. 1, pp. 59–67, jan 2009. 48

[155] U. Givon, G. Zeilig, and A. Achiron, "Gait analysis in multiple sclerosis: characterization of temporal-spatial parameters using GAITRite functional ambulation system." *Gait & posture*, vol. 29, no. 1, pp. 138–142, jan 2009. 48

[156] M. H. Cameron and S. Lord, "Postural control in multiple sclerosis: implications for fall prevention." *Current neurology and neuroscience reports*, vol. 10, no. 5, pp. 407–412, sep 2010. 48, 80

[157] M. G. Benedetti, R. Piperno, L. Simoncini, P. Bonato, A. Tonini, and S. Giannini, "Gait abnormalities in minimally impaired multiple sclerosis

patients." *Multiple sclerosis (Houndmills, Basingstoke, England)*, vol. 5, no. 5, pp. 363–368, oct 1999. 48

[158] R. Mazumder, C. Murchison, D. Bourdette, and M. Cameron, "Falls in people with multiple sclerosis compared with falls in healthy controls." *PloS one*, vol. 9, no. 9, p. e107620, 2014. 49

[159] J. M. Huisinga, J. M. Yentes, M. L. Filipi, and N. Stergiou, "Postural control strategy during standing is altered in patients with multiple sclerosis," *Neuroscience Letters*, vol. 524, no. 2, pp. 124–128, 2012. [Online]. Available: http://www.sciencedirect.com/science/article/pii/S0304394012009433 49

[160] D. Frzovic, M. E. Morris, and L. Vowels, "Clinical tests of standing balance: Performance of persons with multiple sclerosis," *Archives of Physical Medicine and Rehabilitation*, vol. 81, no. 2, pp. 215–221, 2000. [Online]. Available: http://www.sciencedirect.com/science/article/pii/S0003999300901448 49

[161] J. E. Freund, D. M. Stetts, and S. Vallabhajosula, "Relationships between trunk performance, gait and postural control in persons with multiple sclerosis." *NeuroRehabilitation*, vol. 39, no. 2, pp. 305–317, jun 2016. 49

[162] M. A. Rocca, R. Gatti, F. Agosta, P. Broglia, P. Rossi, E. Riboldi, M. Corti, G. Comi, and M. Filippi, "Influence of task complexity during coordinated hand and foot movements in MS patients with and without fatigue : AA kinematic and functional MRI study," *Journal of Neurology*, 2009. 49, 80

[163] M. Gandolfi, D. Munari, C. Geroin, A. Gajofatto, M. D. Benedetti, A. Midiri, F. Carla, A. Picelli, A. Waldner, and N. Smania, "Sensory integration balance training in patients with multiple sclerosis: A

randomized, controlled trial," *Multiple Sclerosis Journal*, vol. 21, no. 11, pp. 1453–1462, jan 2015. [Online]. Available: https://doi.org/10.1177/1352458514562438 50

[164] L. V. Kalia and A. E. Lang, "Parkinson's disease," *The Lancet*, vol. 386, no. 9996, pp. 896–912, 2015. [Online]. Available: http://dx.doi.org/10.1016/S0140-6736(14)61393-3 50, 51, 52, 53

[165] A. Suppa, A. Kita, G. Leodori, A. Zampogna, E. Nicolini, P. Lorenzi, R. Rao, and F. Irrera, "L-DOPA and freezing of gait in Parkinson's disease: Objective assessment through a wearable wireless system," *Frontiers in Neurology*, vol. 8, no. AUG, 2017. 50

[166] D. Hirtz, D. J. Thurman, K. Gwinn-Hardy, M. Mohamed, A. R. Chaudhuri, and R. Zalutsky, "How common are the "common" neurologic disorders?" *Neurology*, vol. 68, no. 5, pp. 326–337, jan 2007. 50

[167] L. Horsfall, I. Petersen, K. Walters, and A. Schrag, "Time trends in incidence of Parkinson's disease diagnosis in UK primary care." *Journal of neurology*, vol. 260, no. 5, pp. 1351–1357, may 2013. 51

[168] A. Ascherio and M. A. Schwarzschild, "The epidemiology of Parkinson's disease: risk factors and prevention," *The Lancet Neurology*, vol. 15, no. 12, pp. 1257–1272, 2016. [Online]. Available: http://dx.doi.org/10.1016/S1474-4422(16)30230-7 51

[169] M. A. Nalls, N. Pankratz, C. M. Lill, C. B. Do, D. G. Hernandez, M. Saad, A. L. DeStefano, E. Kara, J. Bras, M. Sharma, C. Schulte, M. F. Keller, S. Arepalli, C. Letson, C. Edsall, H. Stefansson, X. Liu, H. Pliner, J. H. Lee, R. Cheng, M. A. Ikram, J. P. A. Ioannidis, G. M. Hadjigeorgiou, J. C. Bis, M. Martinez, J. S. Perlmutter, A. Goate, K. Marder, B. Fiske,

M. Sutherland, G. Xiromerisiou, R. H. Myers, L. N. Clark, K. Stefansson, J. A. Hardy, P. Heutink, H. Chen, N. W. Wood, H. Houlden, H. Payami, A. Brice, W. K. Scott, T. Gasser, L. Bertram, N. Eriksson, T. Foroud, and A. B. Singleton, "Large-scale meta-analysis of genome-wide association data identifies six new risk loci for Parkinson's disease." *Nature genetics*, vol. 46, no. 9, pp. 989–993, sep 2014. 51

[170] H. Braak and K. Del Tredici, "Neuroanatomy and pathology of sporadic Parkinson's disease." *Advances in anatomy, embryology, and cell biology*, vol. 201, pp. 1–119, 2009. 51

[171] M. Selikhova, D. R. Williams, P. A. Kempster, J. L. Holton, T. Revesz, and A. J. Lees, "A clinico-pathological study of subtypes in Parkinson's disease." *Brain : a journal of neurology*, vol. 132, no. Pt 11, pp. 2947–2957, nov 2009. 52

[172] T. Virmani, C. B. Moskowitz, J.-P. Vonsattel, and S. Fahn, "Clinicopathological characteristics of freezing of gait in autopsy-confirmed Parkinson's disease." *Movement disorders : official journal of the Movement Disorder Society*, vol. 30, no. 14, pp. 1874–1884, dec 2015. 52

[173] S. D. Kim, N. E. Allen, C. G. Canning, and V. S. C. Fung, "Parkinson disease." *Handbook of clinical neurology*, vol. 159, pp. 173–193, 2018. 52, 53

[174] M. A. Hely, J. G. L. Morris, W. G. J. Reid, and R. Trafficante, "Sydney Multicenter Study of Parkinson's disease: non-L-dopa-responsive problems dominate at 15 years." *Movement disorders : official journal of the Movement Disorder Society*, vol. 20, no. 2, pp. 190–199, feb 2005. 53

[175] A. J. Hughes, S. E. Daniel, and A. J. Lees, "Improved accuracy of clinical diagnosis of Lewy body Parkinson's disease." *Neurology*, vol. 57, no. 8, pp. 1497–1499, oct 2001. 53

[176] D. W. Dickson, H. Braak, J. E. Duda, C. Duyckaerts, T. Gasser, G. M. Halliday, J. Hardy, J. B. Leverenz, K. Del Tredici, Z. K. Wszolek, and I. Litvan, "Neuropathological assessment of Parkinson's disease: refining the diagnostic criteria." *The Lancet. Neurology*, vol. 8, no. 12, pp. 1150–1157, dec 2009. 53

[177] X. Shen, I. S. K. Wong-Yu, and M. K. Y. Mak, "Effects of Exercise on Falls, Balance, and Gait Ability in Parkinson's Disease: A Meta-analysis." *Neurorehabilitation and neural repair*, vol. 30, no. 6, pp. 512–527, jul 2016. 53

[178] G. Abbruzzese, L. Avanzino, R. Marchese, and E. Pelosin, "Action Observation and Motor Imagery: Innovative Cognitive Tools in the Rehabilitation of Parkinson's Disease," *Parkinson's Disease*, vol. 2015, 2015. 54, 128

[179] V. Gallese, L. Fadiga, L. Fogassi, and G. Rizzolatti, "Action recognition in the premotor cortex." *Brain : a journal of neurology*, vol. 119 (Pt 2, pp. 593–609, apr 1996. 54, 127

[180] G. Rizzolatti and L. Craighero, "The Mirror Neuron System," *Annual Review of Neuroscience*, vol. 27, no. 1, pp. 169–192, jun 2004. [Online]. Available: https://doi.org/10.1146/annurev.neuro.27.070203.144230 54, 127

[181] E. Pelosin, L. Avanzino, M. Bove, P. Stramesi, A. Nieuwboer, and G. Abbruzzese, "Action observation improves freezing of gait in patients with

Parkinson's disease," *Neurorehabilitation and Neural Repair*, vol. 24, no. 8, pp. 746–752, 2010. 54, 128, 140

[182] J. Nonnekes and A. Nieuwboer, "Towards personalized rehabilitation for gait impairments in Parkinson's disease," *Journal of Parkinson's Disease*, vol. 8, no. s1, pp. S101–S106, 2018. 54

[183] C. D. Hacker, J. S. Perlmutter, S. R. Criswell, B. M. Ances, and A. Z. Snyder, "Resting state functional connectivity of the striatum in Parkinson's disease." *Brain : a journal of neurology*, vol. 135, no. Pt 12, pp. 3699–3711, dec 2012. 55

[184] R. C. Helmich, L. C. Derikx, M. Bakker, R. Scheeringa, B. R. Bloem, and I. Toni, "Spatial remapping of cortico-striatal connectivity in Parkinson's disease." *Cerebral cortex (New York, N.Y. : 1991)*, vol. 20, no. 5, pp. 1175–1186, may 2010. 55

[185] D. Putcha, R. S. Ross, A. Cronin-Golomb, A. C. Janes, and C. E. Stern, "Altered intrinsic functional coupling between core neurocognitive networks in Parkinson's disease." *NeuroImage. Clinical*, vol. 7, pp. 449–455, 2015. 55

[186] M. Sharman, R. Valabregue, V. Perlbarg, L. Marrakchi-Kacem, M. Vidailhet, H. Benali, A. Brice, and S. Lehericy, "Parkinson's disease patients show reduced cortical-subcortical sensorimotor connectivity." *Movement disorders : official journal of the Movement Disorder Society*, vol. 28, no. 4, pp. 447–454, apr 2013. 55

[187] C. Y. Luo, X. Y. Guo, W. Song, Q. Chen, B. Cao, J. Yang, Q. Y. Gong, and H.-F. Shang, "Functional connectome assessed using graph theory in drug-naive Parkinson's disease." *Journal of neurology*, vol. 262, no. 6, pp. 1557–1567, jun 2015. 55

[188] J. Kim, M. Criaud, S. S. Cho, M. Diez-Cirarda, A. Mihaescu, S. Coakeley, C. Ghadery, M. Valli, M. F. Jacobs, S. Houle, and A. P. Strafella, "Abnormal intrinsic brain functional network dynamics in Parkinson's disease." *Brain : a journal of neurology*, vol. 140, no. 11, pp. 2955–2967, nov 2017. 55

[189] J. M. Shine, E. Matar, P. B. Ward, M. J. Frank, A. A. Moustafa, M. Pearson, S. L. Naismith, and S. J. G. Lewis, "Freezing of gait in Parkinson's disease is associated with functional decoupling between the cognitive control network and the basal ganglia." *Brain : a journal of neurology*, vol. 136, no. Pt 12, pp. 3671–3681, dec 2013. 55

[190] T. Hanakawa, Y. Katsumi, H. Fukuyama, M. Honda, T. Hayashi, J. Kimura, and H. Shibasaki, "Mechanisms underlying gait disturbance in Parkinson's disease," *Brain*, vol. 122, no. 7, pp. 1271–1282, 1999. 55, 139

[191] A. Maillet, S. Thobois, V. Fraix, J. Redoute, D. Le Bars, F. Lavenne, P. Derost, F. Durif, B. R. Bloem, P. Krack, P. Pollak, and B. Debu, "Neural substrates of levodopa-responsive gait disorders and freezing in advanced Parkinson's disease: a kinesthetic imagery approach." *Human brain mapping*, vol. 36, no. 3, pp. 959–980, mar 2015. 55, 140

[192] A. H. Snijders, I. Leunissen, M. Bakker, S. Overeem, R. C. Helmich, B. R. Bloem, and I. Toni, "Gait-related cerebral alterations in patients with Parkinson's disease with freezing of gait," *Brain*, vol. 134, no. 1, pp. 59–72, 2011. 55, 128, 140

[193] M. M. Schoonheim and M. Filippi, "Functional plasticity in MS: Friend or foe?" *Neurology*, vol. 79, no. 14, pp. 1418–1419, 2012. 57

[194] P. Pantano, N. Petsas, F. Tona, and E. Sbardella, "The role of fMRI to assess plasticity of the motor system in MS," *Frontiers in Neurology*, vol. 6, no. MAR, pp. 6–9, 2015. 58

[195] M. Martino, P. Magioncalda, Z. Huang, B. Conio, N. Piaggio, N. W. Duncan, G. Rocchi, A. Escelsior, V. Marozzi, A. Wolff, M. Inglese, M. Amore, and G. Northoff, "Contrasting variability patterns in the default mode and sensorimotor networks balance in bipolar depression and mania." *Proceedings of the National Academy of Sciences of the United States of America*, vol. 113, no. 17, pp. 4824–4829, apr 2016. 58, 61

[196] G. Buzsaki and A. Draguhn, "Neuronal oscillations in cortical networks." *Science (New York, N.Y.)*, vol. 304, no. 5679, pp. 1926–1929, jun 2004. 58

[197] X.-N. Zuo, A. Di Martino, C. Kelly, Z. E. Shehzad, D. G. Gee, D. F. Klein, F. X. Castellanos, B. B. Biswal, and M. P. Milham, "The oscillating brain: complex and reliable." *NeuroImage*, vol. 49, no. 2, pp. 1432–1445, jan 2010. 58, 64, 74

[198] M. Penttonen and G. Buzsáki, "Natural logarithmic relationship between brain oscillators," *Thalamus and Related Systems*, vol. 2, no. 2, pp. 145–152, 2003. 58

[199] N. Egorova, M. Veldsman, T. Cumming, and A. Brodtmann, "Fractional amplitude of low-frequency fluctuations (fALFF) in post-stroke depression." *NeuroImage. Clinical*, vol. 16, pp. 116–124, 2017. 58

[200] W. J. Brownlee and D. H. Miller, "Clinically isolated syndromes and the relationship to multiple sclerosis," *Journal of Clinical Neuroscience*, vol. 21, no. 12, pp. 2065–2071, 2015. [Online]. Available: http://dx.doi.org/10.1016/j.jocn.2014.02.026 58

[201] C. H. Polman, S. C. Reingold, B. Banwell, M. Clanet, J. A. Cohen, M. Filippi, K. Fujihara, E. Havrdova, M. Hutchinson, L. Kappos, F. D. Lublin, X. Montalban, and P. O. Connor, "Diagnostic Criteria for Multiple Sclerosis : 2010 Revisions to the McDonald Criteria," *Annals of Neurology*, 2011. 59, 115

[202] M. Battaglini, M. Jenkinson, and N. De Stefano, "Evaluating and reducing the impact of white matter lesions on brain volume measurements," *Human Brain Mapping*, vol. 33, no. 9, pp. 2062–2071, 2012. 60, 87, 116

[203] Q. H. Zou, C. Z. Zhu, Y. Yang, X. N. Zuo, X. Y. Long, Q. J. Cao, Y. F. Wang, and Y. F. Zang, "An improved approach to detection of amplitude of low-frequency fluctuation (ALFF) for resting-state fMRI: Fractional ALFF," *Journal of Neuroscience Methods*, vol. 172, no. 1, pp. 137–141, 2008. 61

[204] A. R. Laird, S. B. Eickhoff, K. Li, D. A. Robin, D. C. Glahn, and P. T. Fox, "Investigating the functional heterogeneity of the default mode network using coordinate-based meta-analytic modeling." *The Journal of neuroscience : the official journal of the Society for Neuroscience*, vol. 29, no. 46, pp. 14 496–14 505, nov 2009. 63

[205] M. R. Brier, J. B. Thomas, A. Z. Snyder, T. L. Benzinger, D. Zhang, M. E. Raichle, D. M. Holtzman, J. C. Morris, and B. M. Ances, "Loss of intranetwork and internetwork resting state functional connections with Alzheimer's disease progression." *The Journal of neuroscience : the official journal of the Society for Neuroscience*, vol. 32, no. 26, pp. 8890–8899, jun 2012. 63

[206] M. A. Rocca, P. Valsasina, V. M. Leavitt, M. Rodegher, M. Radaelli, G. C.

Riccitelli, V. Martinelli, F. Martinelli-Boneschi, A. Falini, G. Comi, and M. Filippi, "Functional network connectivity abnormalities in multiple sclerosis: Correlations with disability and cognitive impairment." *Multiple sclerosis (Houndmills, Basingstoke, England)*, p. 1352458517699875, mar 2017. 75

[207] X. Di, E. H. Kim, C.-C. Huang, S.-J. Tsai, C.-P. Lin, and B. B. Biswal, "The influence of the amplitude of low-frequency fluctuations on resting-state functional connectivity." *Frontiers in human neuroscience*, vol. 7, p. 118, 2013. 75

[208] R. H. Benedict, J. Deluca, G. Phillips, N. LaRocca, L. D. Hudson, and R. Rudick, "Validity of the Symbol Digit Modalities Test as a cognition performance outcome measure for multiple sclerosis," *Multiple Sclerosis*, vol. 23, no. 5, pp. 721–733, 2017. 76

[209] B. O. Turner, B. Lopez, T. Santander, and M. B. Miller, "One dataset , many conclusions : BOLD variability ' s complicated relationships with age and motion artifacts," *Brain Imaging and Behavior*, pp. 115–127, 2015. 77

[210] Y. Lajoie, N. Teasdale, J. D. Cole, M. Burnett, C. Bard, M. Fleury, R. Forget, J. Paillard, and Y. Lamarre, "Gait of a deafferented subject without large myelinated sensory fibers below the neck." *Neurology*, vol. 47, no. AUGUST, pp. 109–115, 1996. 79

[211] B. Bloem, J. H. J. Allum, M. Carpenter, J. Verschuuren, and F. Honegger, "Triggering of balance corrections and compensatory strategies in a patient with total leg proprioceptive loss," *Experimental Brain Research*, vol. 142, no. 1, pp. 91–107, 2002. 79

[212] S. Gilman, "Joint position sense and vibration sense : anatomical organisation and assessment," *Journal of Neurology, Neurosurgery and Psychiatry*, pp. 473–478, 2002. 79

[213] R. Dobson and G. Giovannoni, "Multiple sclerosis – a review," *European Journal of Neurology*, vol. 26, no. 1, pp. 27–40, 2019. 80

[214] A. Scalfari, A. Neuhaus, A. Degenhardt, G. P. Rice, P. A. Muraro, M. Daumer, and G. C. Ebers, "The natural history of multiple sclerosis: a geographically based study 10: relapses and long-term disability." *Brain : a journal of neurology*, vol. 133, no. Pt 7, pp. 1914–1929, jul 2010. 80

[215] A. Jamali, E. Sadeghi-Demneh, N. Fereshtenajad, and S. Hillier, "Somatosensory impairment and its association with balance limitation in people with multiple sclerosis." *Gait & posture*, vol. 57, pp. 224–229, sep 2017. 80

[216] L. Filli, T. Sutter, C. S. Easthope, T. Killeen, C. Meyer, K. Reuter, L. Lorincz, M. Bolliger, M. Weller, A. Curt, D. Straumann, M. Linnebank, and B. Zorner, "Profiling walking dysfunction in multiple sclerosis: characterisation, classification and progression over time." *Scientific reports*, vol. 8, no. 1, p. 4984, mar 2018. 80

[217] S. Maggioni, A. Melendez-Calderon, E. van Asseldonk, V. Klamroth-Marganska, L. Lünenburger, R. Riener, and H. van der Kooij, "Robot-aided assessment of lower extremity functions: a review," *Journal of NeuroEngineering and Rehabilitation*, vol. 13, no. 1, p. 72, 2016. 80

[218] O. Ciccarelli, A. T. Toosy, J. F. Marsden, C. M. Wheeler-Kingshott, D. H. Miller, P. M. Matthews, and A. J. Thompson, "Functional response to active and passive ankle movements with clinical correlations in patients

with primary progressive multiple sclerosis." *Journal of neurology*, vol. 253, no. 7, pp. 882–891, jul 2006. 80

[219] P. Pantano, C. Mainero, D. Lenzi, F. Caramia, G. D. Iannetti, M. C. Piattella, I. Pestalozza, S. Di Legge, L. Bozzao, and C. Pozzilli, "A longitudinal fMRI study on motor activity in patients with multiple sclerosis," *Brain*, vol. 128, no. 9, pp. 2146–2153, 2005. 80

[220] S. Niam, W. Cheung, P. E. Sullivan, S. Kent, and X. Gu, "Balance and physical impairments after stroke," *Archives of Physical Medicine and Rehabilitation*, vol. 80, no. 10, pp. 1227–1233, 1999. 80

[221] M. H. J. Fanchamps, H. Gensicke, J. Kuhle, L. Kappos, J. H. J. Allum, and Ö. Yaldizli, "Screening for balance disorders in mildly affected multiple sclerosis patients," *Journal of neurology*, vol. 259, no. 7, pp. 1413–1419, 2012. 80

[222] B. W. Fling, G. G. Dutta, H. Schlueter, M. H. Cameron, and F. B. Horak, "Associations between proprioceptive neural pathway structural connectivity and balance in people with multiple sclerosis," *Frontiers in human neuroscience*, vol. 8, 2014. 80, 85, 140

[223] D. S. Peterson, G. Gera, F. B. Horak, and B. W. Fling, "Corpus Callosum Structural Integrity Is Associated With Postural Control Improvement in Persons With Multiple Sclerosis Who Have Minimal Disability." *Neurorehabilitation and neural repair*, vol. 31, no. 4, pp. 343–353, apr 2017. 80

[224] J. C. Eliassen, K. Baynes, and M. S. Gazzaniga, "Anterior and posterior callosal contributions to simultaneous bimanual movements of the hands and fingers." *Brain : a journal of neurology*, vol. 123 Pt 12, pp. 2501–2511, dec 2000. 81

[225] F. Lin, C. Yu, Y. Liu, K. Li, and H. Lei, "Diffusion tensor group tractography of the corpus callosum in clinically isolated syndrome," *American Journal of Neuroradiology*, vol. 32, no. 1, pp. 92–98, 2011. 81

[226] F. Marini, V. Squeri, P. Morasso, J. Konczak, and L. Masia, "Robot-Aided Mapping of Wrist proprioceptive acuity across a 3D workspace," *PloS one*, vol. 11, no. 8, p. e0161155, 2016. 81

[227] S. P. Dukelow, T. M. Herter, K. D. Moore, M. J. Demers, J. I. Glasgow, S. D. Bagg, K. E. Norman, and S. H. Scott, "Quantitative assessment of limb position sense following stroke." *Neurorehabilitation and neural repair*, vol. 24, no. 2, pp. 178–187, feb 2010. 81

[228] S. E. Findlater, J. A. Desai, J. A. Semrau, J. M. Kenzie, C. Rorden, T. M. Herter, S. H. Scott, and S. P. Dukelow, "Central perception of position sense involves a distributed neural network - Evidence from lesion-behavior analyses," *Cortex*, vol. 79, pp. 42–56, 2016. 81

[229] N. Elangovan, A. Herrmann, and J. Konczak, "Assessing proprioceptive function: evaluating joint position matching methods against psychophysical thresholds," *Physical Therapy*, vol. 94, no. 4, pp. 553–561, 2014. 81

[230] R. Iandolo, A. Bellini, C. Saiote, I. Marre, G. Bommarito, N. Oesingmann, L. Fleysher, G. L. Mancardi, M. Casadio, and M. Inglese, "Neural correlates of lower limbs proprioception: An fMRI study of foot position matching." *Human brain mapping*, vol. 39, no. 5, pp. 1929–1944, may 2018. 82, 90, 109

[231] R. A. Clark, A. L. Bryant, Y. Pua, P. McCrory, K. Bennell, and M. Hunt, "Validity and reliability of the Nintendo Wii Balance Board for assessment of standing balance," *Gait & posture*, vol. 31, no. 3, pp. 307–310, 2010. 85

[232] J. D. Holmes, M. E. Jenkins, A. M. Johnson, M. A. Hunt, and R. A. Clark, "Validity of the Nintendo Wii®balance board for the assessment of standing balance in Parkinson's disease," *Clinical Rehabilitation*, vol. 27, no. 4, pp. 361–366, 2013. 85

[233] H. L. Bartlett, L. H. Ting, and J. T. Bingham, "Accuracy of force and center of pressure measures of the Wii Balance Board." *Gait & posture*, vol. 39, no. 1, pp. 224–228, jan 2014. 85, 86

[234] D. J. Goble, B. L. Cone, and B. W. Fling, "Using the Wii Fit as a tool for balance assessment and neurorehabilitation: the first half decade of "Wii-search"," *Journal of neuroengineering and rehabilitation*, vol. 11, no. 1, p. 12, 2014. 85

[235] G. Severini, S. Straudi, C. Pavarelli, M. Da Roit, C. Martinuzzi, L. Di Marco Pizzongolo, and N. Basaglia, "Use of Nintendo Wii Balance Board for posturographic analysis of Multiple Sclerosis patients with minimal balance impairment." *Journal of neuroengineering and rehabilitation*, vol. 14, no. 1, p. 19, mar 2017. 85, 86

[236] M. Pau, G. Coghe, C. Atzeni, F. Corona, G. Pilloni, M. G. Marrosu, E. Cocco, and M. Galli, "Novel characterization of gait impairments in people with multiple sclerosis by means of the gait profile score." *Journal of the neurological sciences*, vol. 345, no. 1-2, pp. 159–163, oct 2014. 85

[237] L. Castelli, L. Stocchi, M. Patrignani, G. Sellitto, M. Giuliani, and L. Prosperini, "We-Measure: Toward a low-cost portable posturography for patients with multiple sclerosis using the commercial Wii balance board," *Journal of the neurological sciences*, vol. 359, no. 1, pp. 440–444, 2015. 85

[238] L. Baratto, P. G. Morasso, C. Re, and G. Spada, "A new look at posturographic analysis in the clinical context: sway-density versus other parameterization techniques." pp. 246–270, 2002. 85, 86

[239] M. Salavati, M. R. Hadian, M. Mazaheri, H. Negahban, I. Ebrahimi, S. Talebian, A. H. Jafari, M. A. Sanjari, S. M. Sohani, and M. Parnianpour, "Test-retest reliability [corrected] of center of pressure measures of postural stability during quiet standing in a group with musculoskeletal disorders consisting of low back pain, anterior cruciate ligament injury and functional ankle instability." *Gait & posture*, vol. 29, no. 3, pp. 460–464, apr 2009. 86

[240] R. W. Cox, "AFNI: Software for Analysis and Visualization of Functional Magnetic Resonance Neuroimages," *Computers and Biomedical Research*, vol. 29, pp. 162–173, 1996. 88

[241] F. Segonne, A. M. Dale, E. Busa, M. Glessner, D. Salat, H. K. Hahn, and B. Fischl, "A hybrid approach to the skull stripping problem in MRI." *NeuroImage*, vol. 22, no. 3, pp. 1060–1075, jul 2004. 88, 131

[242] M. Jenkinson, P. Bannister, M. Brady, and S. Smith, "Improved optimization for the robust and accurate linear registration and motion correction of brain images." *NeuroImage*, vol. 17, no. 2, pp. 825–841, oct 2002. 88, 89, 131, 133

[243] S. M. Smith, M. Jenkinson, M. W. Woolrich, C. F. Beckmann, T. E. J. Behrens, H. Johansen-Berg, P. R. Bannister, M. De Luca, I. Drobnjak, D. E. Flitney, R. K. Niazy, J. Saunders, J. Vickers, Y. Zhang, N. De Stefano, J. M. Brady, and P. M. Matthews, "Advances in functional and structural MR

image analysis and implementation as FSL." *NeuroImage*, vol. 23 Suppl 1, pp. S208–19, jan 2004. 88, 131

[244] M. W. Woolrich, S. Jbabdi, B. Patenaude, M. Chappell, S. Makni, T. Behrens, C. Beckmann, M. Jenkinson, and S. M. Smith, "Bayesian analysis of neuroimaging data in FSL." *NeuroImage*, vol. 45, pp. S173–S186, 2009. 88, 131

[245] M. W. Woolrich, B. D. Ripley, M. Brady, and S. M. Smith, "Temporal Autocorrelation in Univariate Linear Modeling of FMRI Data," *NeuroImage*, vol. 14, no. 6, pp. 1370–1386, dec 2001. 88, 131

[246] Y. Zhang, M. Brady, and S. Smith, "Segmentation of brain MR images through a hidden Markov random field model and the expectation-maximization algorithm," *IEEE Transactions on Medical Imaging*, vol. 20, no. 1, pp. 45–57, 2001. 88, 132

[247] D. N. Greve and B. Fischl, "Accurate and robust brain image alignment using boundary-based registration," *NeuroImage*, vol. 48, no. 1, pp. 63–72, 2009. 88

[248] S. B. Eickhoff, T. Paus, S. Caspers, M. H. Grosbras, A. C. Evans, K. Zilles, and K. Amunts, "Assignment of functional activations to probabilistic cytoarchitectonic areas revisited," *NeuroImage*, vol. 36, no. 3, pp. 511–521, 2007. 89, 133

[249] S. Mori, S. Wakana, P. C. M. van Zijl, and L. Nagae-Poetscher, "MRI Atlas of Human White Matter." *1st ed. Elsevier Science*, 2005. 89

[250] J. L. R. Andersson, M. Jenkinson, and S. Smith, "Non-linear registration aka Spatial normalisation FMRIB Technial Report TR07JA2,"

In Practice, no. June, p. 22, 2007. [Online]. Available: http://fmrib.medsci.ox.ac.uk/analysis/techrep/tr07ja2/tr07ja2.pdf 89

[251] P. Thoumie and E. Mevellec, "Relation between walking speed and muscle strength is affected by somatosensory loss in multiple sclerosis." *Journal of neurology, neurosurgery, and psychiatry*, vol. 73, no. 3, pp. 313–315, sep 2002. 109

[252] N. E. Fritz, R. E. R. Marasigan, P. A. Calabresi, S. D. Newsome, and K. M. Zackowski, "The impact of dynamic balance measures on walking performance in multiple sclerosis." *Neurorehabilitation and neural repair*, vol. 29, no. 1, pp. 62–69, jan 2015. 109

[253] G. L. Shulman, D. L. W. Pope, S. V. Astafiev, M. P. McAvoy, A. Z. Snyder, and M. Corbetta, "Right hemisphere dominance during spatial selective attention and target detection occurs outside the dorsal frontoparietal network." *The Journal of neuroscience : the official journal of the Society for Neuroscience*, vol. 30, no. 10, pp. 3640–3651, mar 2010. 110

[254] F. du Boisgueheneuc, R. Levy, E. Volle, M. Seassau, H. Duffau, S. Kinkingnehun, Y. Samson, S. Zhang, and B. Dubois, "Functions of the left superior frontal gyrus in humans: a lesion study." *Brain : a journal of neurology*, vol. 129, no. Pt 12, pp. 3315–3328, dec 2006. 110

[255] C. Keysers, J. H. Kaas, and V. Gazzola, "Somatosensation in social perception." *Nature reviews. Neuroscience*, vol. 11, no. 6, pp. 417–428, jun 2010. 110

[256] M. Schurz, M. G. Tholen, J. Perner, R. B. Mars, and J. Sallet, "Specifying the brain anatomy underlying temporo-parietal junction activations for theory of mind: A review using probabilistic atlases from different imaging

modalities." *Human brain mapping*, vol. 38, no. 9, pp. 4788–4805, sep 2017. 110

[257] J. Limanowski and F. Blankenburg, "Integration of Visual and Proprioceptive Limb Position Information in Human Posterior Parietal, Premotor, and Extrastriate Cortex." *The Journal of neuroscience : the official journal of the Society for Neuroscience*, vol. 36, no. 9, pp. 2582–2589, mar 2016. 110

[258] T. N. Mackenzie, A. Z. Bailey, P. Y. Mi, P. Tsang, C. B. Jones, and A. J. Nelson, "Human area 5 modulates corticospinal output during movement preparation." *Neuroreport*, vol. 27, no. 14, pp. 1056–1060, sep 2016. 110

[259] M. Jueptner, K. M. Stephan, C. D. Frith, D. J. Brooks, R. S. Frackowiak, and R. E. Passingham, "Anatomy of motor learning. I. Frontal cortex and attention to action." *Journal of neurophysiology*, vol. 77, no. 3, pp. 1313–1324, mar 1997. 110

[260] M. J. Lowe, E. B. Beall, K. E. Sakaie, K. A. Koenig, L. Stone, R. A. Marrie, and M. D. Phillips, "Resting state sensorimotor functional connectivity in multiple sclerosis inversely correlates with transcallosal motor pathway transverse diffusivity." *Human brain mapping*, vol. 29, no. 7, pp. 818–827, jul 2008. 111

[261] J. Gooijers, K. Caeyenberghs, H. M. Sisti, M. Geurts, M. H. Heitger, A. Leemans, and S. P. Swinnen, "Diffusion tensor imaging metrics of the corpus callosum in relation to bimanual coordination: effect of task complexity and sensory feedback." *Human brain mapping*, vol. 34, no. 1, pp. 241–252, jan 2013. 111

[262] M. A. Rocca, P. Valsasina, M. Absinta, G. Riccitelli, M. E. Rodegher, P. Misci, P. Rossi, A. Falini, G. Comi, and M. Filippi, "Default-mode net-

work dysfunction and cognitive impairment in progressive MS," *Neurology*, 2010. 114, 121, 125

[263] A. Ceccarelli, M. A. Rocca, P. Valsasina, M. Rodegher, A. Falini, G. Comi, and M. Filippi, "Structural and functional magnetic resonance imaging correlates of motor network dysfunction in primary progressive multiple sclerosis," *European Journal of Neuroscience*, vol. 31, no. 7, pp. 1273–1280, 2010. 114, 121

[264] G. Boffa, A. Tacchino, E. Sbragia, S. Schiavi, A. Droby, N. Piaggio, G. Bommarito, G. Girardi, G. L. Mancardi, G. Brichetto, and M. Inglese, "Preserved brain functional plasticity after upper limb task-oriented rehabilitation in progressive multiple sclerosis." *European journal of neurology*, vol. 27, no. 1, pp. 77–84, jan 2020. 114

[265] D. W. Langdon, M. P. Amato, J. Boringa, B. Brochet, F. Foley, S. Fredrikson, P. Hämäläinen, H. P. Hartung, L. Krupp, I. K. Penner, A. T. Reder, and R. H. Benedict, "Recommendations for a brief international cognitive assessment for multiple sclerosis (BICAMS)," *Multiple Sclerosis Journal*, vol. 18, no. 6, pp. 891–898, 2012. 115

[266] B. A. Parmenter, S. M. Testa, D. J. Schretlen, B. Weinstock-Guttman, and R. H. Benedict, "The utility of regression-based norms in interpreting the minimal assessment of cognitive function in multiple sclerosis (MACFIMS)," *Journal of the International Neuropsychological Society*, vol. 16, no. 1, pp. 6–16, 2010. 115

[267] J. D. Power, K. A. Barnes, A. Z. Snyder, B. L. Schlaggar, and S. E. Petersen, "Spurious but systematic correlations in functional connectivity MRI networks arise from subject motion," *NeuroImage*,

vol. 59, no. 3, pp. 2142–2154, feb 2012. [Online]. Available: http://www.sciencedirect.com/science/article/pii/S1053811911011815 116

[268] L. Parkes, B. Fulcher, M. Yucel, and A. Fornito, "An evaluation of the efficacy, reliability, and sensitivity of motion correction strategies for resting-state functional MRI." *NeuroImage*, vol. 171, pp. 415–436, may 2018. 116

[269] B. Fischl, M. I. Sereno, R. B. Tootell, and A. M. Dale, "High-resolution intersubject averaging and a coordinate system for the cortical surface." *Human brain mapping*, vol. 8, no. 4, pp. 272–284, 1999. 116

[270] R. S. Desikan, F. Segonne, B. Fischl, B. T. Quinn, B. C. Dickerson, D. Blacker, R. L. Buckner, A. M. Dale, R. P. Maguire, B. T. Hyman, M. S. Albert, and R. J. Killiany, "An automated labeling system for subdividing the human cerebral cortex on MRI scans into gyral based regions of interest." *NeuroImage*, vol. 31, no. 3, pp. 968–980, jul 2006. 116

[271] A. Schaefer, R. Kong, E. M. Gordon, T. O. Laumann, X.-N. Zuo, A. J. Holmes, S. B. Eickhoff, and B. T. T. Yeo, "Local-Global Parcellation of the Human Cerebral Cortex from Intrinsic Functional Connectivity MRI," *Cerebral Cortex*, vol. 28, no. 9, pp. 3095–3114, 2018. [Online]. Available: https://academic.oup.com/cercor/article/28/9/3095/3978804 116

[272] D. E. Meskaldji, S. Morgenthaler, and D. Van De Ville, "New measures of brain functional connectivity by temporal analysis of extreme events," *Proceedings - International Symposium on Biomedical Imaging*, vol. 2015-July, pp. 26–29, 2015. 117

[273] M. Newman and M. E. J. Newman, "Mathematics of networks," *Networks*, pp. 109–167, 2010. 117

[274] B. Zhang and S. Horvath, "A general framework for weighted gene co-expression network analysis." *Statistical applications in genetics and molecular biology*, vol. 4, p. Article17, 2005. 117

[275] Y. Wang, E. Ghumare, R. Vandenberghe, and P. Dupont, "Comparison of Different Generalizations of Clustering Coefficient and Local Efficiency for Weighted Undirected Graphs." *Neural computation*, vol. 29, no. 2, pp. 313–331, feb 2017. 117

[276] U. Brandes, "A faster algorithm for betweenness centrality," *The Journal of Mathematical Sociology*, vol. 25, no. 2, pp. 163–177, 2001. [Online]. Available: https://doi.org/10.1080/0022250X.2001.9990249 117

[277] A. Krishnan, L. J. Williams, A. R. McIntosh, and H. Abdi, "Partial Least Squares (PLS) methods for neuroimaging: a tutorial and review." *NeuroImage*, vol. 56, no. 2, pp. 455–475, may 2011. 118

[278] M. A. Rocca, C. Gavazzi, D. M. Mezzapesa, A. Falini, B. Colombo, M. Mascalchi, G. Scotti, G. Comi, and M. Filippi, "A functional magnetic resonance imaging study of patients with secondary progressive multiple sclerosis." *NeuroImage*, vol. 19, no. 4, pp. 1770–1777, aug 2003. 121

[279] A. Droby, K. S. L. Yuen, M. Muthuraman, S.-C. Reitz, V. Fleischer, J. Klein, R.-M. Gracien, U. Ziemann, R. Deichmann, F. Zipp, and S. Groppa, "Changes in brain functional connectivity patterns are driven by an individual lesion in MS: a resting-state fMRI study." *Brain imaging and behavior*, vol. 10, no. 4, pp. 1117–1126, dec 2016. 124

[280] C. H. Park, W. H. Chang, S. H. Ohn, S. T. Kim, O. Y. Bang, A. Pascual-Leone, and Y. H. Kim, "Longitudinal changes of resting-state functional

connectivity during motor recovery after stroke," *Stroke*, vol. 42, no. 5, pp. 1357–1362, 2011. 124

[281] F. De Vico Fallani, J. Richiardi, M. Chavez, and S. Achard, "Graph analysis of functional brain networks: Practical issues in translational neuroscience," *Philosophical Transactions of the Royal Society B: Biological Sciences*, vol. 369, no. 1653, 2014. 125

[282] G. Buccino, A. Solodkin, and S. L. Small, "Functions of the Mirror Neuron System : Implications for," *Rehabilitation*, vol. 19, no. 1, pp. 55–63, 2006. 128, 140

[283] E. Poliakoff, A. Galpin, J. Dick, P. Moore, and S. P. Tipper, "The effect of viewing graspable objects and actions in Parkinson's disease." *Neuroreport*, vol. 18, no. 5, pp. 483–487, mar 2007. 128

[284] S. Marceglia, M. Fiorio, G. Foffani, S. Mrakic-Sposta, M. Tiriticco, M. Locatelli, E. Caputo, M. Tinazzi, and A. Priori, "Modulation of beta oscillations in the subthalamic area during action observation in Parkinson's disease." *Neuroscience*, vol. 161, no. 4, pp. 1027–1036, jul 2009. 128

[285] M. Alegre, M. C. Rodriguez-Oroz, M. Valencia, M. Perez-Alcazar, J. Guridi, J. Iriarte, J. A. Obeso, and J. Artieda, "Changes in subthalamic activity during movement observation in Parkinson's disease: is the mirror system mirrored in the basal ganglia?" *Clinical neurophysiology : official journal of the International Federation of Clinical Neurophysiology*, vol. 121, no. 3, pp. 414–425, mar 2010. 128

[286] F. Tremblay, G. Leonard, and L. Tremblay, "Corticomotor facilitation associated with observation and imagery of hand actions is impaired in Parkin-

son's disease." *Experimental brain research*, vol. 185, no. 2, pp. 249–257, feb 2008. 128

[287] T. Heida, N. R. Poppe, C. C. de Vos, M. J. A. M. van Putten, and J. P. P. van Vugt, "Event-related mu-rhythm desynchronization during movement observation is impaired in Parkinson's disease." *Clinical neurophysiology : official journal of the International Federation of Clinical Neurophysiology*, vol. 125, no. 9, pp. 1819–1825, sep 2014. 128

[288] D. S. Peterson, K. A. Pickett, R. Duncan, J. Perlmutter, and G. M. Earhart, "Gait-related brain activity in people with Parkinson disease with freezing of gait," *PLoS ONE*, vol. 9, no. 3, pp. 1–9, 2014. 128, 140

[289] F. Agosta, R. Gatti, E. Sarasso, M. A. Volonte, E. Canu, A. Meani, L. Sarro, M. Copetti, E. Cattrysse, E. Kerckhofs, G. Comi, A. Falini, and M. Filippi, "Brain plasticity in Parkinson's disease with freezing of gait induced by action observation training." *Journal of neurology*, vol. 264, no. 1, pp. 88–101, jan 2017. 128, 140

[290] E. Canu, F. Agosta, E. Sarasso, M. A. Volonte, S. Basaia, T. Stojkovic, E. Stefanova, G. Comi, A. Falini, V. S. Kostic, R. Gatti, and M. Filippi, "Brain structural and functional connectivity in Parkinson's disease with freezing of gait." *Human brain mapping*, vol. 36, no. 12, pp. 5064–5078, dec 2015. 128

[291] A. J. Hughes, S. E. Daniel, L. Kilford, and A. J. Lees, "Accuracy of clinical diagnosis of idiopathic Parkinson's disease: a clinico-pathological study of 100 cases." *Journal of neurology, neurosurgery, and psychiatry*, vol. 55, no. 3, pp. 181–184, mar 1992. 129

[292] M. F. Folstein, S. E. Folstein, and P. R. McHugh, “”Mini-mental state”. A practical method for grading the cognitive state of patients for the clinician.” *Journal of psychiatric research*, vol. 12, no. 3, pp. 189–198, nov 1975. 129

[293] C. G. e. a. Goetz, “Movement Disorder Society-Sponsored Revision of the Unified Parkinson’s Disease Rating Scale (MDS-UPDRS): Scale presentation and clinimetric testing results,” *Movement Disorders*, vol. 23, no. 15, pp. 2129–2170, 2008. 129

[294] C. G. Goetz, W. Poewe, O. Rascol, C. Sampaio, G. T. Stebbins, C. Counsell, N. Giladi, R. G. Holloway, C. G. Moore, G. K. Wenning, M. D. Yahr, and L. Seidl, “Movement Disorder Society Task Force report on the Hoehn and Yahr staging scale: Status and recommendations,” *Movement Disorders*, vol. 19, no. 9, pp. 1020–1028, 2004. 129

[295] N. Giladi, J. Tal, T. Azulay, O. Rascol, D. J. Brooks, E. Melamed, W. Oertel, W. H. Poewe, F. Stocchi, and E. Tolosa, “Validation of the Freezing of Gait Questionnaire in patients with Parkinson’s disease,” *Movement Disorders*, vol. 24, no. 5, pp. 655–661, 2009. 129

[296] M. Jenkinson, C. F. Beckmann, T. E. J. Behrens, M. W. Woolrich, and S. M. Smith, “FSL.” *NeuroImage*, vol. 62, no. 2, pp. 782–790, aug 2012. 131

[297] F. Malouin, C. L. Richards, P. L. Jackson, F. Dumas, and J. Doyon, “Brain activations during motor imagery of locomotor-related tasks: A PET study,” *Human Brain Mapping*, vol. 19, no. 1, pp. 47–62, 2003. 138, 141

[298] K. Iseki, T. Hanakawa, J. Shinozaki, M. Nankaku, and H. Fukuyama, "Neural mechanisms involved in mental imagery and observation of gait," *NeuroImage*, vol. 41, no. 3, pp. 1021–1031, 2008. 139

[299] A. E. Cavanna and M. R. Trimble, "The precuneus: A review of its functional anatomy and behavioural correlates," *Brain*, vol. 129, no. 3, pp. 564–583, 2006. 139, 141